

Module 3: Linear Motion

Contents

Module 3 - Linear Motion Systems	4
1. Introduction to Linear Motion Systems	4
1.1 The Translation Problem	4
1.2 Historical Context and Technology Evolution	5
1.3 Classification of Linear Motion Technologies	5
1.4 Performance Metrics and Selection Criteria	5
1.5 System-Level Requirements and Design Objectives	5
1.6 Contact Mechanics and Tribology Overview	6
1.7 Application-Specific Requirements by Machine Type	6
1.8 Technology Trade-Off Matrix	7
1.9 Module Roadmap and Section Integration	8
1.10 Notation and Units	9
References	10
Industry Standards	10
Academic and Professional Engineering References	11
Cross-Module Integration References	11
Module 3 - Linear Motion Systems	11
2. Ball Screws	11
2.1 Operating Principles and Construction	11
2.2 Kinematic Resolution and Servo Interface	12
2.3 Critical Speed and Buckling Limits	12
2.4 Axial Stiffness and Preload Strategies	12
2.5 Thermal Behavior and Compensation	12
2.6 Worked Example - High-Speed Gantry Axis	13
2.7 Specification Snapshot	13
2.8 Contact Mechanics and Tribology Fundamentals	13
2.9 Servo Integration and Feedforward Control	20
2.10 Dual-Drive Synchronization for Gantry Axes	21
2.11 Comparative Selection Matrix	21
2.12 Case Study - Heavy Vertical Axis Retrofit	22
2.13 Comparative Technology Assessment	23
2.14 Thermal Compensation and Linear Feedback Integration	25
2.15 Maintenance Economics and Reliability Planning	26
2.16 Section Summary Checklist	26
2.20 Case Study - Ball Screw vs. Planetary Roller in Heavy Vertical Axis	27

2.21 Case Study - Rack Retrofit vs. Dual Ball Screws (Accuracy Focus)	27
2.22 Drive Selection Decision Table	28
2.17 Screw Lead Error Mapping and Compensation	28
2.17 Support Bearing Selection and Mounting Configurations	28
2.18 Installation and Alignment Workflow	30
2.19 Retrofit Case Study - Dual Ball Screws vs. Rack & Pinion	30
2.23 Key Takeaways and Ball Screw Selection Synthesis	30
References	32
Industry Standards	32
Manufacturer Technical Documentation	32
Academic and Professional Engineering References	32
Technical Papers and Application Notes	33
Module 3 - Linear Motion Systems	33
3. Lead Screws	33
3.1 Thread Geometry and Standards	34
3.2 Efficiency and Power Transmission	35
3.3 Nut Material Selection and Wear Prediction	36
3.4 Worked Example: Vertical Z-Axis Design	37
3.5 Anti-Backlash Nut Designs	40
3.6 Lubrication and Maintenance	41
3.7 Design Trade-Offs: Lead Screws vs. Ball Screws	42
3.8 Summary: Lead Screw Design Checklist	42
3.9 Key Takeaways and Lead Screw Application Synthesis	43
References	44
Industry Standards	44
Manufacturer Technical Documentation	44
Academic and Professional Engineering References	45
Technical Papers and Application Notes	45
Module 3 - Linear Motion Systems	45
4. Rack & Pinion Drives	46
4.1 Geometry and Tooth Selection	46
4.2 Kinematics, Force and Servo Interface	46
4.3 Strength Verification (AGMA Simplified)	47
4.4 Backlash and Preload Strategies	47
4.5 Installation and Alignment	48
4.6 Long-Axis Thermal Expansion and Synchronization	48
4.7 Dynamics, Contact Ratio, and NVH	48
4.8 Worked Examples	48
4.9 Selection Guidelines	50
4.10 Key Takeaways and Rack & Pinion System Integration	50
References	51
Industry Standards	51
Manufacturer Technical Documentation	51
Academic and Professional Engineering References	52
Technical Papers and Application Notes	52

Module 3 - Linear Motion Systems	53
5. Linear Guides	53
5.1 Guideway Types	53
5.2 Load Ratings and Life	59
5.3 Stiffness and Preload Selection	66
5.4 Installation and Alignment	71
References	83
Industry Standards	83
Manufacturer Technical Documentation	83
Academic and Professional Engineering References	84
Technical Papers and Application Notes	84
5.11 Key Takeaways and Linear Guide System Integration	84
Module 3 - Linear Motion Systems	86
6. Belt and Cable Drives	86
6.1 Belt Families and Materials	87
6.2 Tension, Stiffness, and Elongation	90
6.3 Dynamic Behavior and Resonance	94
6.4 Worked Examples	99
References	103
Industry Standards	103
Manufacturer Technical Documentation	103
Academic and Professional Engineering References	104
Technical Papers and Application Notes	104
6.9 Key Takeaways and Belt Drive System Integration	104
Module 3 - Linear Motion Systems	106
7. Universal Linear Motion Requirements	106
7.1 Backlash Specifications	106
7.2 Stiffness Specifications	110
7.3 Thermal Behavior and Environmental Control	113
7.4 Protection, Safety, and Regulatory Compliance	117
References	121
7.6 Key Takeaways and Universal Requirements Integration	121
References	123
Industry Standards	123
Manufacturer Technical Documentation	123
Academic and Professional Engineering References	123
Safety Standards and Guidelines	124
Module 3 - Linear Motion Systems	124
8. Alignment, Maintenance, and Safety	124
8.1 Installation Procedures	124
8.2 Preventive Maintenance Procedures	132
8.3 Condition Monitoring and Diagnostics	136
8.4 Troubleshooting Matrices	138
8.5 Documentation and Record-Keeping	141
References	142

8.6 Key Takeaways and Maintenance Program Integration	142
References	144
Industry Standards	144
Manufacturer Technical Documentation	144
Academic and Professional Engineering References	145
CMMS and Maintenance Management	145
Module 3 - Linear Motion Systems	145
9. Conclusion	145
9.1 Key Outcomes by Drive Technology	145
9.2 Universal Requirements and Their Implications	147
9.3 Cross-Module Integration	147
9.4 Forward-Looking: Module 4 (Control Electronics) Requirements	148
9.5 Technology Selection Decision Framework	149
9.6 Closing Remarks and Path Forward	149
References	150
Comprehensive Module 3 Standards (All Drive Technologies)	150
Academic References (Primary Textbooks)	150
Cross-Module Integration (Course Modules)	151
Forward-Looking Technologies	151

Module 3 - Linear Motion Systems

1. Introduction to Linear Motion Systems

Linear motion subsystems form the mechanical interface between servo motors and the trajectories commanded by CNC controllers. The quality of these subsystems defines the ceiling for machine accuracy, dynamic bandwidth, and long-term reliability. Unlike rotary axes, linear axes must convert torque into straight-line motion while resisting thermal drift, contamination, and multi-directional loads without accumulating backlash.

1.1 The Translation Problem

Professional CNC machines must:

1. **Convert rotary to linear motion** with predictable kinematics and minimal lost motion.
2. **Maintain positional accuracy** under variable cutting forces and thermal gradients.
3. **Minimize parasitic errors** such as backlash, hysteresis, and compliance.
4. **Resist disturbances** from process forces, acceleration transients, and environmental vibration.
5. **Operate continuously** with manageable maintenance over multi-year duty cycles.

Balancing these demands forces trade-offs among stiffness, friction, speed capability, cost, and manufacturability. The remainder of this module develops design methodologies for achieving those trade-offs.

1.2 Historical Context and Technology Evolution

- **1940s** - Recirculating ball bearings enable practical rolling-element linear guides.
- **1950s** - Ball screw actuators enter early NC machines.
- **1970s** - Precision profile rails with ground raceways standardize high stiffness.
- **1990s** - High-speed ball screws adopt optimized ball return and surface hardening.
- **2000s** - Direct-drive linear motors gain adoption for high-acceleration stages.
- **2010s+** - Hybrid motion systems combine multiple drive technologies with active compensation.

1.3 Classification of Linear Motion Technologies

- **Screw-Based Drives** - Ball screws, lead screws, planetary roller screws.
- **Rack & Pinion Drives** - Spur or helical racks with pinions and reduction gearboxes.
- **Belt & Cable Drives** - Timing belts (GT2, HTD, AT) or steel cable transmissions.
- **Direct Linear Actuators** - Linear motors, pneumatic/hydraulic cylinders.
- **Guide Rails** - Profile rails, box ways, cylindrical guides, crossed rollers, air bearings.

1.4 Performance Metrics and Selection Criteria

Performance Metric	Typical Specification Range	Primary Determinants
Positioning accuracy	+/-5 µm to +/-0.1 µm	Drive lead accuracy, encoder resolution, thermal stability
Repeatability	+/-2 µm to +/-0.05 µm	Backlash, preload, servo stiffness
Maximum velocity	0.5 m/s to 5 m/s	Critical speed, lead, gearbox ratio
Maximum acceleration	0.5 g to 5 g	Moving mass, actuator force, inertia ratio
Static stiffness	50 N/µm to 500 N/µm	Preload, contact mechanics, structure
Load capacity	100 N to 100 kN	Rolling element rating, gear strength
Thermal sensitivity	5 µm/°C to 0.5 µm/°C	Materials, cooling, compensation

1.5 System-Level Requirements and Design Objectives

Axis level specifications cascade from machine-level goals. Accuracy budgeting often uses the root-sum-square (RSS) approach:

$$\epsilon_{\text{pos}} = \sqrt{\epsilon_{\text{geom}}^2 + \epsilon_{\text{therm}}^2 + \epsilon_{\text{servo}}^2 + \epsilon_{\text{backlash}}^2}$$

To achieve +/-0.025 mm positioning on a gantry axis, backlash should be <0.01 mm, and thermal drift constrained under +/-0.012 mm via compensation.

Native axis resolution derives from drive lead and encoder density:

$$r_{\text{axis}} = \frac{L_{\text{lead}}}{N_{\text{enc}} \cdot N_{\text{gear}}}$$

where L_{lead} is screw/belt pitch, N_{enc} is counts per motor revolution, and N_{gear} is total reduction ratio.

Axis stiffness sets deflection under cutting load:

$$\delta = \frac{F_{\text{axis}}}{k_{\text{axis}}}, \quad \frac{1}{k_{\text{axis}}} = \frac{1}{k_{\text{drive}}} + \frac{1}{k_{\text{bearing}}} + \frac{1}{k_{\text{structure}}}$$

High-precision machining centers target $k_{\text{axis}} \geq 100 \text{ N}/\mu\text{m}$ to keep deflection below 0.01 mm under 1 kN.

Dynamic response must support servo bandwidth. The fundamental natural frequency of the axis mechanism is

$$f_n = \frac{1}{2\pi} \sqrt{\frac{k_{\text{axis}}}{m_{\text{eq}}}}$$

and should exceed five times the servo bandwidth to preserve stability margins.

1.6 Contact Mechanics and Tribology Overview

- **Rolling contacts** (ball screw grooves, profile rail races) rely on Hertzian contact theory to predict stress and deflection.
- **Sliding contacts** (lead screw nuts, box ways) require PV (pressure-velocity) analysis to prevent adhesive wear.
- **Mixed lubrication regimes** exist wherever preload increases contact stress; grease or oil selection must support elastohydrodynamic films.
- **Contamination control** via scrapers, wipers, bellows, or positive-pressure enclosures is essential for life expectancy.

1.7 Application-Specific Requirements by Machine Type

Linear motion system specifications vary dramatically across CNC machine classes, driven by accuracy, speed, load capacity, and cost constraints:

Precision Machining Centers (Vertical Mills, Horizontal Mills): - Positioning accuracy: +/- 0.002-0.010 mm (+/-2-10 μm) - Repeatability: +/- 0.001-0.005 mm - Axis stiffness: 100-300 N/ μm (minimize deflection under 5-20 kN cutting forces) - Travel length: 500-2,000 mm (X/Y axes), 300-800 mm (Z-axis) - Speed: 15-40 m/min rapids, 0.5-8 m/min cutting feeds - Technology: Ground ball screws (ISO Grade 3-5), precision profile rails (accuracy class H or P) - Cost: \$2,000-15,000 per axis depending on travel length and preload class

High-Speed Routers and Gantry Systems: - Positioning accuracy: +/- 0.025-0.100 mm (adequate for wood, plastics, aluminum) - Repeatability: +/- 0.010-0.050 mm - Axis stiffness: 50-150 N/ μm (lower cutting forces enable compliance) - Travel length: 1,000-3,000 mm (X/Y), 150-300

mm (Z) - Speed: 30-100 m/min rapids (emphasis on throughput, cycle time reduction) - Technology: Rolled ball screws or rack & pinion (helical racks for X/Y gantry >2 m), belt drives for Z-axis - Cost: \$800-4,000 per axis (economies of scale for gantry beam fabrication)

Plasma and Waterjet Cutters: - Positioning accuracy: +/-0.050-0.200 mm (kerf width 0.8-3.0 mm dominates tolerance) - Repeatability: +/-0.025-0.100 mm - Axis stiffness: 20-80 N/µm (process forces 50-500 N, minimal deflection impact) - Travel length: 2,000-6,000 mm (X/Y gantry for 1.5 x 3 m to 2 x 6 m tables) - Speed: 10-30 m/min cutting, 40-80 m/min rapids - Technology: Rack & pinion (module 2-4 spur or helical, dual-pinion anti-backlash), linear profile rails - Cost: \$3,000-12,000 per axis (long travel dominates cost, rack segments \$150-400/m)

Laser Cutting and Engraving (CO₂, Fiber, Diode): - Positioning accuracy: +/-0.010-0.050 mm (fiber laser spot diameter 25-150 µm, CO₂ 150-400 µm) - Repeatability: +/-0.005-0.025 mm (vector engraving reveals backlash as corner rounding) - Axis stiffness: 30-100 N/µm (reaction forces minimal, but deceleration loads 500-2,000 N from lightweight gantry at 2-5 g) - Travel length: 600-1,500 mm (desktop CO₂), 1,000-3,000 mm (industrial fiber) - Speed: 50-300 m/min rapids (CoreXY/H-bot kinematics enable 1-5 g acceleration) - Technology: GT2/HTD timing belts (steel-reinforced or aramid core), cylindrical linear guides or V-slot extrusions - Cost: \$400-2,500 per axis (belt drives lowest cost, dual-belt preload adds \$200-400)

Large-Format FDM 3D Printers (Module 11 Integration): - Positioning accuracy: +/-0.050-0.200 mm (layer adhesion and extrusion width 0.4-1.0 mm dominate dimensional tolerance) - Repeatability: +/-0.020-0.100 mm (Z-layer registration critical, XY less sensitive) - Axis stiffness: 20-60 N/µm (process forces <50 N, but vibration causes ringing artifacts) - Travel length: 300-1,000 mm (build volume cube or rectangular prism) - Speed: 80-300 mm/s printing, 150-400 mm/s travel moves - Technology: GT2 belts (CoreXY for XY speed, belt drive for X/Y, lead screw or ball screw for Z-axis), linear rods or MGN rails - Cost: \$150-1,200 per axis (hobbyist to professional-grade, cost scales with build volume)

1.8 Technology Trade-Off Matrix

Selection among drive technologies involves multi-dimensional trade-offs. The table below quantifies typical performance boundaries guiding preliminary technology selection before detailed analysis (Sections 2-6):

	Travel Length	Load Capacity		Efficiency	Cost/Meter	Typical Applications
Technology		Accuracy	Speed			
Ball Screw	0.3-3.0 m	+/- 0.005-0.020 mm	0.3-1.0 m/s	5-50 kN	90-96%	\$500-3,000
		+/- 0.020 mm				Mills, lathes, precision routers
		+/- 0.05-0.100 mm				
Lead Screw	0.2-1.5 m	+/- 0.025-0.100 mm	0.05-0.3 m/s	1-10 kN	20-40%	\$100-600
		+/- 0.05 mm				Manual mills, Z-axis, vertical lifts
		+/- 0.100 mm				
Rack & Pinion	2-50 m	+/- 0.030-0.150 mm	0.5-2.0 m/s	10-100 kN	85-95%	\$150-500
		+/- 0.150 mm				Gantry routers, plasma, waterjet
		+/- 0.200 mm				

Technology	Travel Length	Load Capacity			Efficiency	Cost/Meter	Typical Applications
		Accuracy	Speed				
Timing Belt	0.5-6 m	+/- 0.030-0.150 mm	1.0-5.0 m/s	0.5-5 kN	95-98%	\$50-300	Laser cutters, FDM printers, pick-place
Linear Motor	0.5-10 m	+/- 0.001-0.010 mm	2.0-10 m/s	0.5-20 kN	70-85%	\$2,000-10,000	Semiconductor, PCB drill, high-speed inspection

Key observations: - Ball screws dominate 0.3-2 m range where +/-0.010 mm accuracy required and travel <3 m avoids critical speed limits - Racks enable long travel (3-50 m) at moderate accuracy (+/-0.050-0.150 mm) for plasma/waterjet/router gantries - Belts provide highest speed/cost ratio for applications tolerating +/-0.050 mm or using linear encoders (closing position loop on table, not motor) - Lead screws retain niche for vertical Z-axes requiring fail-safe (self-locking when $\lambda < \arctan(\mu)$, typically $\lambda < 5^\circ$) - Linear motors excel in specialized high-speed applications but cost 5-20x alternative technologies

1.9 Module Roadmap and Section Integration

Module 3 systematically builds linear motion expertise through nine sections, progressing from individual component technologies (Sections 2-6) through universal system requirements (Section 7), practical alignment and maintenance (Section 8), and synthesis with decision frameworks (Section 9):

Section 2 - Ball Screws: Detailed analysis of recirculating ball screw mechanics including critical speed limits (whip resonance $n_{cr} \propto d_r/L^2$), Euler buckling under compressive loads, preload strategies (2-13% of C_a via double-nut or oversized balls), Hertzian contact stiffness, ISO 3408 life ratings, thermal expansion compensation, and specification selection balancing accuracy (ground vs. rolled), lead (5-20 mm), and diameter (16-63 mm). Worked examples size screws for representative CNC axes demonstrating critical speed checks, buckling safety factors, and stiffness budgets.

Section 3 - Lead Screws: Analysis of ACME, square, and trapezoidal thread geometries emphasizing self-locking condition ($\lambda < \phi$, where lead angle $\lambda = \arctan(L/\pi d_{mean})$ and friction angle $\phi = \arctan(\mu)$), efficiency penalties (20-40% vs. 90%+ ball screws), PV (pressure \times velocity) limits for nut materials (bronze 0.5-1.5 MPa·m/s, polymer 2-3 MPa·m/s), and vertical axis safety applications. Compares bronze vs. polymer nut trade-offs (bronze higher load but lower PV; polymer lower friction, self-lubricating, but more compliant).

Section 4 - Rack & Pinion: Covers spur and helical rack geometry, AGMA bending stress and contact stress verification (ensuring $\sigma_b < 150-600$ MPa and $\sigma_c < 1,000-1,500$ MPa to prevent tooth breakage and pitting), segment alignment and pitch matching (+/-0.010-0.020 mm segment-to-segment to avoid torque spikes), dual-pinion anti-backlash mechanisms (spring-loaded opposing pinions with 50-200 N preload), and long-axis electronic gantry synchronization (cross-coupling controllers maintaining <0.02 mm racking under asymmetric loads). Worked examples demonstrate gear mesh force calculations and segment alignment tolerance analysis.

Section 5 - Linear Guides: Comprehensive treatment of profile rail bearing systems including ISO 14728-1 life rating ($L_{10} = (C/P)^{3.33} \times 10^6$ mm with load correction factors for hardness, temperature, contamination, lubrication), preload classes (Z0/ZA/ZB/ZC = 1%/2%/5%/8% of static load rating C_0), stiffness modeling via Hertzian contact ($k \propto F^{1/3}$, so doubling preload increases stiffness ~26%), installation tolerances (rail straightness +/-0.015 mm/m, parallelism +/-0.020 mm/m, mounting surface flatness +/-0.010 mm/m), and contamination protection (contact seals, magnetic scrapers, bellows). Compares profile rail types: miniature (MGN7-MGN15, 1-8 kN ratings), standard (HGH15-HGH45, 5-60 kN), heavy (HGW35-HGW65, 30-120 kN).

Section 6 - Belt & Cable Drives: Analysis of timing belt mechanics including tension-stiffness relationship ($k = EA/L$ where effective modulus E and cross-sectional area A depend on reinforcement: steel 200 GPa, aramid 70 GPa, fiberglass 40 GPa), resonance prediction ($f_n = \frac{1}{2L} \sqrt{T/\mu}$ typically 10-30 Hz for 1-3 m spans), pulley tooth engagement (GT2 2 mm pitch, HTD 3/5/8 mm, AT10 10 mm), CoreXY kinematics (decoupling XY motion via dual-belt crossed configuration enabling lightweight print head), thermal expansion (steel $\alpha = +11.5 \times 10^{-6}$ K⁻¹ vs. aramid $\alpha = -2.0 \times 10^{-6}$ K⁻¹ enabling passive compensation with aluminum frame), and dual-belt anti-backlash (opposing belts with differential preload, or single belt with spring-loaded idlers).

Section 7 - Universal Requirements: Establishes four categories of requirements all linear motion systems must satisfy regardless of technology: (1) **Backlash specifications** (measurement per ISO 230-2, targets <=0.005 mm precision machines to <=0.100 mm plasma tables), (2) **Stiffness requirements** (10-200 N/μm depending on application, measured per ASME B5.54, combining drive/guide/coupling/frame stiffnesses in series), (3) **Thermal behavior** (steel $\alpha = 11.5 \times 10^{-6}$ K⁻¹, aluminum 23.6×10^{-6} K⁻¹, active compensation algorithms, environmental control +/-0.2-3°C), (4) **Safety systems** (E-stops, interlocked guards, Z-axis brakes >=120% mass, lock-out/tagout procedures). Provides quantitative specifications enabling technology-agnostic comparison.

Section 8 - Alignment & Maintenance: Practical procedures for initial installation alignment (laser alignment achieving +/-0.010-0.020 mm over 1-3 m, dial indicator techniques, surface preparation via grinding/scraping to +/-0.010 mm/m flatness) and preventive maintenance schedules (lubrication intervals 200-500 hours, inspection procedures for wear/contamination, predictive maintenance via vibration/temperature monitoring, troubleshooting decision trees for common failure modes: premature bearing failure from overload/contamination, backlash growth from nut wear, accuracy drift from thermal effects or encoder damage).

Section 9 - Conclusion: Synthesizes Sections 2-8 via technology selection decision tree (prioritizing travel length □ accuracy □ speed □ load capacity □ safety □ cost), cross-module integration (frame stiffness from Module 1, Z-axis gravity loads from Module 2, servo sizing for Module 4, cutting forces from Modules 5-8), and forward-looking considerations (linear motors, active vibration damping, smart bearings with embedded sensors for condition monitoring, hybrid systems combining multiple drive types with electronic synchronization).

1.10 Notation and Units

Symbol	Description	Units	Typical Range
L_{lead}	Lead per revolution (screw/belt pitch)	mm/rev	5-20
d_s	Screw nominal diameter	mm	16-63
d_r	Screw root diameter (for stress analysis)	mm	12-50
k_{axis}	Effective axis stiffness	N/ μm	10-200
k_{drive}	Drive stiffness (screw, belt, rack)	N/ μm	50-500
k_{bearing}	Linear guide stiffness	N/ μm	100-800
m_{carriage}	Moving mass (gantry + tooling)	kg	5-150
C or C_a	Dynamic load rating (axial for screws, radial for guides)	N	5,000-80,000
C_0	Static load rating	N	10,000-150,000
μ	Coefficient of friction (rolling or sliding)	dimensionless	0.002-0.10
ϵ_{pos}	Positioning error (RSS combination)	mm	0.001-0.200
f_n	Natural frequency (axis or belt resonance)	Hz	10-300
α	Coefficient of thermal expansion	$\mu\text{m}/\text{m}\cdot^{\circ}\text{C}$ or K ⁻¹	11.5 (steel), 23.6 (aluminum)
n_{cr}	Critical rotational speed (screw whip)	rpm	500-5,000

Total: 1,529 words | 4 equations | 0 worked examples | 3 tables

References

Industry Standards

1. **ISO 3408 Series (2006)** - Ball screws - Parts 1-5: Vocabulary, nominal dimensions, acceptance conditions, load ratings, rigidities
2. **ISO 14728 Series (2017)** - Rolling bearings - Linear motion rolling bearings - Parts 1-3: Dynamic load ratings, static load ratings, lubrication
3. **ISO 230-2:2014** - Test code for machine tools - Part 2: Determination of accuracy and repeatability of positioning
4. **ASME B5.54-2005 (R2019)** - Methods for Performance Evaluation of Computer Numerically Controlled Machining Centers
5. **AGMA 2001-D04** - Fundamental Rating Factors and Calculation Methods for Involute Spur and Helical Gear Teeth (for rack and pinion systems)

Academic and Professional Engineering References

6. **Slocum, A.H. (1992).** *Precision Machine Design*. Englewood Cliffs, NJ: Prentice Hall. ISBN: 978-0-13-690918-7
 - Comprehensive reference on precision mechanical systems: kinematic couplings, bearing systems, thermal management, alignment procedures
7. **Budynas, R.G. & Nisbett, J.K. (2020).** *Shigley's Mechanical Engineering Design* (11th ed.). New York: McGraw-Hill Education. ISBN: 978-0-07-339820-4
 - Chapters 11 (screws), 13-14 (gears), 16 (rolling bearings) covering fundamental mechanical component design
8. **Norton, R.L. (2020).** *Machine Design: An Integrated Approach* (6th ed.). Hoboken, NJ: Pearson. ISBN: 978-0-13-481834-4
 - Machine design methodology, power screws, gears, bearings with comprehensive worked examples
9. **Juvinal, R.C. & Marshek, K.M. (2020).** *Fundamentals of Machine Component Design* (6th ed.). Hoboken, NJ: Wiley. ISBN: 978-1-119-32176-9
 - Foundational mechanical design covering screws, gears, rolling bearings with stress analysis and life prediction

Cross-Module Integration References

10. **Modules 1-2** - Machine frame design, structural stiffness analysis, Z-axis gravity compensation (covered in course Module 1: Mechanical Frame and Module 2: Vertical Axis)
 11. **Module 4** - Servo motor sizing, encoder selection, control bandwidth limitations (covered in course Module 4: Motion Control Systems)
 12. **Modules 5-8** - Process-specific cutting forces and accuracy requirements: Module 5 (Milling), Module 6 (Turning), Module 7 (Fiber Laser), Module 8 (Waterjet)
 13. **Module 11** - Large-format FDM 3D printer motion systems case study integrating belt drives, linear guides, and thermal management
-

Module 3 - Linear Motion Systems

2. Ball Screws

2.1 Operating Principles and Construction

Ball screws employ hardened steel balls recirculating within helical grooves cut into a screw shaft and nut. Rolling contact yields efficiencies >90% and allows aggressive preload to remove backlash. Precision ground screws offer ISO Grade 3 accuracy (+/-8 µm/300 mm), while rolled screws achieve +/-50 µm/300 mm for cost-sensitive machines.

2.2 Kinematic Resolution and Servo Interface

Linear resolution depends on screw lead and encoder density. For a 10 mm lead screw coupled directly to a 20 000 count/rev encoder:

$$r_{\text{axis}} = \frac{10}{20\,000} = 0.0005 \text{ mm per count}$$

Servo tuning must ensure command updates remain below the mechanical resolution to avoid quantization-induced limit cycles. Gear reductions increase torque and resolution but reduce maximum linear speed.

2.3 Critical Speed and Buckling Limits

The critical speed for screw whipping is

$$n_{\text{cr}} = \frac{4.76 \times 10^6 k d_s}{L^2}$$

with d_s in millimeters, L the free length, and k the end-fixity factor (0.25 fixed-free, 1.0 fixed-supported, 1.36 fixed-fixed). Compressive loading requires Euler buckling verification:

$$F_{\text{cr}} = \frac{\pi^2 EI}{(K_e L)^2}$$

where $I = \frac{\pi d_r^4}{64}$ (use root diameter d_r) and K_e is the effective length factor (fixed-free $K_e = 2.0$, pinned-pinned $K_e = 1.0$, fixed-pinned $K_e \approx 0.70$, fixed-fixed $K_e = 0.50$). Applying a safety factor of 2-3 prevents catastrophic failure under crash loads.

2.4 Axial Stiffness and Preload Strategies

The axial stiffness of a preloaded ball screw is

$$k_{\text{drive}} = \frac{C_a}{\delta_{\text{allow}}}$$

where δ_{allow} is the allowable elastic deflection at the dynamic load rating. Double-nut systems apply differential preload to eliminate backlash; single-nut designs use oversized balls or offset pitch sections. Typical preload classes (ISO P0-P5) correspond to 2%, 5%, 8%, or 13% of dynamic load rating. Excess preload raises friction and temperature, so designers target 3-5% for continuous-duty axes.

2.5 Thermal Behavior and Compensation

Frictional heating lengthens the screw, introducing positional drift. Thermal growth can be estimated via

$$\Delta L = \alpha L_0 \Delta T$$

with $\alpha \approx 11 \times 10^{-6} /^\circ\text{C}$ for steel. Mitigation options include locating the fixed bearing near the motor, using dual temperature sensors with software compensation, or implementing liquid-cooling jackets on high-duty screws.

2.6 Worked Example - High-Speed Gantry Axis

Given: 2.0 m travel, 25 mm screw diameter, 10 mm lead, fixed-supported mounting ($k = 0.57$), axis mass 45 kg, maximum feed 25 m/min.

1. Critical speed check

$$n_{\text{cr}} = \frac{4.76 \times 10^6 \cdot 0.57 \cdot 25}{2000^2} \approx 1700 \text{ rpm}$$

Required rotational speed for 25 m/min is $N = \frac{25000}{10} = 2500 \text{ rpm}$ \square unacceptable.
Solution: increase lead to 20 mm or use dual-screw drive.

2. Buckling load (fixed-pinned approximation $K_e = 0.70$; 25 mm screw with root diameter $d_r \approx 20 \text{ mm}$ so $I = \pi d_r^4 / 64 = 7.85 \times 10^{-9} \text{ m}^4$)

$$F_{\text{cr}} = \frac{\pi^2 (210 \text{ GPa}) (7.85 \times 10^{-9} \text{ m}^4)}{(0.70 \times 2 \text{ m})^2} \approx 8.3 \times 10^3 \text{ N}$$

With 2x safety, allowable compressive load $\approx 4.1 \text{ kN}$.

3. Stiffness

If preload equals 5% of C_a and $\delta_{\text{allow}} = 0.01 \text{ mm}$, then $k_{\text{drive}} \approx 500 \text{ N}/\mu\text{m}$. Combined with bearing and structure results in overall stiffness near 120 N/ μm , adequate for router-class machining.

2.7 Specification Snapshot

Parameter	Typical Ball Screw Value	Design Considerations
Lead accuracy	$\pm 8 \mu\text{m}/300 \text{ mm}$ (ground)	Thermal growth management
Efficiency	0.90–0.96	Increases with larger lead
Preload class	3–5% of C_a	Balances stiffness and heat
Lubrication	Grease (centralized) or oil-air	Interval 8–24 hours
Seal options	Contact wipers, labyrinth	Match environment severity

2.8 Contact Mechanics and Tribology Fundamentals

Reliable ball screw operation depends on engineered contact interfaces that balance load capacity with low friction. This section develops the analytical foundation for understanding rolling element bearings, deriving Hertzian contact stress for ball-on-raceway interfaces, modeling lubrication regimes from boundary to elastohydrodynamic, predicting bearing fatigue life using ISO standards, and quantifying how surface finish, lubrication viscosity, and preload influence stiffness and longevity.

2.8.1 Hertzian Contact Theory for Rolling Elements Point Contact: Ball on Raceway

When a spherical ball of radius R presses against a flat raceway with normal force F_n , the elastic deformation creates a circular contact patch. Hertz (1881) derived the contact radius and pressure distribution for linearly elastic, homogeneous, isotropic materials.

Contact Radius:

$$a = \left(\frac{3F_n R}{4E^*} \right)^{1/3}$$

where the effective elastic modulus E^* combines the properties of both contacting materials:

$$\frac{1}{E^*} = \frac{1 - \nu_1^2}{E_1} + \frac{1 - \nu_2^2}{E_2}$$

For steel-on-steel ($E_1 = E_2 = 200$ GPa, $\nu_1 = \nu_2 = 0.3$):

$$E^* = \frac{E}{1 - \nu^2} = \frac{200 \times 10^9}{1 - 0.09} = 2.198 \times 10^{11} \text{ Pa}$$

Maximum Contact Pressure (at center of contact patch):

$$p_{\max} = \frac{3F_n}{2\pi a^2}$$

Combining the expressions:

$$p_{\max} = \left(\frac{6F_n E^{*2}}{\pi^3 R^2} \right)^{1/3}$$

2.8.2 Worked Example: Ball Screw Contact Stress Given: - Ball diameter: $d_{ball} = 6.35$ mm (1/4", common in SFU1605) - Ball radius: $R = 3.175$ mm = 0.003175 m - Load per ball: $F_n = 400$ N (typical with 4 active balls, 1600 N total thrust) - Material: Steel, $E^* = 2.198 \times 10^{11}$ Pa

Calculate: Contact patch radius and maximum pressure

Solution:

Step 1: Contact radius

$$a = \left(\frac{3 \times 400 \times 0.003175}{4 \times 2.198 \times 10^{11}} \right)^{1/3}$$

$$a = \left(\frac{3.81}{8.792 \times 10^{11}} \right)^{1/3} = (4.334 \times 10^{-12})^{1/3} = 1.630 \times 10^{-4} \text{ m} = 0.163 \text{ mm}$$

Step 2: Maximum pressure

$$p_{\max} = \frac{3 \times 400}{2\pi(1.630 \times 10^{-4})^2} = \frac{1200}{1.668 \times 10^{-7}} = 7.19 \times 10^9 \text{ Pa} = 7.19 \text{ GPa}$$

Result Interpretation and Correction: - Contact patch diameter: $2a \approx 0.33$ mm (very small, concentrated contact) - The computed 7.19 GPa exceeds recommended limits for hardened bearing steel. Practical design guidance targets $p_{\max} \lesssim 3.0$ GPa for 60-62 HRC to ensure robust

rolling-contact fatigue life. - Therefore, the initial assumption (400 N per ball with 6.35 mm balls) is overly aggressive. Reduce per-ball load and/or increase ball diameter, or change preload strategy.

Corrective Design Options: - Reduce per-ball load by increasing the number of simultaneously load-carrying balls (more contacts in the load zone) and moderating preload. - Increase ball diameter (larger radius lowers contact pressure as $p_{\max} \propto R^{-2/3}$). - Use a double-nut with lower preload per nut, or switch to planetary roller screw for very high loads.

Recalculated Example (Compliant Design): - Choose ball diameter 9.525 mm (3/8", $R = 4.7625$ mm) and design for per-ball normal load $F_n = 60$ N (via increased loaded balls and moderated preload). - Using the same formula:

$$p_{\max} = \left(\frac{6F_n E^{*2}}{\pi^3 R^2} \right)^{1/3} \approx 2.9 \text{ GPa}$$

- This satisfies the ≤ 3 GPa guideline and significantly improves rolling-contact fatigue margin.

Dimensional Verification:

$$[p_{\max}] = \frac{N}{m^2} = Pa \quad \checkmark$$

$$[a] = \left(\frac{N \cdot m}{Pa} \right)^{1/3} = \left(\frac{N \cdot m}{N/m^2} \right)^{1/3} = (m^3)^{1/3} = m \quad \checkmark$$

2.8.3 Bearing Life Prediction: ISO 281 Standard Rolling contact fatigue (RCF) arises from repeated Hertzian stress cycles that initiate subsurface cracks, eventually propagating to the surface and causing spalling. The **L10 life** is the operating duration (revolutions or hours) before 10% of a population fails.

Basic Dynamic Load Rating

The **dynamic load rating C** is the constant radial load (for radial bearings) or axial load (for thrust bearings, ball screws) that a bearing can sustain for 1 million revolutions with 90% survival probability.

L10 Life (million revolutions):

$$L_{10} = \left(\frac{C}{P} \right)^p$$

where: - L_{10} = rated life (million revolutions) - C = dynamic load capacity (N), from manufacturer catalog - P = equivalent dynamic load (N), actual operating load - p = exponent: 3 for ball bearings, 10/3 for roller bearings

L10 Life in Operating Hours:

$$L_{10h} = \frac{L_{10} \times 10^6}{60n}$$

where n = rotational speed (rpm)

2.8.4 Worked Example: Ball Screw Life Calculation Given: - Ball screw: SFU1605 (16 mm nominal, 5 mm lead) - Dynamic load rating: $C = 3500$ N (manufacturer spec, e.g., THK or HIWIN catalog) - Operating load: $F_a = 1200$ N (continuous axial thrust from cutting forces) - Operating speed: $n = 1200$ rpm - Load factor: $f_w = 1.3$ (moderate shock, intermittent cutting)

Calculate: L10 life in hours

Solution:

Step 1: Equivalent load with load factor

$$P = F_a \times f_w = 1200 \times 1.3 = 1560 \text{ N}$$

Step 2: L10 life in million revolutions

$$L_{10} = \left(\frac{3500}{1560} \right)^3 = (2.244)^3 = 11.30 \text{ million revolutions}$$

Step 3: Convert to operating hours

$$L_{10h} = \frac{11.30 \times 10^6}{60 \times 1200} = \frac{11.30 \times 10^6}{72000} = 157 \text{ hours}$$

Result Interpretation: - **157 hours** (approximately 1 month of single-shift operation) seems short! - This is because load utilization is high: $P/C = 1560/3500 = 0.446$ (44.6%) - **Guideline:** For long life (>10,000 hours), keep $P/C < 0.15$

Improved Design: Specify larger screw: SFU2005 with $C = 7800$ N

$$\begin{aligned} P &= 1200 \times 1.3 = 1560 \text{ N} \\ L_{10} &= \left(\frac{7800}{1560} \right)^3 = (5.0)^3 = 125 \text{ million rev} \\ L_{10h} &= \frac{125 \times 10^6}{72000} = 1736 \text{ hours } (11\times \text{improvement}) \end{aligned}$$

Further Improvement with Load Reduction: Use counterbalance on vertical axis to reduce gravity load: - Net load: $P = 600 \times 1.3 = 780$ N - $L_{10} = (7800/780)^3 = (10)^3 = 1000$ million rev - $L_{10h} = 13,889$ hours (acceptable for precision CNC)

2.8.5 Friction Modeling Across Lubrication Regimes Friction in linear motion systems varies dramatically with velocity, load, and lubrication quality. The **Stribeck curve** characterizes this behavior.

The Stribeck Curve

Friction coefficient μ depends on the **Sommerfeld number**:

$$S = \frac{\eta v}{P}$$

where: - η = dynamic viscosity (Pa·s) - v = sliding velocity (m/s) - P = contact pressure (Pa)

Three Regimes:

- Boundary Lubrication** (low S): Metal-to-metal contact, $\mu \approx 0.10-0.20$, high wear
- Mixed Lubrication** (intermediate S): Partial fluid film, $\mu \approx 0.05-0.10$, Stribeck effect (friction drops with velocity)
- Hydrodynamic Lubrication** (high S): Full film separation, $\mu \approx 0.001-0.01$, viscous shear only

Stribeck Friction Model:

$$F_{friction} = [F_c + (F_s - F_c)e^{-(v/v_s)^2}] \operatorname{sgn}(v) + Bv$$

where: - F_s = static friction (breakaway force at $v = 0$) - F_c = Coulomb friction (high-speed asymptote) - v_s = Stribeck velocity (transition speed) - B = viscous friction coefficient

Typical Values for Preloaded Ball Screw: - $F_s = 20 \text{ N}$ - $F_c = 8 \text{ N}$ - $v_s = 0.01 \text{ m/s}$ - $B = 40 \text{ N}\cdot\text{s/m}$

Servo Feedforward Compensation:

To reduce tracking error, apply feedforward torque:

$$T_{ff} = \frac{L_{lead}}{2\pi} F_{friction}(v_{cmd})$$

This preemptively counteracts friction, improving contouring accuracy from ~40 μm to <5 μm .

2.8.6 Lubrication System Design Grease Lubrication

Advantages: - Simple, no external pump - Seals in contaminants - Long relubrication intervals (500-2000 hours)

Disadvantages: - Heat dissipation limited - Viscosity changes with temperature - Can migrate or dry out

Grease Selection: - NLGI grade 2 (most common, peanut-butter consistency) - Lithium complex base for wide temperature range (-20°C to +120°C) - EP (extreme pressure) additives for boundary lubrication

Oil-Air Lubrication

Principle: Compressed air (4-6 bar) carries atomized oil droplets to bearing contacts.

Advantages: - Minimal oil consumption (0.01-0.05 mL/hour per bearing) - Excellent cooling (continuous air flow removes heat) - Prevents contamination buildup - Suitable for high-speed operation (>5000 rpm)

System Components: - Oil reservoir and metering pump - Air-oil mixing valve - Distribution manifold to each bearing - Drain collection (oil collects after passing through bearing)

Typical Flow Rate:

$$Q_{oil} = 0.02 \text{ mL/h per bearing contact}$$

For a ball screw with 2 support bearings and 1 ballnut (3 total): $Q_{total} = 0.06 \text{ mL/h}$

Minimum Film Thickness (Hamrock-Dowson Equation)

For point contact (ball on raceway):

$$h_{min} = 3.63 \frac{R\alpha^{0.6}(UE^*)^{0.68}}{W^{0.073}}$$

where: - R = ball radius (m) - α = pressure-viscosity coefficient (m^2/N), $\sim 1.5 \times 10^{-8}$ for mineral oil - $U = \eta_0 v$ = speed parameter ($Pa \cdot m/s$) - η_0 = ambient pressure dynamic viscosity ($Pa \cdot s$) - $W = F_n/(E^* R^2)$ = load parameter (dimensionless)

Film Thickness Ratio:

$$\lambda = \frac{h_{min}}{R_q}$$

where R_q = RMS surface roughness (typically 0.1-0.4 μm for ground raceways)

Classification: - $\lambda < 1$: Boundary lubrication (asperity contact) - $1 < \lambda < 3$: Mixed lubrication - $\lambda > 3$: Full-film hydrodynamic lubrication

Design Goal: Maintain $\lambda > 3$ during normal operation to maximize life.

2.8.7 Contamination Effects and Seal Selection Contaminants (chips, dust, coolant) cause abrasive wear and surface pitting, dramatically reducing bearing life.

Life Reduction Factor:

$$a_{ISO} = 0.1 \text{ to } 1.0$$

where 1.0 = perfectly clean, 0.1 = severely contaminated

Modified Life:

$$L_{10,clean} = a_{ISO} \times L_{10}$$

Example: A ball screw with calculated $L_{10h} = 5000$ hours in a dirty plasma cutting environment ($a_{ISO} = 0.3$) has actual life:

$$L_{10,actual} = 0.3 \times 5000 = 1500 \text{ hours}$$

Seal Types:

Seal Type	Contamination Protection	Friction Penalty	Application
Felt wipers	Moderate	Low	Light dust, general CNC
Labyrinth seals	Good	Very low	High speed, minimal contact
Contact lip seals	Excellent	Moderate	Plasma, waterjet, heavy chips
Bellows/boots	Excellent	None	Complete enclosure, vertical axes

Seal Type	Contamination Protection	Friction Penalty	Application
Positive pressure	Excellent	None	Clean air purge keeps dust out

2.8.8 Worked Example: Bearing Life with Contamination **Given:** - Ball screw: SFU2005, $C = 7800 \text{ N}$ - Operating load: $P = 1000 \text{ N}$ - Speed: $n = 1000 \text{ rpm}$ - Environment: Plasma cutting table, heavy metal dust - Contamination factor: $a_{ISO} = 0.25$

Calculate: Actual service life

Solution:

Step 1: Ideal L10 life

$$L_{10} = \left(\frac{7800}{1000} \right)^3 = (7.8)^3 = 474.6 \text{ million rev}$$

$$L_{10h,clean} = \frac{474.6 \times 10^6}{60 \times 1000} = 7910 \text{ hours}$$

Step 2: Apply contamination factor

$$L_{10h,actual} = 0.25 \times 7910 = 1978 \text{ hours}$$

Result: Expect ball screw replacement every ~2000 hours (approx. 1 year of single-shift operation)

Mitigation: - Install contact lip seals at ballnut: a_{ISO} improves to 0.6 \square Life = 4746 hours - Add bellows enclosure: a_{ISO} improves to 0.9 \square Life = 7119 hours

2.8.9 Summary: Contact Mechanics Design Principles

Design Objective	Analytical Tool	Target Metric
Prevent surface yield	Hertzian contact stress	$p_{max} < 0.9 \times p_{yield,hardened}$ (~3 GPa for 60 HRC steel)
Ensure adequate life	ISO 281 L10 calculation	$P/C < 0.15$ for >10,000 hour life
Minimize friction variability	Stribeck curve analysis	Operate in hydrodynamic regime ($\lambda > 3$)
Optimize lubrication	Film thickness prediction	Maintain $h_{min} > 3R_q$
Protect from contamination	Seal selection + life factor	$a_{ISO} > 0.6$ with appropriate seals

Cross-Reference to Other Modules: - **Module 1 (Mechanical Frame):** Contact mechanics informs rail mounting flatness requirements to avoid edge loading - **Module 2 (Vertical Axis):** Bearing life calculations guide counterbalance design to reduce gravity loads - **Module 4 (Control Electronics):** Friction models enable feedforward compensation for improved servo tracking

2.9 Servo Integration and Feedforward Control

Effective ball screw utilization demands servo dynamics that complement mechanical stiffness. The reflected inertia of the linear payload is

$$J_{\text{ref}} = \frac{m_{\text{carriage}} L_{\text{lead}}^2}{(2\pi)^2}$$

and should remain within a 1:1-5:1 ratio relative to the servo rotor inertia J_m to maintain adequate phase margin. The total torque required from the motor combines inertial, frictional, and process loads with screw efficiency η :

$$T_{\text{req}} = \frac{L_{\text{lead}}}{2\pi\eta} (m_{\text{carriage}}a + F_{\text{friction}} + F_{\text{process}})$$

where F_{friction} is drawn from the Stribeck model and F_{process} includes cutting or tooling forces.

Servo feedforward terms further reduce tracking error. The position command $x(t)$ converts to motor angle $\theta(t)$ via $\theta = \frac{2\pi}{L_{\text{lead}}}x$. Velocity and acceleration feedforward components become

$$\dot{\theta}_{\text{ff}} = \frac{2\pi}{L_{\text{lead}}} \dot{x}, \quad T_{\text{ff}} = J_{\text{eq}} \frac{2\pi}{L_{\text{lead}}} \ddot{x} + \frac{L_{\text{lead}}}{2\pi\eta} F_{\text{friction}}(\dot{x})$$

with $J_{\text{eq}} = J_m + J_{\text{ref}}$. Implementing these terms enables contouring errors below 5 μm on well-preloaded screws.

Worked Example - Servo Sizing and Feedforward Given: 750 W servo ($J_m = 1.4 \times 10^{-3}$ $\text{kg}\cdot\text{m}^2$) driving a 16 mm lead screw; moving mass 35 kg; target acceleration 2.0 g; Coulomb friction 10 N.

1. Reflected inertia

$$J_{\text{ref}} = \frac{35 \times 0.016^2}{(2\pi)^2} = 7.1 \times 10^{-4} \text{ kg}\cdot\text{m}^2$$

Inertia ratio $J_{\text{ref}}/J_m = 0.51$ (acceptable).

2. Peak torque demand (assume $\eta = 0.92$)

$$T_{\text{req}} = \frac{0.016}{2\pi \times 0.92} (35 \times 2.0 \times 9.81 + 10) \approx 1.9 \text{ N}\cdot\text{m}$$

With efficiency included, a 2.4 N·m continuous servo has margin; higher accelerations will still demand a larger motor.

3. Feedforward torque at 1.6 g

$$T_{\text{ff}} = (1.4 + 0.71) \times 10^{-3} \frac{2\pi}{0.016} \times 15.7 + \frac{0.016}{2\pi} \times 10 = 2.45 \text{ N}\cdot\text{m}$$

Remaining controller effort handles disturbances and compliance.

Proper servo sizing ensures acceleration targets are achievable without overheating, while feed-forward minimizes steady-state error caused by friction and inertia mismatch.

2.10 Dual-Drive Synchronization for Gantry Axes

Long gantries often employ twin ball screws with independent servos to prevent torsional windup. Design steps include:

1. **Mechanical alignment:** Establish datum blocks at each end; phase screws within +/-0.05° before closing the loop.
2. **Electronic gearing:** Designate a master servo and command the slave to track master position while regulating cross-coupled error $e_c = x_L - x_R$.
3. **Racking stiffness verification:** The gantry torsional stiffness k_{torsion} links differential displacement Δx to tool-tip error:

$$\theta = \frac{\Delta x}{2L_g}, \quad \delta_{\text{tool}} = \theta \cdot L_{\text{tool}}$$

Maintaining $\delta_{\text{tool}} < 0.02$ mm with $L_g = 2.5$ m and $L_{\text{tool}} = 0.4$ m demands $\Delta x < 6.4$ μm.

Worked Example - Cross-Coupled Error Budget **Given:** Gantry width 2.2 m, torsional stiffness 1.8×10^5 N·mm/rad, maximum differential thrust 250 N.

1. Racking torque $M = FL_g/2 = 275\,000$ N·mm.
2. Angular twist $\theta = M/k_{\text{torsion}} = 1.53$ mrad.
3. Tool-tip error at 350 mm offset: $\delta = 0.535$ mm (unacceptable).
4. Required cross-coupled suppression: reduce Δx to 5 μm via high-gain synchronization and periodic orthogonality calibration.

Recommended practice:

- Run a synchronization routine after homing that sweeps the gantry length while recording linear scale feedback.
- Apply adaptive feedforward to balance torque between servos; alarm if current mismatch exceeds 15%.
- Inspect for differential wear quarterly by measuring ball screw backlash on each side; re-preload nuts if difference exceeds 0.01 mm.

2.11 Comparative Selection Matrix

Screw Size	Lead (mm)	Max Practical Speed (rpm)	Critical Length (fixed-fixed) (mm)	Axial Stiffness @ 5% C_a (N/ μ m)	Typical Cost (USD)	Representative Application
Ø16 C7	5	2 000	1 250	220	180	Compact Z-axes, benchtop routers
Ø20 C5	10	3 000	1 800	310	420	Medium X/Y axes <=1.5 m travel
Ø25 C5	10	2 600	2 200	420	520	Fabrication gantries, plasma tables
Ø32 C5	20	2 200	2 800	510	860	Dual-drive routers, woodworking cells
Ø40 C3	20	1 800	3 400	640	1 350	Precision machining centers, heavy Z

Guidelines: - Select Ø25/Ø32 screws for travel >2 m to balance stiffness and critical speed.
 - Favor C5 ground screws when positioning tolerance must stay within +/-12 μ m/m.
 - Upgrade to C3 ground screws when integrating linear scales and thermal compensation.

2.12 Case Study - Heavy Vertical Axis Retrofit

Objective: Retrofit a vertical machining center with a 400 kg spindle head while achieving 4 m/min feed and safe power-loss holding.

1. **Screw choice:** Ø40, 12 mm lead double-nut screw, $C_a = 20\ 300$ N.
2. **Load management:** Counterbalance system (gas spring + brake) reduces net moving load to 150 N; preload 5% C_a maintains backlash-free operation.
3. **Critical speed:** For 1.2 m span, fixed-fixed:

$$n_{cr} = \frac{4.76 \times 10^6 \times 1.36 \times 40}{1200^2} = 1\ 800 \text{ rpm}$$

Command speed 333 rpm \square safe margin.

4. **Buckling:** Euler load > 110 kN; with safety factor 3, allowable 37 kN still far above operating load.

5. **Servo sizing:** Required torque at 1.0 g acceleration

$$T = \frac{0.012}{2\pi} (400 \times 9.81 + 150) = 7.6 \text{ N}\cdot\text{m}$$

Select 2.5 kW servo (11 N·m continuous) with normally-on brake.

6. **Thermal strategy:** Circulate cooled oil through hollow screw to limit temperature rise to 8°C
 □ thermal growth $\Delta L = 0.38$ mm, compensated via linear scale feedback.

Result: retrofit meets performance and safety objectives, demonstrating how analytical tools in Section 2 guide real-world upgrades.

2.13 Comparative Technology Assessment

Although ball screws are the default choice for many CNC axes, alternative actuators can deliver superior performance in specific use cases. Table 2-4 benchmarks a high-performance ball screw against a planetary roller screw and an ironless linear motor for a 1.5 m travel axis requiring +/-0.02 mm accuracy.

Attribute	Ball Screw ($\varnothing 32$, 20 mm lead)	Planetary Roller Screw ($\varnothing 25$, 10 mm lead)	Ironless Linear Motor
Continuous thrust (N)	8 000	14 000	7 500
Peak thrust (N)	12 000	22 000	15 000
Max speed (m/min)	80	60	150
Stiffness at 5% preload (N/ μm)	510	680	220 (air bearing)
Efficiency (%)	92	88	100 (no contact)
Thermal drift ($\mu\text{m}/^\circ\text{C}$ over 1.5 m)	13	11	2 (with cooling)
Maintenance interval	1000 h (grease)	600 h (forced oil)	2 000 h (filter change)
Typical system cost (USD)	3 800	6 500	14 000

Attribute	Ball Screw ($\varnothing 32$, 20 mm lead)	Planetary Roller Screw ($\varnothing 25$, 10 mm lead)	Ironless Linear Motor
Best-fit application	General-purpose gantry	Heavy press-feed/drilling	High-speed pick-and-place/laser

Planetary roller screws provide higher stiffness and thrust density by distributing load across multiple line contacts, but the additional rolling elements and recirculation hardware complicate lubrication. Linear motors eliminate backlash and reach extreme speeds, yet they require precision temperature management and sophisticated control hardware.

Worked Example - Throughput vs. Cost Scenario: Compare cycle time and cost per thousand cycles for the three actuators. The axis carries 40 kg, traverses 1.5 m per stroke, and includes a 0.4 s dwell at each end. Motion follows a triangular velocity profile with acceleration limited by available thrust.

1. Acceleration limit

$$a = \frac{F_{\text{cont}}}{m}$$

Ball screw: 200 m/s² (practically limited to 30 m/s² to avoid exciting structure); planetary roller: limit to 45 m/s²; linear motor: limit to 60 m/s².

2. Half-stroke time

$$t_{\frac{1}{2}} = 2\sqrt{\frac{d}{a}}$$

- Ball screw: $t_{\frac{1}{2}} = 0.447$ s
- Planetary roller: $t_{\frac{1}{2}} = 0.365$ s
- Linear motor: $t_{\frac{1}{2}} = 0.316$ s

3. Cycle time including dwell

$$t_{\text{cycle}} = 2t_{\frac{1}{2}} + 0.4$$

- Ball screw: 1.294 s \square 745 cycles/h
- Planetary roller: 1.130 s \square 888 cycles/h
- Linear motor: 1.032 s \square 969 cycles/h

4. Cost per thousand cycles

$$C_{1000} = \frac{\text{System Cost}}{(t_{\text{cycle}}^{-1} \times 1000)}$$

- Ball screw: \$5.10
- Planetary roller: \$7.32

- Linear motor: \$14.45

Interpretation: Linear motors deliver about 30% higher throughput than ball screws but at nearly three times the capital cost per thousand cycles. Planetary roller screws provide a 19% throughput gain with moderate cost increase, making them attractive when thrust density or stiffness, rather than top speed, constrains performance.

2.14 Thermal Compensation and Linear Feedback Integration

Even with careful mechanical design, temperature gradients along a ball screw introduce elongation errors that can exceed +/-0.02 mm over long travels. Closed-loop compensation uses linear encoders or dual temperature probes to mitigate these effects. The thermal elongation predicted by

$$\Delta L = \alpha L_0 \Delta T$$

can be corrected by applying a temperature-dependent offset to the command position:

$$x_{\text{comp}} = x_{\text{cmd}} - \alpha L_0 (T_{\text{screw}} - T_{\text{datum}})$$

where T_{datum} is the reference temperature recorded during calibration.

When linear scales are installed, the numerical controller combines rotary encoder data with direct position feedback. The blended position error is

$$e_{\text{blend}} = w_e \left(\theta \frac{L_{\text{lead}}}{2\pi} - x_{\text{scale}} \right) + (1 - w_e) e_{\text{servo}}$$

with weighting factor $0 \leq w_e \leq 1$ set according to scale resolution and servo bandwidth.

Worked Example - Dual Temperature Probe Compensation Given: 1.8 m axis, steel screw ($\alpha = 11 \times 10^{-6} /^{\circ}\text{C}$), fixed bearing at motor end, temperature sensors show $T_{\text{motor}} = 42^{\circ}\text{C}$, $T_{\text{idler}} = 30^{\circ}\text{C}$. Assume linear gradient.

1. Average temperature rise relative to 20°C ambient:

$$\Delta T_{\text{avg}} = \frac{(42 - 20) + (30 - 20)}{2} = 16^{\circ}\text{C}$$

2. Predicted elongation

$$\Delta L = 11 \times 10^{-6} \times 1.8 \times 16 = 0.317 \text{ mm}$$

3. Compensation command

$$x_{\text{comp}} = x_{\text{cmd}} - 0.317 \text{ mm}$$

Installing a 1 μm-resolution linear scale eliminates the need for open-loop temperature compensation; the scale directly senses the thermal drift. However, designers must still manage servo loop stability by blending encoder and scale feedback (typical $w_e = 0.7$ for stiff axes).

- Best Practices:**
- Locate fixed bearing near the heat source (motor) so thermal growth accumulates in the free end.
 - Use hollow screws with forced fluid circulation on high-duty axes.
 - Calibrate temperature-lag constants during machine warm-up and store them in the controller for adaptive compensation.
 - When using linear scales, mount them on thermally stable substructures (granite, Invar) to avoid mirror-image expansion.

2.15 Maintenance Economics and Reliability Planning

Ball screw life ultimately depends on lubrication, contamination control, and preload retention. A preventive maintenance (PM) schedule balances downtime cost with component replacement.

Maintenance Task	Interval	Tools/Consumables	Estimated Downtime	Typical Cost (USD)	Failure Risk if Skipped
Grease replenishment (centralized manifold)	Every 160 operating hours	NLGI-2 grease, manual pump	15 min	8	Accelerated wear, preload loss
Oil-air reservoir refill	Monthly	ISO VG32 oil	10 min	12	Dry running, thermal spikes
Backlash verification	Quarterly	1 µm indicator, 400 N force fixture	30 min	0 (labor only)	Positioning drift, chatter
Seal inspection / replacement	Semiannual	Blade replacement wipers, solvent	45 min	65	Abrasive contamination
Screw-nut preload check	Annual	Torque wrench, strain gauge	90 min	120	Catastrophic nut failure

The total annual maintenance cost for a dual-screw gantry (two axes) is roughly \$1 100 in consumables and labor. Compare this with the \$4 500 price of replacing both screws: timely PM reduces long-term cost by a factor of four and minimizes unscheduled downtime.

Reliability Modeling MTBF (mean time between failures) for a ball screw can be estimated by combining L₁₀ life with PM effectiveness:

$$\text{MTBF} = L_{10h} \times a_{\text{PM}} \times a_{\text{env}}$$

where a_{PM} captures maintenance quality (0.7 for reactive maintenance, 1.2 for proactive) and a_{env} accounts for contamination (0.3-1.0). For the heavy Z-axis retrofit example: $L_{10h} = 7\,100$ h, $a_{\text{PM}} = 1.2$, $a_{\text{env}} = 0.8$ \square $\text{MTBF} \approx 6\,816$ h (~3.5 years at 2 000 h/year).

2.16 Section Summary Checklist

Before finalizing a ball screw axis design, validate the following:

- Backlash limited to $\leq 10 \mu\text{m}$ through appropriate preload class.
- Critical speed margin $\geq 30\%$ above commanded rotational speed.
- Buckling safety factor ≥ 2.5 under worst-case compression.
- Thermal compensation strategy defined (temperature sensors or linear scales).
- Servo inertia ratio between 1:1 and 5:1, with feedforward tuned for friction model.
- Contamination mitigation in place (contact seals, bellows, positive pressure if required).
- Maintenance plan documented with lubrication intervals, inspection methods, and spare inventory.

These checkpoints ensure mechanical, control, and operational considerations remain aligned prior to expanding the remaining sections of Module 3.

2.20 Case Study - Ball Screw vs. Planetary Roller in Heavy Vertical Axis

Objective: Select a drive for a 350 kg vertical load, 0.4 m travel, 3 m/min, requiring high thrust and safety.

Parameter	Ball Screw ($\varnothing 40$, 12 mm)	Planetary Roller ($\varnothing 25$, 10 mm)
C_a / thrust (cont./peak)	20 kN / 35 kN	35 kN / 55 kN
Efficiency η	0.92	0.88
Critical speed margin	High ($n_{cr} \approx 1,800$ rpm; 3 m/min) □ 250 rpm	High (lower rpm)
Axial stiffness (5% C_a)	~ 640 N/ μm	~ 820 N/ μm
Self-locking	No	Yes (with low lead)
Cost (system)	\$	

Torque for 1.0 g accel (ignoring friction for brevity):

$$T = \frac{L_{\text{lead}}}{2\pi\eta}(ma + mg) \approx \frac{0.012}{2\pi \cdot 0.92}(350 \cdot 9.81 + 350 \cdot 9.81) = 14.4 \text{ N}\cdot\text{m}$$

Planetary roller delivers greater stiffness and thrust density, reducing deflection and brake reliance (with low lead, partial self-locking). For a safety-critical heavy Z, the planetary roller wins despite higher cost; otherwise a $\varnothing 40$ ball screw suffices with a robust brake.

2.21 Case Study - Rack Retrofit vs. Dual Ball Screws (Accuracy Focus)

Existing 3.0 m X-axis with module-2 spur rack shows 0.12 mm backlash (compensated). Target is < 0.01 mm bidirectional accuracy for precision milling.

Metric	Rack (existing)	Dual Ø32 Ball Screws
Backlash	0.12 mm	0.006 mm
Static stiffness	48 N/ μm	220 N/ μm
Surface finish (R_a)	1.8-2.5 μm	0.8-1.2 μm
Cycle time	Baseline	-4% (marginal)
Retrofit cost	-	\$9,800

Conclusion: If accuracy/finish is the driver, dual ball screws justify cost; if throughput is primary and 0.05-0.10 mm accuracy is adequate, keep the rack and improve compensation/tensioning.

2.22 Drive Selection Decision Table

Requirement	Recommended Drive	Rationale
Long travel (>2 m), moderate accuracy	Rack & pinion	Unlimited length, good speed, low cost
High accuracy (<+/-0.02 mm), medium thrust	Ball screw	High efficiency, low backlash, good stiffness
Heavy thrust, safety-critical vertical	Planetary roller screw	Highest thrust/stiffness, partial self-locking
Ultra-high speed (>100 m/min)	Linear motor	Zero backlash, highest acceleration
Dirty environment, low cost	Lead screw	Tolerant to contamination, simple

2.17 Screw Lead Error Mapping and Compensation

Manufacturing tolerances introduce periodic and cumulative lead error in ball screws. Mapping and compensation reduce positioning error by measuring the actual screw advance versus command and applying corrections in the controller.

Procedure: 1. Mount a laser interferometer along the axis and home to the machine datum. 2. Command incremental moves (e.g., 10 mm) over the full travel while logging actual vs. commanded position. 3. Generate an error table $e(x)$ at fixed intervals (e.g., 5 mm). 4. Load $e(x)$ into the CNC controller's compensation table; enable interpolation between points. 5. Verify by repeating the measurement; residual error typically drops by 60-90%.

Worked Example: An X-axis with +/-18 μm peak-to-peak lead error over 1.5 m is mapped at 5 mm intervals. After enabling compensation, residual error measured by the laser is +/-5 μm . Combined with the Section 2 thermal strategy (temperature sensors + linear scale blending), total positioning error remains within +/-10 μm across the full travel.

2.17 Support Bearing Selection and Mounting Configurations

The bearing arrangement at each screw end governs axial constraint, critical speed, and stiffness. Table 2-5 summarizes common configurations.

Arrangement	Description	Axial Constraint	Critical-Speed Factor k	Typical Use
Fixed-Floating	Preloaded angular-contact bearing (ACB) pair at drive end + single radial bearing	One direction	0.57	Medium-duty axes <1.5 m where thermal growth dominates
Fixed-Supported	Preloaded ACB pair + duplex ACB with light preload	Bidirectional (compliant)	0.80	High-speed axes needing improved critical-speed margin
Fixed-Fixed	Duplex ACBs at both ends, both preloaded	Bidirectional (rigid)	1.36	Precision machines demanding symmetric stiffness

The equivalent dynamic bearing load is

$$P = XF_r + YF_a$$

with coefficients X , Y defined by contact angle (for 40° ACBs, $X = 0.57$, $Y = 1.04$). Life in hours follows

$$L_{10h} = \frac{(C/P)^p \times 10^6}{60n}$$

where $p = 3$ for ball bearings and n is screw rpm.

Worked Example - Fixed-Fixed Bearing Sizing **Given:** Axial thrust 5 kN, radial load 0.2 kN, speed 2 000 rpm, target life 20 000 h. Compute required bearing rating.

1. Equivalent load

$$P = 0.57 \times 0.2 + 1.04 \times 5.0 = 5.30 \text{ kN}$$

2. Dynamic rating

$$C = P \left(\frac{L_{10h} 60n}{10^6} \right)^{1/3} = 5.30(2.4) = 12.7 \text{ kN}$$

3. Selection - Duplex 7005C bearings ($C = 13.5$ kN) satisfy the requirement. The fixed-fixed layout raises the critical-speed factor to $k = 1.36$, increasing allowable rpm by 138% versus fixed-floating. When both ends are fixed, pre-stretch the screw during assembly to absorb thermal growth.

2.18 Installation and Alignment Workflow

Consistent results require a structured alignment process:

1. **Prepare datums** - Scrape or grind bearing seats/nut pads to $\leq 10 \mu\text{m}$ flatness per metre.
2. **Install fixed support** - Bolt and dowel the fixed-end housing; verify squareness to the rail datum within 0.02 mm.
3. **Assemble nut and screw** - Maintain cleanliness; avoid losing preload balls.
4. **Fit floating support** - Leave bolts snug to permit axial self-alignment.
5. **Align screw** - Rotate while gauging runout; shim until mid-span TIR $< 0.02 \text{ mm}$.
6. **Couple motor** - Torque flexible coupling fasteners while monitoring end-play.
7. **Run-in** - Operate at 10% speed for 15 min, ramping to full speed; ensure temperature rise $< 15^\circ\text{C}$ and current draw within spec.
8. **Lock & document** - Final torque floating support, record backlash/stiffness/encoder offsets for maintenance baselines.

2.19 Retrofit Case Study - Dual Ball Screws vs. Rack & Pinion

Metric	Rack & Pinion (Existing)	Dual Ø32 Ball Screws
Backlash (compensated)	0.12 mm	0.006 mm
Static stiffness (N/ μm)	48	220
Achievable acceleration (m/s^2)	18	28
Maintenance interval	200 h lubrication	1 000 h lubrication
Annual maintenance cost	\$1 400	\$900
Retrofit hardware cost	–	\$9 800
Scrap rate	3.0%	0.8%
Throughput change	Baseline	+12%

With 2 400 operating hours per year and average part value \$80, scrap reduction saves \$4 224 annually. Throughput gains add \$11 500, totalling \$15 724/year. Simple payback on the \$9 800 retrofit is about 7.5 months, in addition to qualitative improvements (surface finish, acoustic noise, servo tuning window).

2.23 Key Takeaways and Ball Screw Selection Synthesis

Key Takeaways:

1. **Critical speed limits** via whipping resonance $n_{\text{cr}} = \frac{4.76 \times 10^6 k d_r}{L^2}$ constrain maximum rotational speed—example: 25 mm diameter screw over 2 m span (fixed-supported $k = 0.57$) limits to 1,700 rpm requiring lead increase or dual-screw configuration for high-speed axes; Euler buckling $F_{\text{cr}} = \frac{\pi^2 EI}{(K_e L)^2}$ sets compressive load safety factor 2-3× preventing catastrophic failure under crash loads or vertical axis gravity preload
2. **Preload selection** balancing stiffness against life—ISO preload classes P0-P5 (2-13% of dynamic rating C) with typical 3-5% for continuous duty providing $k_{\text{drive}} = 100\text{-}300 \text{ N}/\mu\text{m}$ via Hertzian contact stiffness ($k \propto F^{1/3}$); double-nut configurations (differential or offset

pitch) eliminate backlash to <0.005 mm enabling +/-0.002-0.010 mm positioning accuracy for precision machining centers; excess preload >8% increases friction torque 30-60% and reduces L_{10} life by 40-60%

3. **ISO 3408 life rating** $L_{10} = \left(\frac{C}{P}\right)^3 \times 10^6$ revolutions predicts 90% survival probability under equivalent axial load P (including radial and moment loads via load factors $f_w = 1.5\text{-}2.5$ for standard mounting); hardness correction f_H (0.6-1.0 for softer materials), contamination factor f_C (0.3-1.0 for harsh environments), and temperature derating f_T (<1.0 above 100°C) adjust nominal rating—example: $C = 30$ kN screw under 5 kN axial load achieves $L_{10} = 216 \times 10^6$ revolutions = 18,000 hours at 200 rpm
4. **Thermal expansion compensation** critical for long axes—steel screws grow 11.5 $\mu\text{m}/\text{m}\cdot^\circ\text{C}$ causing +/-23 μm positioning error over 2 m axis with +/-10°C ambient swing; mitigation strategies: (1) locate fixed bearing near motor centralizing growth, (2) dual RTD sensors (+/-0.5°C accuracy) enabling software correction $x_{\text{corrected}} = x_{\text{cmd}} \times [1 + \alpha(T - T_{\text{ref}})]$ reducing error to <10 μm , (3) liquid cooling jackets for high-duty screws maintaining <5°C temperature rise, (4) lead error mapping compensating manufacturing tolerances (+/-8-50 μm peak-to-peak) by 60-90% via controller compensation tables
5. **Ground vs rolled screws** trading accuracy against cost—ground screws (ISO Grade 3-5: +/-8-16 $\mu\text{m}/300$ mm lead accuracy) cost \$800-5,000 for 16-40 mm diameter enabling precision machining applications, rolled screws (+/-50-100 $\mu\text{m}/300$ mm) cost \$200-1,500 adequate for routers/plasma where tolerance +/-0.025-0.100 mm; ground screws require through-hardened alloy steel (58-62 HRC) with precision lapping achieving Ra 0.2-0.4 μm raceway finish, rolled screws cold-form threads strain-hardening surface (45-55 HRC) with Ra 0.8-1.6 μm
6. **Efficiency advantages** of 90-96% (vs 20-40% lead screws) reducing motor torque and heat generation—example: 5 kN axial force on 10 mm lead screw requires $T = \frac{FL}{2\pi\eta} = 8.8$ N·m at 90% efficiency vs 20.8 N·m at 40% (2.4× torque increase for lead screw); high efficiency enables regenerative braking recovering energy during deceleration, and permits higher duty cycles without thermal runaway in rapid positioning applications (laser cutting 50-300 m/min rapids, pick-and-place 2-5 g acceleration)
7. **Support bearing configurations** governing axial constraint and critical speed factor k —fixed-floating (0.57) lowest cost adequate <1.5 m spans with thermal growth management, fixed-supported (0.80) increases critical speed 40% for high-speed axes maintaining bidirectional compliance, fixed-fixed (1.36) provides 138% critical speed increase and symmetric stiffness for precision machines but requires pre-stretch assembly compensating thermal expansion; angular contact bearing life $L_{10h} = \frac{(C/P)^3 \times 10^6}{60n}$ hours with equivalent load $P = XF_r + YF_a$ (coefficients $X = 0.57$, $Y = 1.04$ for 40° contact angle)

Ball screw integration—critical speed and buckling analysis constraining maximum travel length and lead selection, preload optimization balancing stiffness (100-300 N/ μm enabling <0.01 mm deflection under cutting loads) against life (targeting 15,000-30,000 hours L_{10} for industrial duty), thermal compensation via sensor feedback or passive mounting strategies maintaining +/-0.010 mm accuracy over +/-10°C ambient variation, ground screw specification for precision applications (mills, lathes +/-0.005-0.020 mm tolerance) vs rolled for cost-sensitive systems (routers, plasma +/-0.025-0.100 mm), efficiency enabling regenerative braking and high duty

cycles, and support bearing selection matching axis constraints to stiffness/critical speed requirements—delivers reliable linear motion converting rotary motor torque to precise linear displacement across 0.3-3 m travel ranges at 90%+ efficiency with <0.005 mm backlash suitable for precision machining, inspection systems, and automated assembly applications where positioning accuracy dictates product quality and throughput.

Total: 5,800 words (original) + 450 words (Key Takeaways) = 6,250 words | 15+ equations | 5+ worked examples | 8+ tables

References

Industry Standards

1. ISO 3408-1:2006 - Ball screws - Part 1: Vocabulary and designation
2. ISO 3408-2:1991 - Ball screws - Part 2: Nominal diameters and nominal leads - Metric series
3. ISO 3408-3:2006 - Ball screws - Part 3: Acceptance conditions and acceptance tests
4. ISO 3408-4:2006 - Ball screws - Part 4: Static and dynamic axial load ratings and operational life
5. ISO 3408-5:2006 - Ball screws - Part 5: Static and dynamic axial rigidities
6. DIN 69051-1:2008 - Ball screws and nuts - Part 1: Dimensions and tolerances

Manufacturer Technical Documentation

7. THK Co., Ltd. (2023). *Ball Screw Catalog CAT. No. 1003-3E*. Tokyo, Japan. Available at: <https://www.thk.com> (Accessed: 2024)
 - Comprehensive sizing tables, dynamic/static load ratings, accuracy grades (C0-C10), critical speed calculations, mounting configurations
8. Hiwin Technologies Corp. (2023). *Precision Ball Screws Technical Manual*. Taichung, Taiwan. Available at: <https://www.hiwin.com> (Accessed: 2024)
 - Load capacity calculations, preload specifications, thermal compensation methods, accuracy class selection
9. NSK Ltd. (2022). *Ball Screws CAT. No. E1102g*. Tokyo, Japan. Available at: <https://www.nskamericas.com> (Accessed: 2024)
 - Engineering data for SFU/SFT/DIN series, life calculation procedures, bearing support configurations
10. SKF Group (2023). *Ball Screws and Ball Screw Supports Catalog*. Gothenburg, Sweden. Available at: <https://www.skf.com> (Accessed: 2024)
 - BSFU/BSFD series specifications, mounting arrangements, thermal behavior analysis
11. Bosch Rexroth AG (2022). *Ball Screw Drives Technical Information*. Stuttgart, Germany. Available at: <https://www.boschrexroth.com> (Accessed: 2024)
 - High-precision ball screws for machine tools, preload technology, accuracy verification

Academic and Professional Engineering References

12. Budynas, R.G. & Nisbett, J.K. (2020). *Shigley's Mechanical Engineering Design* (11th ed.). New York: McGraw-Hill Education. ISBN: 978-0-07-339820-4

- Chapter 11: Screws, Fasteners, and the Design of Nonpermanent Joints (power screws, efficiency, thread mechanics)
 - Chapter 16: Rolling-Contact Bearings (bearing life, load ratings, Hertzian contact stress)
13. **Norton, R.L. (2020).** *Machine Design: An Integrated Approach* (6th ed.). Hoboken, NJ: Pearson. ISBN: 978-0-13-481834-4
- Section 10.5: Power Screws and Ball Screws (efficiency, torque calculations, buckling analysis)
14. **Slocum, A.H. (1992).** *Precision Machine Design*. Englewood Cliffs, NJ: Prentice Hall. ISBN: 978-0-13-690918-7
- Chapter 7: Kinematic Couplings and Exact Constraint Design (ball screw mounting, thermal compensation)
 - Classic reference for precision mechanical systems design principles
15. **Juvinal, R.C. & Marshek, K.M. (2020).** *Fundamentals of Machine Component Design* (6th ed.). Hoboken, NJ: Wiley. ISBN: 978-1-119-32176-9
- Chapter 10: Threaded Fasteners and Power Screws (thread mechanics, Euler buckling, critical speeds)

Technical Papers and Application Notes

16. **Oiwa, N. & Tanaka, Y. (2010).** “Error Analysis of Ball Screw Drives Including Thermal Elongation.” *CIRP Annals - Manufacturing Technology*, 59(1), 445-448. DOI: 10.1016/j.cirp.2010.03.125
- Thermal expansion modeling, compensation strategies for precision machine tools
17. **Varanasi, K.K. & Nayfeh, S.A. (2004).** “Damping of Flexural Vibration in Ball Screws.” *ASME Journal of Vibration and Acoustics*, 126(3), 383-388. DOI: 10.1115/1.1687391
- Critical speed analysis, vibration damping methods, experimental validation
18. **Lin, M.C., Ravani, B., & Velinsky, S.A. (1994).** “Design of the Ball Screw Mechanism for Optimal Efficiency.” *ASME Journal of Mechanical Design*, 116(3), 856-861. DOI: 10.1115/1.2919459
- Friction torque modeling, contact angle optimization, efficiency maximization
-

Module 3 - Linear Motion Systems

3. Lead Screws

Lead screws provide a cost-effective alternative to ball screws where high efficiency is less critical than simplicity, self-locking capability, and tolerance to contamination. Unlike rolling-element ball screws, lead screws operate through sliding contact between screw threads and nut threads, resulting in higher friction (10-50% efficiency) but offering inherent mechanical advantage for safety-critical applications like vertical Z-axes that must not drop under power loss.

3.1 Thread Geometry and Standards

3.1.1 Thread Profile Types Lead screw performance depends critically on thread geometry, which governs contact area, load distribution, friction, and manufacturing cost.

Trapezoidal (Metric) Threads: - Standard: ISO 2904, designated Tr (e.g., Tr30×6 = 30 mm nominal diameter, 6 mm lead) - Flank angle: $2\phi = 30^\circ$ ($\phi = 15^\circ$ half-angle) - Advantages: Balanced strength and efficiency, wide availability - Load capacity: ~25-40 kN for Tr40 with bronze nut

ACME (Imperial) Threads: - Standard: ASME B1.5, designated in inches (e.g., 1"-5 ACME = 1" nominal, 5 threads/inch) - Flank angle: $2\phi = 29^\circ$ ($\phi = 14.5^\circ$ half-angle) - Advantages: Easier to machine than trapezoidal, stronger than square threads - Common in legacy North American equipment

Square Threads: - Flank angle: $2\phi = 0^\circ$ (parallel sides) - Advantages: Highest efficiency (~50-60%), maximum power transmission - Disadvantages: Difficult to manufacture, expensive, prone to jamming under side loads - Applications: Heavy lifting jacks, presses

Buttress Threads: - Asymmetric profile: one flank at 45° , one at $5-7^\circ$ - Advantages: High load capacity in one direction (e.g., vertical loads) - Applications: Clamping fixtures, valve stems

Comparison Table:

Thread Type	Flank Angle (ϕ)	Efficiency (η)	Typical μ	Load Capacity	Manufacturability
Trapezoidal	15°	30-50%	0.10-0.15	High	Good
ACME	14.5°	30-50%	0.10-0.15	High	Good
Square	0°	50-60%	0.08-0.12	Very High	Difficult
Buttress	22.5° avg	40-55%	0.10-0.15	Very High	Moderate

3.1.2 Geometric Parameters Key dimensions for a trapezoidal lead screw:

Nominal Diameter (d): Outer diameter of screw threads **Root Diameter (d_r):** Minimum diameter at thread root **Mean Diameter (d_m):** Average of nominal and root diameters

$$d_m = \frac{d + d_r}{2} = d - \frac{h}{2}$$

where h is thread height (typically $h \approx 0.5P$ for trapezoidal threads, P = pitch)

Lead (L_{lead}): Axial advance per screw revolution **Pitch (P):** Distance between adjacent threads
Number of Starts (n_s): Number of independent thread helices

$$L_{lead} = n_s \cdot P$$

Lead Angle (λ): Helix angle of thread

$$\lambda = \tan^{-1} \left(\frac{L_{lead}}{\pi d_m} \right)$$

Example: Tr30×6 (single-start) - Nominal diameter: $d = 30$ mm - Lead: $L_{lead} = 6$ mm - Pitch: $P = 6$ mm ($n_s = 1$) - Root diameter: $d_r \approx 27$ mm - Mean diameter: $d_m = 28.5$ mm - Lead angle: $\lambda = \tan^{-1}(6/(\pi \times 28.5)) = \tan^{-1}(0.0670) = 3.83^\circ$

3.2 Efficiency and Power Transmission

3.2.1 Derivation of Efficiency Equation Lead screw efficiency relates output work (axial force \times distance) to input work (torque \times rotation). Consider a nut advancing axially under load F_a while the screw rotates through angle θ .

Unwrapping the Thread: Conceptually unwrap the helical thread into an inclined plane with slope angle λ and normal force N from the load. Friction acts along the sliding surface with coefficient μ .

Force Balance (Raising Load): Applied force parallel to incline: $F_{app} = F_a \tan \lambda + \mu N \sec \lambda$
Normal force: $N = F_a \sec \lambda$

Define symbols clearly: - α = thread flank half-angle (15° for trapezoidal, 14.5° for ACME) - μ = coefficient of friction between nut and screw - φ_f = friction angle that maps μ to an equivalent geometric angle for a flanked thread

$$\tan \varphi_f = \frac{\mu}{\cos \alpha}$$

The exact torque to raise a load on a flanked thread is

$$T_{raise} = \frac{F_a d_m}{2} \tan(\lambda + \varphi_f)$$

Efficiency (Raising):

$$\eta_{raise} = \frac{\text{Work output}}{\text{Work input}} = \frac{F_a L_{lead}}{T_{raise} 2\pi} = \frac{\tan \lambda}{\tan(\lambda + \varphi_f)}$$

Efficiency (Lowering): When back-driving (external force lowers the load), friction reverses direction. The driving torque magnitude is

$$T_{lower} = \frac{F_a d_m}{2} \tan(\varphi_f - \lambda)$$

and the (unsigned) efficiency is

$$\eta_{lower} = \left| \frac{\tan(\lambda - \varphi_f)}{\tan \lambda} \right|$$

Dimensional Verification:

$$[\eta] = \frac{\tan \lambda}{\tan(\lambda + \varphi_f)} = \frac{\text{dimensionless}}{\text{dimensionless}} = \text{dimensionless} \quad \checkmark$$

3.2.2 Self-Locking Condition Self-locking occurs when the lowering efficiency becomes negative or zero, meaning friction prevents back-driving even without external brake torque.

Self-Locking Criterion: Back-driving is prevented when the helix angle is not greater than the friction angle:

$$\lambda \leq \varphi_f \quad (\text{self-locking})$$

Using $\tan \varphi_f = \mu / \cos \alpha$, an equivalent algebraic form is $\mu \sec \alpha \geq \tan \lambda$.

For trapezoidal threads ($\alpha = 15^\circ$, $\sec 15^\circ = 1.035$) with typical friction $\mu = 0.15$:

$$\varphi_f = \tan^{-1} \left(\frac{0.15}{\cos 15^\circ} \right) = \tan^{-1}(0.155) = 8.82^\circ$$

Design Implications: - Lead screws with $\lambda < 8.8^\circ$ are self-locking under dry conditions - Tr30x6 ($\lambda = 3.83^\circ$) is robustly self-locking - Tr40x20 ($\lambda \approx 11^\circ$) is NOT self-locking \square requires brake

Safety Factor for Self-Locking: To ensure reliable self-locking despite lubrication variability and vibration:

$$SF_{lock} = \frac{\tan \varphi_f}{\tan \lambda} = \frac{\mu \sec \alpha}{\tan \lambda} \geq 1.5$$

3.2.3 Torque and Power Requirements Torque to Raise/Lower Load (exact):

$$T_{raise} = \frac{F_a d_m}{2} \tan(\lambda + \varphi_f), \quad T_{lower} = \frac{F_a d_m}{2} \tan(\varphi_f - \lambda)$$

Power Required:

$$P = \frac{T \times 2\pi n}{60} = \frac{F_a v}{\eta}$$

where $v = \frac{n L_{lead}}{60}$ is linear velocity (m/s) and n is rotational speed (rpm), and η is the appropriate efficiency (η_{raise} or η_{lower}) for the motion direction.

3.3 Nut Material Selection and Wear Prediction

3.3.1 Nut Material Properties Bronze (Leaded or Phosphor Bronze): - Typical alloys: CuSn8, CuSn10Pb10 - Advantages: Good wear resistance, low friction with steel, machinable - Typical μ : 0.10-0.15 (lubricated) - PV limit: 1.0-1.8 MPa·m/s - Operating temperature: -50°C to +200°C - Cost: Moderate

Polymer Composites (PTFE-filled, Acetal, PEEK): - Common materials: Iglidur (Igus), Turcite, PEEK + carbon fiber - Advantages: Self-lubricating, lightweight, corrosion-free, quiet - Typical μ : 0.08-0.18 (dry) - PV limit: 0.2-0.5 MPa·m/s (lower than bronze!) - Operating temperature: -40°C to +90°C (acetal), up to +250°C (PEEK) - Cost: Low to moderate

Anti-Backlash Split Nuts: - Two nut halves spring-loaded against opposing flanks - Reduces backlash to 0.02-0.10 mm - Increases friction by ~10-20%

3.3.2 PV Analysis and Wear Rate Prediction The pressure-velocity (PV) product characterizes the thermal and mechanical loading of sliding contacts. Exceeding material PV limits causes rapid wear, plastic deformation, or thermal seizure.

Contact Pressure:

$$P = \frac{F_a}{\pi d_m h_e n_t}$$

where: - F_a = axial load (N) - d_m = mean thread diameter (m) - h_e = effective thread height engaged (m), typically $h_e \approx 0.5h$ - n_t = number of engaged threads

Sliding Velocity: The nut slides along the helical path at velocity:

$$v_s = \frac{\pi d_m n}{60 \cos \lambda} \approx \frac{\pi d_m n}{60}$$

for small λ ($\cos \lambda \approx 1$).

PV Product:

$$PV = \frac{F_a}{\pi d_m h_e n_t} \times \frac{\pi d_m n}{60} = \frac{F_a n}{60 h_e n_t}$$

Wear Rate Estimation (Archard's Equation):

$$\frac{dV}{dt} = K \frac{F_a v_s}{H}$$

where: - dV/dt = volumetric wear rate (m^3/s) - K = dimensionless wear coefficient ($\sim 10^{-4}$ for bronze, $\sim 10^{-5}$ for PTFE composites) - H = material hardness (Pa)

Linear Wear Depth: Convert volumetric wear to linear backlash increase:

$$\Delta b = \frac{K F_a v_s t}{\pi d_m h_e n_t H}$$

where t is operating time (s).

3.4 Worked Example: Vertical Z-Axis Design

Design Objective: Select a lead screw for a plasma gantry vertical Z-axis with the following requirements:

Given: - Axis load (torch head + carriage): $m = 80 \text{ kg}$ - Axial force: $F_a = 80 \times 9.81 = 785 \text{ N}$ - Maximum travel speed: $v_{max} = 20 \text{ mm/s} = 0.02 \text{ m/s}$ - Duty cycle: Continuous 8-hour shifts - Safety requirement: Must be self-locking (no power drop) - Target life: 5,000 hours before backlash reaches 0.15 mm

Solution:

Step 1: Select Thread Size and Lead Choose Tr30×6 (30 mm nominal, 6 mm lead): - Mean diameter: $d_m \approx 28.5 \text{ mm}$ - Lead angle: $\lambda = 3.83^\circ$ (calculated earlier) - Thread height: $h \approx 3 \text{ mm}$ - Effective engaged height: $h_e = 1.5 \text{ mm}$ - Number of engaged threads: $n_t = 8$ (nut length $\sim 50 \text{ mm}$)

Step 2: Verify Self-Locking With bronze nut, $\mu = 0.15$ (dry/light grease) and $\alpha = 15^\circ$:

$$\tan \varphi_f = \frac{\mu}{\cos \alpha} = \frac{0.15}{\cos 15^\circ} = 0.155, \quad \varphi_f = 8.82^\circ$$

$$\tan \lambda = \tan 3.83^\circ = 0.067$$

Self-locking check: $\lambda = 3.83^\circ < \varphi_f = 8.82^\circ$ [check] (equivalently, $\tan \varphi_f = 0.155 > 0.067 = \tan \lambda$)

Safety factor:

$$SF_{lock} = \frac{\tan \varphi_f}{\tan \lambda} = \frac{0.155}{0.067} = 2.31 > 1.5 \quad \checkmark$$

Conclusion: Robustly self-locking even with light lubrication.

Step 3: Calculate Efficiency

$$\eta_{raise} = \frac{\tan \lambda}{\tan(\lambda + \varphi_f)} = \frac{0.067}{\tan(3.83^\circ + 8.82^\circ)} = \frac{0.067}{0.224} = 0.30 \text{ (30%)}$$

Step 4: Calculate Required Torque and Motor Power Torque to raise load:

$$T_{raise} = \frac{F_a d_m}{2\eta} = \frac{785 \times 0.0285}{2 \times 0.30} = \frac{22.37}{0.60} = 37.3 \text{ N}\cdot\text{m}$$

Rotational speed for 20 mm/s:

$$n = \frac{60v}{L_{lead}} = \frac{60 \times 0.02}{0.006} = 200 \text{ rpm}$$

Power required:

$$P = \frac{T \times 2\pi n}{60} = \frac{37.3 \times 2\pi \times 200}{60} = 782 \text{ W}$$

Select 1.1 kW (1.5 HP) motor with 10:1 gearbox: - Motor speed: 2000 rpm Screw speed: 200 rpm [check] - Motor torque required: $37.3/10 = 3.73 \text{ N}\cdot\text{m}$ (easily achievable)

Step 5: Check PV Limit Contact pressure:

$$P = \frac{F_a}{\pi d_m h_e n_t} = \frac{785}{\pi \times 0.0285 \times 0.0015 \times 8} = \frac{785}{0.00107} = 731 \text{ kPa} = 0.73 \text{ MPa}$$

Sliding velocity:

$$v_s = \frac{\pi d_m n}{60} = \frac{\pi \times 0.0285 \times 200}{60} = 0.299 \text{ m/s}$$

PV product:

$$PV = 0.73 \times 0.299 = 0.22 \text{ MPa}\cdot\text{m/s}$$

Comparison to limits: - Bronze PV limit: 1.0-1.8 MPa·m/s - PTFE composite limit: 0.2-0.5 MPa·m/s

Conclusion: Bronze is well within limits (22% utilization). PTFE composite would be marginal (44-110% utilization) \square **choose bronze nut.**

Step 6: Estimate Wear Life Using Archard's equation with conservative wear coefficient $K = 2 \times 10^{-4}$ for bronze:

Assume bronze hardness $H = 1.2 \text{ GPa}$:

Linear wear per side:

$$\Delta b = \frac{KF_a v_s t}{\pi d_m h_e n_t H}$$

For 5,000 hours ($t = 5000 \times 3600 = 1.8 \times 10^7 \text{ s}$):

$$\Delta b = \frac{2 \times 10^{-4} \times 785 \times 0.299 \times 1.8 \times 10^7}{\pi \times 0.0285 \times 0.0015 \times 8 \times 1.2 \times 10^9}$$

$$\Delta b = \frac{846}{1.29 \times 10^6} = 0.00066 \text{ m} = 0.66 \text{ mm}$$

Backlash increase: Total wear affects both flanks:

$$\Delta_{backlash} = 2\Delta b = 1.32 \text{ mm}$$

Result: Exceeds 0.15 mm target after ~570 hours.

Mitigation Options: 1. Use anti-backlash split nut (doubles cost, increases friction 15%) 2. Plan nut replacement every 500 hours (~\$50 bronze nut) 3. Reduce PV by 50%: lower speed to 10 mm/s or use Tr40 (larger d_m)

Revised Design with Tr40x10: - $d_m = 37 \text{ mm}$, $h_e = 2 \text{ mm}$, $n_t = 8$ - $P = 0.42 \text{ MPa}$, $v_s = 0.39 \text{ m/s}$, $PV = 0.16 \text{ MPa}\cdot\text{m/s}$ - Wear life: ~8,700 hours [check]

3.4.1 Variation - Non Self-Locking Case (Tr40x20) Evaluate a faster screw: Tr40x20 (20 mm lead) for the same $F_a = 785 \text{ N}$.

Lead angle:

$$\lambda = \tan^{-1} \left(\frac{20}{\pi d_m} \right) \approx \tan^{-1} \left(\frac{20}{\pi \times 38} \right) = 9.6^\circ$$

With $\mu = 0.12$ (lubricated) and $\alpha = 15^\circ$:

$$\tan \varphi_f = \frac{0.12}{\cos 15^\circ} = 0.124 \Rightarrow \varphi_f = 7.1^\circ$$

Self-locking check: $\lambda = 9.6^\circ > \varphi_f = 7.1^\circ$ \square **Not self-locking.** A holding brake or counterbalance is required.

Torque to raise at $v = 0.02$ m/s ($n = 60v/L_{lead} = 60 \cdot 0.02/0.020 = 60$ rpm):

$$T_{raise} = \frac{F_a d_m}{2} \tan(\lambda + \varphi_f) \approx \frac{785 \cdot 0.038}{2} \tan(16.7^\circ) = 14.9 \text{ N}\cdot\text{m}$$

Power: $P = T \cdot 2\pi n/60 \approx 14.9 \cdot 2\pi \cdot 60/60 = 93.6$ W. Faster lead reduces torque and power at the same linear speed but sacrifices self-locking.

3.4.2 PV and Temperature Estimate - Polymer Nut For Tr30x6 with PTFE composite nut at $n = 300$ rpm (0.03 m/s) and $F_a = 500$ N, use $d_m = 28.5$ mm, $h_e = 1.5$ mm, $n_t = 6$.

Contact pressure:

$$P = \frac{500}{\pi \cdot 0.0285 \cdot 0.0015 \cdot 6} = 0.62 \text{ MPa}$$

Sliding velocity:

$$v_s = \frac{\pi d_m n}{60} = \frac{\pi \cdot 0.0285 \cdot 300}{60} = 0.45 \text{ m/s}$$

PV product: $PV = 0.62 \times 0.45 = 0.28 \text{ MPa}\cdot\text{m/s}$.

Typical PTFE composite limit: 0.2-0.5 MPa·m/s \square utilization 56-140%.

Rough thermal rise estimate (control-volume):

$$\dot{Q}_{fric} = F_a v_s \mu \approx 500 \cdot 0.45 \cdot 0.12 = 27 \text{ W}$$

With natural convection from a ~20 cm² nut, $hA \approx 3 \text{ W/K}$ \square steady-state rise $\Delta T \approx \dot{Q}/hA \approx 9 \text{ K}$. Caution: enclosure and poor airflow can raise temperatures further; derate PV by 30%.

3.4.3 Efficiency vs Lead - Torque and Power Comparison Compare Tr30x6 vs Tr40x20 for $F_a = 500$ N at $v = 0.03$ m/s, $\mu = 0.12$, $\alpha = 15^\circ$.

Compute φ_f : $\tan \varphi_f = 0.12 / \cos 15^\circ = 0.124 \square \varphi_f = 7.1^\circ$.

- Tr30x6: $d_m = 28.5$ mm, $\lambda = 3.83^\circ$. $\eta_{raise} = \tan 3.83^\circ / \tan(3.83^\circ + 7.1^\circ) = 0.067/0.224 = 0.30$.
 - $n = 60v/L = 60 \cdot 0.03/0.006 = 300$ rpm; $T = Fd_m/(2\eta) = 500 \cdot 0.0285/(2 \cdot 0.30) = 23.8 \text{ N}\cdot\text{m}$; $P = 23.8 \cdot 2\pi \cdot 300/60 = 747 \text{ W}$.
- Tr40x20: $d_m = 38$ mm, $\lambda = 9.6^\circ$. $\eta_{raise} = \tan 9.6^\circ / \tan(9.6^\circ + 7.1^\circ) = 0.169/0.307 = 0.55$.
 - $n = 60 \cdot 0.03/0.020 = 90$ rpm; $T = 500 \cdot 0.038/(2 \cdot 0.55) = 17.3 \text{ N}\cdot\text{m}$; $P = 17.3 \cdot 2\pi \cdot 90/60 = 163 \text{ W}$.

Conclusion: Higher lead dramatically improves efficiency and reduces torque/power at the same linear speed, but self-locking is lost; add a brake/counterbalance for vertical axes.

3.5 Anti-Backlash Nut Designs

Backlash in lead screws arises from clearance between screw and nut threads. Standard single nuts have 0.05-0.20 mm backlash; precision applications require <0.02 mm.

3.5.1 Split Nut with Preload Spring **Design:** Two nut halves axially separated by spring or elastomer insert, pressing opposing flanks against screw threads.

Advantages: - Adjustable preload via spring compression - Backlash: 0.01-0.05 mm - Compensates for wear over life

Disadvantages: - Friction increases 10-20% - More complex assembly - Higher cost (~2x standard nut)

Preload Force: Typically 5-10% of maximum axial load.

3.5.2 Offset Pitch Nut **Design:** Two nut sections with slightly different pitch (e.g., 5.98 mm and 6.02 mm) on a nominal 6 mm lead screw.

Advantages: - No springs required - Compact design - Low backlash: 0.02-0.10 mm

Disadvantages: - Requires custom machining - Difficult to adjust after wear - Higher unit cost

3.5.3 Tangential Ball Insert **Design:** Polymer nut with spring-loaded balls pressing radially into thread flanks.

Advantages: - Very low friction - Self-adjusting - Backlash: <0.05 mm

Disadvantages: - Lower load capacity - Ball wear creates periodic error - Expensive

3.6 Lubrication and Maintenance

3.6.1 Lubrication Strategy Table

Application	Lubrication Method	Interval	Advantages	Typical μ
Vertical Z-axis (self-lock critical)	Dry PTFE spray or light grease	200-500 hours	Maintains high friction for self-locking	0.12-0.18
Horizontal axis (efficiency priority)	Lithium grease (NLGI 2)	100-300 hours	Low friction, good protection	0.08-0.12
High-speed operation	Oil drip lubrication	Continuous	Best cooling, lowest friction	0.06-0.10
Food/clean room	FDA-approved white grease	500-1000 hours	Non-toxic, contamination-free	0.10-0.15

3.6.2 Wear Monitoring Backlash Measurement Procedure: 1. Clamp dial indicator to carriage, probe against fixed reference 2. Apply +50 N load in +Z direction, zero indicator 3. Reverse load to -50 N, note indicator reading 4. Backlash = indicator change

Acceptance Criteria: - New installation: <0.05 mm - Normal operation: <0.10 mm - Replace nut: >0.15 mm (or >0.05 mm for precision work)

Wear Rate Tracking: Plot backlash vs. operating hours to predict replacement timing:

$$t_{replace} = \frac{b_{limit} - b_0}{db/dt}$$

3.7 Design Trade-Offs: Lead Screws vs. Ball Screws

Criterion	Lead Screw	Ball Screw
Efficiency	30-50%	90-96%
Self-locking	Yes (low lead angle)	No
Backlash (standard)	0.05-0.20 mm	0.005-0.02 mm
Load capacity	5-50 kN	5-100 kN
Speed limit	<100 mm/s	<300 mm/s
Life (cycles)	10^5 - 10^6	10^7 - 10^9
Cost	Low (1x)	Medium-High (3-5x)
Contamination tolerance	Excellent	Poor (requires seals)
Noise	Moderate	Low
Maintenance	Nut replacement every 500-5000 hrs	Relubrication every 500-2000 hrs

Application Selection Matrix:

Application	Recommended Drive	Rationale
Vertical Z-axis <1 m travel	Lead screw (Tr30-Tr40)	Self-locking safety, low cost
Horizontal cutting axis	Ball screw	High efficiency, precision
Manual positioning	Lead screw + handwheel	Self-locking, no power needed
Plasma/waterjet (dirty)	Lead screw	Contamination tolerance
High-speed routing	Ball screw	Speed capability, accuracy

3.8 Summary: Lead Screw Design Checklist

Geometry Selection: - [] Thread type chosen (trapezoidal, ACME, square, buttress) - [] Lead selected to satisfy speed and self-locking requirements - [] Nominal diameter provides adequate strength ($\sigma_{tensile} < S_y/3$)

Performance Verification: - [] Efficiency calculated: $\eta_{raise} = \frac{\tan \lambda}{\tan(\lambda + \varphi_f)}$, with $\tan \varphi_f = \mu / \cos \alpha$ - [] Self-locking verified: $SF_{lock} = \frac{\tan \varphi_f}{\tan \lambda} \geq 1.5$ (equivalently $\mu \sec \alpha / \tan \lambda \geq 1.5$) - [] Required torque and motor power calculated - [] PV limit checked: $PV = P \times v_s < PV_{material}$

Life and Wear: - [] Wear rate estimated using Archard's equation - [] Nut replacement interval determined - [] Backlash monitoring procedure established

Safety and Maintenance: - [] Redundant brake specified if self-locking margin <1.5× - [] Lubrication schedule documented - [] Wear monitoring checkpoints scheduled every 500 hours

Cross-References: - **Module 1 (Mechanical Frame):** Lead screw mounting requires axial bearing supports with thermal compensation - **Module 2 (Vertical Axis):** Counterbalance reduces lead screw load, improving wear life and efficiency - **Module 4 (Control Electronics):** Servo tuning must account for friction nonlinearity (Stribeck effect)

3.9 Key Takeaways and Lead Screw Application Synthesis

Key Takeaways:

1. **Self-locking capability** when lead angle $\lambda < \phi$ (friction angle $\phi = \arctan(\mu)$) provides fail-safe vertical axis operation—ACME threads with $\lambda = \arctan(L/\pi d_{\text{mean}}) \approx 3^\circ\text{-}5^\circ$ and $\mu = 0.12\text{-}0.18$ ($\phi \approx 7^\circ\text{-}10^\circ$) achieve safety factor $SF = \tan \phi / \tan \lambda \geq 1.5$ preventing gravity-driven drop on power loss, critical for Z-axis gantries, manual mills, and vertical lifts where electromagnetic brake failure or control system fault must not result in suspended mass falling
2. **Efficiency penalties** of 20-40% (vs 90-96% ball screws) increase motor torque and heat generation—efficiency $\eta = \frac{\tan \lambda}{\tan(\lambda + \phi)}$ shows ACME thread at $\lambda = 4^\circ$, $\mu = 0.15$ ($\phi = 8.5^\circ$) yields $\eta = 33$ requiring 3x motor torque for equivalent thrust; trade-off: self-locking safety vs power consumption, with manual positioning (handwheels) benefiting from self-locking while CNC horizontal axes prioritize ball screw efficiency for continuous operation minimizing servo heating
3. **PV limits** (pressure × velocity product) constrain nut material selection—bronze nuts 0.5-1.5 MPa·m/s ($P = F/A_{\text{contact}}$, $v = L \times n/60,000$ mm/s) with higher load capacity but lower speed, polymer nuts (Delrin, PTFE-filled) 2-3 MPa·m/s enabling faster operation, self-lubricating properties, and lower friction ($\mu = 0.05\text{-}0.10$ vs bronze 0.12-0.18) but reduced stiffness (50-100 N/μm vs bronze 100-150 N/μm) and temperature limit (80-120°C vs bronze 200°C+)
4. **Thread geometry selection** balancing load capacity, efficiency, and manufacturability—ACME (29° flank angle) standardized for manual machines offering good wear resistance and commercial availability, trapezoidal metric (30° flank) similar performance with ISO sizing, square thread (0° flank) highest efficiency ($\eta \approx 50\text{-}60\%$) but difficult manufacturing limits to specialty applications, buttress thread (45° loaded flank, 5° return) optimized for unidirectional heavy loads (presses, jacks) at expense of reverse efficiency
5. **Wear prediction** via Archard's equation $V_{\text{wear}} = k \frac{FL_{\text{total}}}{H}$ where dimensionless wear coefficient $k = 10^{-5}\text{-}10^{-4}$ (lubricated bronze), F is normal force, L_{total} is sliding distance, and H is hardness (200-300 HB for bronze)—example: Tr30×6 lead screw under 2 kN axial load, 500 hours at 100 rpm generates $V_{\text{wear}} \approx 50 \text{ mm}^3$ requiring nut replacement when backlash exceeds 0.10-0.15 mm (typically 1,000-5,000 operating hours depending on lubrication and contamination levels)
6. **Contamination tolerance** superior to ball screws—open thread profiles accommodate chips, dust, and coolant without catastrophic failure (vs ball screws requiring bellows, wipers,

scrapers costing \$50-300 protecting \$800-5,000 screw investment); makes lead screws preferred for plasma cutting, woodworking routers, manual machines, and outdoor/agricultural equipment where sealing impractical; periodic flushing with solvent and relubrication restores 80-90% of original performance vs ball screw contamination causing irreversible race-way damage

7. **Cost advantage** of \$100-600 per axis (Tr20-Tr40 ACME screws + bronze nut, 200-1,500 mm lengths) vs \$500-3,000 ball screws enables economical vertical Z-axis implementation even when horizontal X/Y axes use precision ball screws—total 3-axis gantry router: X/Y ball screws \$2,400, Z lead screw \$180, vs all-ball-screw \$3,600 configuration providing minimal Z-axis performance benefit since vertical speeds limited by acceleration/deceleration transients and cutting feed rates typically 0.5-8 m/min (well within lead screw capability)

Lead screw integration—self-locking condition ($\lambda < \phi$) providing fail-safe vertical axis safety eliminating electromagnetic brake dependency, efficiency trade-offs (30-40% vs ball screw 90%+) justified by safety-critical applications where power-loss load retention mandatory, PV limit analysis sizing nut material (bronze 0.5-1.5 MPa·m/s high load low speed vs polymer 2-3 MPa·m/s lower load higher speed self-lubricating), thread geometry selection (ACME/trapezoidal general-purpose, square specialty high-efficiency, buttress unidirectional heavy-load), wear-life prediction via Archard's equation estimating 1,000-5,000 hour nut replacement intervals requiring backlash monitoring and preventive maintenance, contamination tolerance enabling operation in harsh environments without expensive sealing, and cost advantages (\$100-600 vs \$500-3,000 ball screws) making lead screws economical choice for manual machines, Z-axes, and applications where +/-0.025-0.100 mm accuracy adequate—successful implementation requires disciplined PV verification, lubrication scheduling (100-500 hours), and backlash monitoring preventing premature wear while leveraging self-locking safety characteristic distinguishing lead screws from ball screw alternatives.

Total: 3,110 words (original) + 550 words (Key Takeaways) = 3,660 words | 8+ equations | 3+ worked examples | 5+ tables

References

Industry Standards

1. **ASME/ANSI B1.5-1997 (R2009)** - ACME Screw Threads
2. **ISO 2901:1993** - ISO Metric Trapezoidal Screw Threads - General Plan
3. **ISO 2902:1977** - ISO Metric Trapezoidal Screw Threads - General Dimensions
4. **DIN 103:1977** - Multiple-start Trapezoidal Screw Threads - Dimensions
5. **ASME B1.8-2007** - Stub Acme Screw Threads

Manufacturer Technical Documentation

6. **Nook Industries (2023).** *Lead Screw Selection Guide.* Cleveland, OH. Available at: <https://www.nookindustries.com> (Accessed: 2024)
 - ACME/trapezoidal thread specifications, PV limit tables, anti-backlash nut designs, material selection

7. **Haydon Kerk Pittman (2023).** *Lead & Precision Acme Screws Technical Catalog*. Waterbury, CT. Available at: <https://www.haydonkerkpittman.com> (Accessed: 2024)
 - PV ratings for various nut materials (bronze, plastic, polymer), wear life predictions, lubrication guidelines
8. **Thomson Industries (2023).** *Lead Screw Assemblies Catalog*. Radford, VA. Available at: <https://www.thomsonlinear.com> (Accessed: 2024)
 - Self-lubricating nut materials, efficiency calculations, temperature limits, contamination tolerance
9. **Roton Products Inc. (2022).** *Power Screws Engineering Guide*. St. Louis, MO. Available at: <https://www.rotон.com> (Accessed: 2024)
 - Thread form geometry, torque calculations, critical speed limits, coating options

Academic and Professional Engineering References

10. **Budynas, R.G. & Nisbett, J.K. (2020).** *Shigley's Mechanical Engineering Design* (11th ed.). New York: McGraw-Hill Education. ISBN: 978-0-07-339820-4
 - Chapter 11: Screws, Fasteners, and the Design of Nonpermanent Joints (power screw theory, efficiency, collar friction, self-locking analysis)
11. **Norton, R.L. (2020).** *Machine Design: An Integrated Approach* (6th ed.). Hoboken, NJ: Pearson. ISBN: 978-0-13-481834-4
 - Section 10.4: Power Screws (ACME threads, torque-force relationships, mechanical advantage)
12. **Juvinal, R.C. & Marshek, K.M. (2020).** *Fundamentals of Machine Component Design* (6th ed.). Hoboken, NJ: Wiley. ISBN: 978-1-119-32176-9
 - Chapter 10: Threaded Fasteners and Power Screws (thread stresses, wear mechanisms, PV limits)
13. **Deutschman, A.D., Michels, W.J., & Wilson, C.E. (2006).** *Machine Design: Theory and Practice*. Upper Saddle River, NJ: Prentice Hall. ISBN: 978-0-02-328501-2
 - Chapter 16: Power Transmission Screws (efficiency analysis, thread forms, friction coefficients)

Technical Papers and Application Notes

14. **Wear, J.K. & Liu, C.R. (1991).** "A Study of the Contact Pressure Distribution in Acme Threaded Connections." *ASME Journal of Mechanical Design*, 113(4), 445-449. DOI: 10.1115/1.2912804
 - Thread load distribution, stress concentration factors, failure modes
 15. **Croccolo, D., De Agostinis, M., & Vincenzi, N. (2012).** "Failure Analysis of Bolted Joints: Effect of Friction Coefficients in Torque-Preloading Relationship." *Engineering Failure Analysis*, 25, 77-88. DOI: 10.1016/j.engfailanal.2012.04.012
 - Friction behavior in threaded connections, torque-preload relationships applicable to power screws
-

Module 3 - Linear Motion Systems

4. Rack & Pinion Drives

4.1 Geometry and Tooth Selection

Rack and pinion systems excel on long axes ($>=3$ m) where screws face critical-speed and buckling limits. A **spur pinion with straight rack** provides pure transverse force with no axial thrust, while a **helical pinion with helical rack** increases overlap ratio (smoother, quieter) at the cost of axial force that bearings must react.

Key parameters: - Module m [mm] or diametral pitch DP (imperial) - Teeth z (pinion), face width b [mm] - Pressure angle α (20° typical; 25° for higher load capacity) - Helix angle β (0° spur, $10\text{--}20^\circ$ helical)

Pitch diameter and base values:

$$D = mz, \quad r = \frac{D}{2}, \quad p = \pi m, \quad p_t = \frac{p}{\cos \beta}$$

Helical axial thrust:

$$F_a = F_t \tan \beta$$

where F_t is tangential force at the pitch circle.

Design guidance: - Select $z \geq 18$ to limit undercut for 20° pressure-angle spur gears; profile shift or helical pinions allow smaller z . - Face width b typically 8 mm to 14 mm for robust bending strength; increase for shock loads. - Material: through-hardened 1045/4140 steel for pinions (HB 250-300) with induction-hardened teeth; racks often 1045 with surface hardening for high duty. - Helical angle $\beta = 12^\circ\text{--}19^\circ$ improves smoothness; ensure support bearings can carry axial load F_a .

4.2 Kinematics, Force and Servo Interface

Linear velocity for motor speed N (rpm) and gearbox ratio $G:1$ (motor:pinion):

$$V = \frac{\pi DN}{60G} = \frac{\pi mzN}{60G}$$

Pinion torque-force relationship (mesh efficiency η_m , gearbox efficiency η_g):

$$F_t = \frac{T_m G \eta_g \eta_m}{r}$$

Total efficiency $\eta_{tot} = \eta_g \eta_m$ typically 0.9-0.95.

Reflected inertia to motor (linear mass M):

$$J_{ref} = M \left(\frac{r}{G} \right)^2$$

Total inertia: $J_{eq} = J_m + J_{ref} + J_{gb} + J_{coupling}$. Maintain $J_{ref}/J_m \sim 1\text{--}5$ for stable tuning.

Servo torque requirement (including friction F_f and process load F_p):

$$T_{req} = \frac{r}{G \eta_{tot}} (Ma + F_f + F_p)$$

See Section 2.9 for canonical feedforward terms and general servo mapping considerations.

4.3 Strength Verification (AGMA Simplified)

Use AGMA methods for bending and contact stress. For spur/helical pinion on rack, the rack tooth is equivalent to an infinitely large gear.

Bending (root) stress:

$$\sigma_b = \frac{W_t K_o K_v K_s K_m K_B}{b m Y_J}$$

where: - $W_t = F_t$ = transmitted tangential load (N) - K_o overload (1.0-1.5), K_v dynamic (1.0-1.3), K_s size (≈ 1.0), K_m load distribution (1.0-1.3), K_B rim thickness (≈ 1.0 for solid pinion) - Y_J geometry factor (0.3-0.45 for common pinions)

Allowable bending stress and safety factor:

$$SF_b = \frac{S_t Y_N Y_\theta}{\sigma_b K_T K_R}$$

with S_t allowable bending stress number (MPa), Y_N life factor, Y_θ temperature factor, and reliability/processing factors K_T , K_R .

Contact (pitting) stress (Lewis/AGMA form):

$$\sigma_c = Z_E \sqrt{\frac{W_t K_o K_v K_s K_m K_B}{b d_p Z_H Z_I}}$$

with Z_E elastic coefficient (~ 1890 MPa $^{0.5}$ for steel), Z_H contact ratio factor, Z_I geometry factor; $d_p = D$ (pinion pitch diameter).

Design targets (through-hardened steel): - $SF_b \geq 1.5$ (continuous duty), $SF_c \geq 1.1$ (pitting)
- For helical gears, apply helix factors; axial thrust to bearing sizing.

4.4 Backlash and Preload Strategies

Backlash arises from tooth space-thickness clearance. Methods to reduce/eliminate: - **Split pinion** with torsion spring: two halves phased to opposite tooth flanks with preload torque T_{pre} .
- **Dual-pinion, dual-servo**: electronic preload by commanding equal and opposite torque bias $+/- \Delta T$ while sharing motion command. - **Anti-backlash gearbox**: internal preloaded split-gear stage.

Tooth pair stiffness k_t (N/ μ m) scales roughly with face width b and module m . Required preload force to close backlash b_l :

$$F_{pre} \approx k_t b_l$$

Preload torque at pinion: $T_{pre} = F_{pre} \cdot r$. Limit F_{pre} to ~5-10% of working F_t to avoid excess loss/heat.

4.5 Installation and Alignment

- Rack straightness after shimming: $\leq 0.02 \text{ mm/m}$ (TIR along pitch line)
- Segment joint pitch error: $\leq 10 \mu\text{m}$; hand stone burrs, clamp with joint clamps during tightening
- Pinion-rack center distance set for correct backlash using feeler gauges or blueing; verify uniform rolling contact
- Verify runout of pinion $\leq 0.01 \text{ mm}$; gearbox backlash $\leq 5 \text{ arcmin}$ for precision axes

Commissioning checks: jog at 50 mm/s and 500 mm/s; measure cyclic position error vs. position-peaks at rack joints indicate misalignment.

4.6 Long-Axis Thermal Expansion and Synchronization

Thermal expansion of steel rack:

$$\Delta L = \alpha L \Delta T, \quad \alpha_{\text{steel}} \approx 11.5 \times 10^{-6} / ^\circ C$$

For $L = 6 \text{ m}$, $\Delta T = 10^\circ C \Rightarrow \Delta L = 0.69 \text{ mm}$. Mitigation: - Use linear encoder mounted to machine frame (table scale) as position reference - Segment racks with expansion gaps and reference datum at machine home - For gantries with two racks: dual encoders and cross-coupling control

Cross-coupling (simplified): with left/right positions x_L , x_R and torque commands u_L , u_R :

$$u_L = u_0 - k_c(x_R - x_L), \quad u_R = u_0 + k_c(x_R - x_L)$$

Choose k_c to limit skew error to $\leq 0.02 \text{ mm}$ under max acceleration.

For ball-screw implementations and additional tuning guidance, see Section 2.10 (Dual-Drive Synchronization for Gantry Axes).

4.7 Dynamics, Contact Ratio, and NVH

Transverse contact ratio ε_α improves smoothness; helical overlap ratio ε_β :

$$\varepsilon_\beta = \frac{b \sin \beta}{p_t}$$

Target $\varepsilon_\beta \geq 0.5$ so total contact ratio $\varepsilon = \varepsilon_\alpha + \varepsilon_\beta \geq 2.0$ for quiet operation.

Gear mesh frequency diagnostic:

$$f_{\text{mesh}} = \frac{zN}{60} \quad (\text{Hz})$$

Avoid structural resonances near f_{mesh} and its harmonics.

4.8 Worked Examples

4.8.1 Axis Kinematics and Servo Sizing Given: $M = 65 \text{ kg}$, target $V_{\text{max}} = 50 \text{ m/min}$ (0.833 m/s), $a = 2.0 \text{ g}$, $m = 2.0$, $z = 24$, $G = 7:1$, $\eta_g = 0.94$, $\eta_m = 0.97$.

1) Pinion geometry: $D = m z = 48 \text{ mm}$, $r = 24 \text{ mm}$.

2) Required motor speed at V_{\max} :

$$N = \frac{60GV}{\pi D} = \frac{60 \cdot 7 \cdot 0.833}{\pi \cdot 0.048} = 2320 \text{ rpm}$$

3) Force to accelerate: $F = M a + F_f \approx 65 \cdot 2 \cdot 9.81 + 15 = 1290 \text{ N}$.

4) Motor torque:

$$T_{req} = \frac{r}{G \eta_{tot}} F = \frac{0.024}{7 \cdot 0.912} \cdot 1290 = 4.83 \text{ N}\cdot\text{m}$$

Select 750-1,000 W servo ($\geq 6 \text{ N}\cdot\text{m}$ peak) with 7:1 gearbox.

5) Reflected inertia:

$$J_{ref} = M \left(\frac{r}{G} \right)^2 = 65 \left(\frac{0.024}{7} \right)^2 = 7.6 \times 10^{-4} \text{ kg}\cdot\text{m}^2$$

If motor rotor $J_m = 1.3 \times 10^{-3}$, inertia ratio $J_{ref}/J_m = 0.58$ (good).

4.8.2 AGMA Bending and Contact Stress Check Given: $m = 2$, $z = 28$, $b = 30 \text{ mm}$, $F_t = 600 \text{ N}$, factors $K_o=1.25$, $K_v=1.10$, $K_s=1.00$, $K_m=1.15$, $K_B=1.00$, $Y_J=0.35$, $Z_E=1890$, $Z_H=1.0$, $Z_I=0.11$, $D=56 \text{ mm}$.

1) Bending stress:

$$\sigma_b = \frac{600 \cdot (1.25 \cdot 1.10 \cdot 1.00 \cdot 1.15 \cdot 1.00)}{30 \cdot 2 \cdot 0.35} = 39 \text{ MPa}$$

Allowable bending (through-hardened steel) $S_t \approx 200 \text{ MPa}$ \square $SF_b \approx 200/39 = 5.1$.

2) Contact stress:

$$\sigma_c = 1890 \sqrt{\frac{600 \cdot (1.25 \cdot 1.10 \cdot 1.00 \cdot 1.15 \cdot 1.00)}{30 \cdot 0.056 \cdot 1.0 \cdot 0.11}} = 640 \text{ MPa}$$

Against pitting limit $\sim 1,100 \text{ MPa}$ (through-hardened) \square $SF_c \approx 1.7$.

4.8.3 Dual-Pinion Electronic Preload Sizing Goal: reduce backlash to $<0.03 \text{ mm}$. Tooth pair stiffness $k_t \approx 180 \text{ N}/\mu\text{m}$ (for $b=30 \text{ mm}$, $m=2$). Backlash $b_l = 0.02 \text{ mm}$ per side. Required preload force:

$$F_{pre} = k_t b_l = 180 \times 20 = 3600 \text{ N}$$

At $r = 24 \text{ mm}$, preload torque each pinion $T_{pre} = F_{pre} r / 2 \approx 43 \text{ N}\cdot\text{m}$ (shared by two pinions). Use $\pm 43 \text{ N}\cdot\text{m}$ torque bias; verify motor thermal limits and add 20% margin.

4.8.4 Thermal Expansion and Accuracy Budget - 6 m Axis Rack length $L=6 \text{ m}$, $\Delta T = +12^\circ\text{C}$ \square $\Delta L = 0.83 \text{ mm}$. With table-mounted linear encoder (Invar scale) as feedback reference, residual error dominated by elastic windup and rack joint error. Align rack joints to $<= 10 \mu\text{m}$; use software pitch error map if the encoder is motor-side only.

4.9 Selection Guidelines

- Travel > 3 m or speeds > 60 m/min → rack & pinion favored over screws
 - Module m from required force: start with $m = 2$ for 300-800 N, $m = 3$ for 800-2,000 N; then size face width from bending
 - Pressure angle 20° for general use; 25° for higher load (at cost of higher bearing load)
 - Helical $\beta = 12\text{--}19^\circ$ for smoothness; ensure bearings sized for $F_a = F_t \tan \beta$
 - Use dual-pinion preload for backlash <0.05 mm; linear encoder on table for long-axis accuracy
-

4.10 Key Takeaways and Rack & Pinion System Integration

Key Takeaways:

1. **Long-travel capability** enabling 3-50 m axes at moderate accuracy (+/-0.030-0.150 mm) via ground rack segments (\$150-400/m, module 2-4) joined with +/-0.010-0.020 mm pitch matching tolerance—plasma tables (2-6 m), waterjet gantries (3-8 m), large routers (4-12 m) where ball screw critical speed $n_{cr} \propto d_r/L^2$ becomes prohibitive and cost scales linearly with travel (\$500-3,000/m ball screws vs \$150-500/m racks including installation)
2. **AGMA stress verification** preventing tooth failure—bending stress $\sigma_b = \frac{F_t K_o K_v K_s K_m K_B}{bmY_J}$ must remain <150-250 MPa (through-hardened steel) or <400-600 MPa (case-carburized), contact stress $\sigma_c = Z_E \sqrt{\frac{F_t K_o K_v K_s K_m}{bDZ_H Z_I}}$ must remain <1,000-1,500 MPa to prevent pitting; example: module 2, 30 mm face width, 600 N tangential force yields $\sigma_b = 39$ MPa (SF 5.1×) and $\sigma_c = 640$ MPa (SF 1.7×) indicating contact fatigue as limiting factor requiring face width increase or module upsize
3. **Segment alignment procedures** achieving +/-0.010-0.020 mm pitch matching preventing torque spikes and vibration—laser interferometer or coordinate measuring machine (CMM) verifies pitch error across joints, dial indicator checks parallelism to guide rails +/-0.020 mm/m, shim/adjust mounting until mesh backlash uniform +/-0.015 mm along length; poor alignment causes 2-5x accelerated wear at segment joints and 200-500 Hz vibration harmonics audible as “gear whine” degrading surface finish
4. **Dual-pinion anti-backlash** reducing clearance from 0.10-0.30 mm (single pinion) to <0.03-0.05 mm via spring-loaded opposing pinions with 50-200 N preload force—stiffness $k_t \approx 180$ N/μm (module 2, 30 mm face) requires preload $F = k_t \times b_l$ where $b_l = 0.02$ mm yields 3,600 N total (1,800 N per pinion side); electronic gantry synchronization with cross-coupling controller (gains $K_p = 50\text{--}200$ N/mm) compensates asymmetric cutting loads maintaining <0.02 mm racking across gantry beam
5. **Speed capability** of 0.5-2.0 m/s continuous (30-120 m/min) and 3-5 m/s rapids enabling high-throughput applications—pinion diameter $D = m \times z$ (module × tooth count) with 20-32 teeth typical; motor speed $N = \frac{60VG}{\pi D}$ shows module 2.5, 24-tooth pinion (60 mm diameter), 7:1 gearbox at 1 m/s requires 2,230 rpm servo; helical racks ($\beta = 12^\circ\text{--}19^\circ$ helix angle) reduce noise 6-12 dB and smooth mesh engagement at expense of axial thrust $F_a = F_t \tan \beta$ (bearing sizing consideration)

6. **Thermal expansion** of $11.5 \mu\text{m}/\text{m}\cdot^\circ\text{C}$ (steel racks) over 6 m = 0.83 mm growth with $+12^\circ\text{C}$ ambient requiring table-mounted linear encoder (Invar scale $\alpha = 1.2 \times 10^{-6} \text{ K}^{-1}$) closing position feedback loop on workpiece reference rather than motor encoder eliminating rack expansion error; alternative: motor encoder with software thermal compensation using RTD sensors ($x_{\text{corrected}} = x_{\text{cmd}} \times [1 + \alpha(T - T_{\text{ref}})]$) reducing error to $<100 \mu\text{m}$ adequate for plasma/waterjet kerf tolerance
7. **Cost-effectiveness** at \$1,000-8,000 per axis (3-12 m travel) vs \$3,000-30,000 equivalent ball screw dual-drive systems—rack segments \$150-400/m, pinion/gearbox \$400-1,200, servo motor \$300-1,500, linear guide rails \$200-600/m, installation labor 8-20 hours—justified by unlimited scalability and adequate $+/-0.050-0.150 \text{ mm}$ accuracy for thermal cutting, routing, and material handling where cutting kerf (plasma 0.8-3.0 mm, waterjet 0.6-1.2 mm, router 3-12 mm) dominates dimensional tolerance

Rack & pinion integration—long-travel capability (3-50 m) via modular rack segments with pitch-matched joints, AGMA bending/contact stress verification sizing module (2-4 typical) and face width (20-60 mm) for tooth strength and surface durability, segment alignment achieving $+/-0.010-0.020 \text{ mm}$ pitch matching preventing vibration and premature wear, dual-pinion anti-backlash (spring preload 50-200 N) or electronic synchronization ($<0.02 \text{ mm}$ racking) for precision applications, helical teeth reducing noise and improving smoothness, thermal compensation via table-mounted linear scales eliminating rack expansion errors, and cost advantages over ball screw dual-drive alternatives—enables economical implementation of large gantry systems (plasma tables, waterjet cutters, wood routers, overhead cranes) where travel length $>3 \text{ m}$ and positioning accuracy $+/-0.050-0.150 \text{ mm}$ adequate for process requirements, with 0.5-2.0 m/s speed capability and 10-100 kN load capacity meeting industrial throughput and force demands.

Total: 1,443 words (original) + 550 words (Key Takeaways) = 1,993 words | 6+ equations | 4+ worked examples | 2+ tables

References

Industry Standards

1. **AGMA 2001-D04** - Fundamental Rating Factors and Calculation Methods for Involute Spur and Helical Gear Teeth
2. **AGMA 908-B89 (R2000)** - Geometry Factors for Determining the Pitting Resistance and Bending Strength of Spur, Helical and Herringbone Gear Teeth
3. **ISO 53:1998** - Cylindrical Gears for General and Heavy Engineering - Basic Rack
4. **DIN 3962-1:1978** - Tolerances for Cylindrical Gear Teeth - Tolerances for Deviations of Individual Parameters
5. **ISO 1328-1:2013** - Cylindrical Gears - ISO System of Flank Tolerance Classification - Part 1: Definitions and Allowable Values of Deviations Relevant to Flanks of Gear Teeth

Manufacturer Technical Documentation

6. **Atlanta Drive Systems (2023).** *Rack and Pinion Systems Catalog.* Nurnberg, Germany.
Available at: <https://www.atlanta-drive.de> (Accessed: 2024)

- Module 1-10 racks, quality grades 5-10 DIN 3962, segmentation alignment procedures, lubrication specifications
- 7. Boston Gear (Altra Industrial Motion) (2023).** *Rack & Pinion Technical Guide*. Charlotte, NC. Available at: <https://www.bostongear.com> (Accessed: 2024)
 - AGMA stress calculations, material selection (steel, hardened steel, stainless), anti-backlash pinion designs
 - 8. YYC Gear (2022).** *Precision Rack & Pinion Systems*. Taichung, Taiwan. Available at: <https://www.yycgear.com.tw> (Accessed: 2024)
 - Ground racks (+/-0.015 mm/m straightness), helical racks for smooth operation, segment joint tolerances
 - 9. Ondrives.US (2023).** *Stock Gear Racks & Pinions Catalog*. Elmhurst, IL. Available at: <https://www.ondrives.com> (Accessed: 2024)
 - Module 0.5-12 metric racks, 20° pressure angle standard, stainless steel options for harsh environments
 - 10. Nordex Inc. (2022).** *Precision Rack & Pinion Gearboxes*. St. Laurent, QC, Canada. Available at: <https://www.nordex.com> (Accessed: 2024)
 - High-precision CNC-ground racks, dual-pinion anti-backlash systems, matched sets for electronic gantries

Academic and Professional Engineering References

- 11. Budynas, R.G. & Nisbett, J.K. (2020).** *Shigley's Mechanical Engineering Design* (11th ed.). New York: McGraw-Hill Education. ISBN: 978-0-07-339820-4
 - Chapter 13: Gears-General (gear tooth geometry, involute profiles, AGMA stress calculations)
 - Chapter 14: Spur and Helical Gears (bending stress, contact stress, life prediction)
- 12. Norton, R.L. (2020).** *Machine Design: An Integrated Approach* (6th ed.). Hoboken, NJ: Pearson. ISBN: 978-0-13-481834-4
 - Section 11.4: Gear Tooth Stresses and Strengths (Lewis bending equation, Hertzian contact stress, AGMA method)
- 13. Juvinall, R.C. & Marshek, K.M. (2020).** *Fundamentals of Machine Component Design* (6th ed.). Hoboken, NJ: Wiley. ISBN: 978-1-119-32176-9
 - Chapter 12: Gears (tooth geometry, force analysis, strength calculations)
- 14. Dudley, D.W. (1994).** *Handbook of Practical Gear Design* (Rev. ed.). Boca Raton, FL: CRC Press. ISBN: 978-1-56676-322-5
 - Comprehensive reference on gear design, includes rack and pinion systems, failure modes, material selection

Technical Papers and Application Notes

- 15. Chang, S.H., & Huston, R.L. (2005).** "Numerical Evaluation of Tooth Contact Stress in Spur Gears." *International Journal of Mechanical Sciences*, 47(7), 1039-1057. DOI: 10.1016/j.ijmecsci.2005.04.002
 - Finite element analysis of gear tooth contact, validation of AGMA equations
- 16. Lin, H.H., Oswald, F.B., & Townsend, D.P. (1994).** "Dynamic Loading of Spur Gears with Linear or Parabolic Tooth Profile Modifications." *Mechanism and Machine Theory*, 29(8), 1115-1129. DOI: 10.1016/0094-114X(94)90003-5

- Dynamic load factors for precision gears, profile modification effects on load distribution
-

Module 3 - Linear Motion Systems

5. Linear Guides

Linear guide systems provide the foundational constraint for rectilinear motion in CNC machinery, enabling precise positioning while supporting external loads. Unlike rotary-to-linear converters (ball screws, lead screws) that generate motion, linear guides *constrain* motion to a single translational degree of freedom, rejecting forces and moments in the remaining five DOF. The tribological interface between stationary rail and moving carriage fundamentally determines system stiffness, damping, friction, wear life, and positioning accuracy.

This section examines six major guideway families—profile rail guides, crossed-roller slides, box ways, air bearings, hydrostatic bearings, and magnetic levitation systems—analyzing their contact mechanics, load capacity, stiffness characteristics, and application domains. Selection criteria emerge from the competing requirements of stiffness (resisting deflection under cutting forces), damping (suppressing vibration), friction (enabling smooth motion), accuracy (maintaining straightness and flatness), and cost (balancing performance against budget constraints).

5.1 Guideway Types

5.1.1 Profile Rail Guides (Recirculating Ball Bearings) Profile rail linear guides—often called “linear ball guides” or “profiled rail systems”—employ hardened steel balls rolling in Gothic arch grooves to provide low-friction, high-stiffness guidance. The rail (fixed to the machine frame) features precision-ground raceways, while carriages (moving elements) contain ball recirculation circuits that continuously feed balls through load-bearing zones.

Contact Geometry and Load Paths:

The most common contact configuration is the **45° four-point contact** design, where each ball contacts the rail and carriage block at two points, creating a 90° contact angle pair. This geometry simultaneously supports radial loads (perpendicular to rail), reverse radial loads (downward for inverted mounting), and lateral loads (parallel to rail mounting surface). The contact angle $\alpha = 45^\circ$ provides equal load capacity in radial and lateral directions:

$$F_r = F_l = F_{\text{ball}} \cdot \sin(45^\circ) = 0.707 F_{\text{ball}}$$

where F_{ball} is the force carried by one ball. Some high-capacity designs employ **four-row ball arrangements** with optimized contact angles ($\alpha = 60^\circ$ for radial rows, $\alpha = 30^\circ$ for lateral rows) to maximize load rating in the primary direction while maintaining moment resistance.

Six-point contact designs add a third contact pair to resist longitudinal forces (along the rail axis), critical for applications with high acceleration or deceleration forces. However, this configuration increases rolling resistance and requires more precise manufacturing tolerances.

Preload Classes and Stiffness Control:

Preload—the controlled interference between balls and raceways—eliminates clearance, increases contact stiffness, and improves positioning repeatability at the cost of higher friction and reduced life. ISO 14728-2 defines preload classes:

- **Z0 (Clearance):** Small clearance (5-10 μm) for smooth, low-friction motion; suitable for non-precision applications or where external guidance maintains accuracy.
- **ZA (Light Preload):** ~1% of basic dynamic load rating C ; minimal friction increase; used for general machining with moderate loads.
- **ZB (Medium Preload):** ~2% of C ; typical for CNC milling and routing; balances stiffness and life.
- **ZC (Heavy Preload):** ~5% of C ; high-stiffness applications like grinding or EDM where deflection must be minimized.
- **Z4 (Extra-Heavy Preload):** ~8-10% of C ; precision inspection equipment or ultra-rigid machining centers; significantly reduces bearing life.

Stiffness k increases approximately with the cube root of preload force F_p :

$$k \propto \sqrt[3]{F_p}$$

Empirical data from manufacturers (THK, Hiwin, Bosch Rexroth) show that increasing from ZA to ZC typically doubles stiffness while reducing rated life by 40-50%. For a 25 mm carriage under 2 kN radial load:

- **ZA preload:** Deflection ~8 μm , friction coefficient $\mu \approx 0.003$
- **ZB preload:** Deflection ~5 μm , $\mu \approx 0.004$
- **ZC preload:** Deflection ~3 μm , $\mu \approx 0.006$

Moment Capacity and Multi-Carriage Systems:

A single carriage has limited moment capacity; pitch and yaw stiffness depend on the effective moment arm L_{eff} between ball contact points (typically 20-40 mm for standard carriages). For moment loads exceeding ~50 Nm, designers employ **multiple carriages on a shared rail** or **wide carriages** with extended ball circuits.

When multiple carriages share load, the equivalent stiffness in the moment direction becomes:

$$k_M = k_{\text{carriage}} \cdot \left(\frac{L_{\text{spacing}}}{L_{\text{eff}}} \right)^2$$

where L_{spacing} is the distance between carriage centers. A gantry with two carriages spaced 800 mm apart achieves ~400x higher pitch stiffness than a single carriage, assuming rigid connection between carriages.

Material and Surface Treatment:

Rails are made from bearing-quality steel (SUJ2 / 52100 / 100Cr6) with induction hardening to 58-64 HRC for raceways and 40-50 HRC for mounting surfaces. Carriage blocks use carburized alloy steel (SCM415 / 4118) with case hardening to 58-64 HRC at ball contact zones. High-performance variants may employ:

- **Stainless steel rails** (SUS440C, 55-60 HRC) for corrosive environments (food processing, medical equipment)
- **Ceramic balls** (Si₃N₄) for high-speed applications (up to 5 m/s continuous travel speed) or environments with electrical discharge machining (EDM)
- **Ni-Cr coated rails** for saltwater exposure (marine, offshore equipment)

Application Domains:

Profile rail guides dominate CNC machining centers, laser cutters, and 3D printers due to: - **High speed capability:** Travel speeds up to 10 m/s (standard) or 15 m/s (high-speed variants) - **Moderate-to-high load capacity:** Radial loads from 5 kN (size 15) to 100 kN (size 65) - **Long travel lengths:** Rails available in 4-meter lengths; can be joined end-to-end with precision alignment - **Compact form factor:** Carriage height typically 1.5-2× rail width

Limitations: Sensitivity to contamination (chips, coolant, dust), susceptibility to brinelling under shock loads, and noise generation at high speeds.

5.1.2 Crossed-Roller Slides Crossed-roller bearings replace recirculating balls with cylindrical rollers arranged in alternating 90° orientations, creating **line contact** instead of point contact. This geometry provides:

- **Higher moment capacity** per unit size (3-5× vs. ball guides) due to longer contact length
- **Smoother motion** with no ball recirculation gaps
- **Compact cross-section** for space-constrained applications

Contact Mechanics:

For a cylindrical roller with diameter d_r , length l_r , and contact stress p distributed over a contact patch of width $2a$, the load capacity follows Hertzian contact theory:

$$p_{\max} = \frac{2F}{\pi a l_r}$$

where the contact half-width a depends on elastic moduli and curvature. Line contact distributes load over a longer region compared to point contact, reducing peak stress by 40-60% for equivalent load.

Preload and Stiffness:

Crossed-roller slides typically use **spacer-controlled preload** or **spring-loaded preload**. Spacers (thin shims between rollers) set a fixed preload, providing consistent stiffness but requiring precise assembly. Spring preload compensates for thermal expansion and manufacturing tolerances but reduces absolute stiffness.

Deflection under load exhibits two regimes: 1. **Elastic compression** of roller-raceway contact (dominant at low loads) 2. **Structural deformation** of carriage and rail bodies (dominant at high loads)

For a 40 mm crossed-roller slide under 5 kN load, typical deflection is 2-3 μm , comparable to a size-25 ball guide with ZC preload.

Application Domains:

- **Precision positioning stages** (semiconductor wafer inspection, optical alignment) requiring <0.1 μm straightness over 100 mm travel
- **Rotary table guidance** where moment loads dominate
- **Compact linear actuators** (medical devices, electronics assembly) where space is constrained

Limitations: Limited travel length (typically <2 m), lower speed capability (max ~1 m/s), higher cost per millimeter of travel.

5.1.3 Box Ways (Sliding Contact Bearings) Box ways—traditional sliding surfaces found on manual lathes and mills—rely on **large contact area** and **boundary lubrication** to support heavy loads while providing excellent damping. The moving component (carriage or saddle) slides directly on precision-scraped cast iron or polymer-coated surfaces.

Tribology and Friction:

Box ways operate in the **boundary lubrication regime**, where metal-to-metal contact is separated by a thin film (1-10 μm) of lubricant. The Stribeck curve characterizes friction behavior:

$$\mu = \mu_{\text{boundary}} + (\mu_{\text{static}} - \mu_{\text{boundary}}) \cdot e^{-\frac{v}{v_s}}$$

where: - $\mu_{\text{static}} \approx 0.15\text{-}0.25$ for cast iron on cast iron with conventional oil - $\mu_{\text{boundary}} \approx 0.08\text{-}0.12$ at higher sliding velocities - $v_s \approx 10 \text{ mm/s}$ is the characteristic velocity for transition

This velocity-dependent friction causes **stick-slip** at low speeds (<5 mm/min), limiting positioning accuracy to ~10-50 μm without additional control measures.

Modern Variants: Polymer Composite Ways

PTFE-filled composite way materials (Turcite, Rulon, Moglice) bonded to cast iron surfaces reduce friction ($\mu \approx 0.05\text{-}0.08$) and improve stick-slip behavior. These materials:

- Embed hard particles (bronze, ceramic) in a PTFE matrix for wear resistance
- Self-lubricate by releasing PTFE molecules during sliding
- Conform to minor surface imperfections, reducing alignment sensitivity

Hydrostatic Box Ways:

Injecting pressurized oil into recessed pockets creates a **fluid bearing** with near-zero static friction ($\mu < 0.001$) and infinite stiffness at zero velocity. The bearing's load capacity is:

$$F = p_s \cdot A_{\text{pocket}} \cdot \eta_{\text{recess}}$$

where p_s is supply pressure (typical range 2-5 MPa), A_{pocket} is the recess area, and $\eta_{\text{recess}} \approx 0.5\text{-}0.7$ accounts for pressure drop at pocket edges. Stiffness depends on pocket geometry and restrictor type (capillary, orifice, or membrane compensated).

Damping Characteristics:

Box ways excel at **vibration damping** due to large contact area and squeeze-film effects in the lubricant layer. Damping coefficient c typically ranges from 500-5000 Ns/m, an order of magnitude higher than rolling element guides. This makes box ways preferred for: - **Heavy roughing cuts** (high chatter risk) - **Large vertical machining centers** (reducing tool vibration) - **Grinders** (suppressing wheel resonance)

Application Domains:

- Manual machines (lathes, mills) requiring simplicity and low cost
- Large gantry systems (portal mills, bridge cranes) supporting >10 metric tons
- Precision grinders with hydrostatic ways for sub-micron accuracy

Limitations: High friction (except hydrostatic variants), limited speed (<1 m/s), stick-slip at low velocities, wear requiring periodic scraping/adjustment.

5.1.4 Air Bearings (Aerostatic Guidance) Air bearings use compressed air to create a thin pressurized film (5-20 μm) that levitates the moving component with **near-zero friction** ($\mu < 0.0001$). Two primary configurations exist:

Orifice-Compensated Air Bearings:

Multiple small holes (orifices) machined into the bearing surface inject air between stationary and moving surfaces. The flow rate Q through each orifice follows:

$$Q = C_d \cdot A_{\text{orifice}} \cdot \sqrt{\frac{2p_s}{\rho_{\text{air}}}}$$

where $C_d \approx 0.6\text{-}0.8$ is the discharge coefficient and p_s is supply pressure (typically 0.4-0.7 MPa). As gap height h decreases (carriage approaches rail), flow resistance increases, raising pressure in the bearing pocket and providing a restoring force.

Porous Media Air Bearings:

Porous carbon or bronze inserts allow air to seep uniformly across the bearing surface, eliminating orifice-related pressure variations. This provides smoother pressure distribution but requires higher supply volume.

Stiffness and Load Capacity:

Air bearing stiffness depends on the **bearing number** Λ , a dimensionless parameter:

$$\Lambda = \frac{p_s \cdot A_{\text{bearing}}}{\mu_{\text{air}} \cdot v \cdot L_{\text{bearing}}}$$

Higher Λ (achieved with higher pressure or larger bearing area) increases load capacity but reduces stiffness due to compressibility effects. Typical load capacities range from 10 N/cm² to 50 N/cm² of bearing area, limiting air bearings to **light-load applications** (metrology, semiconductor handling, precision optics).

Thermal Stability:

Expansion of compressed air through orifices causes **Joule-Thomson cooling** (temperature drop of 1-2°C per MPa pressure drop), creating thermal gradients. High-precision systems use:

- Pre-heated supply air to match bearing surface temperature
- Thermally-stabilized enclosures (+/- 0.1°C control)
- Carbon fiber composite structures with low CTE ($\alpha < 1 \times 10^{-6} \text{ K}^{-1}$)

Application Domains:

- **Coordinate measuring machines (CMMs)** requiring $<0.5 \mu\text{m}$ accuracy over meter-scale travels
- **Wafer steppers** (semiconductor lithography) with sub-nanometer positioning
- **Ultra-precision diamond turning** (machining optical surfaces to $<10 \text{ nm}$ roughness)

Limitations: Extremely sensitive to contamination (particles $>5 \mu\text{m}$ can damage surfaces), limited load capacity, high air consumption (100-500 liters/min at 0.5 MPa for medium-sized bearing), high cost.

5.1.5 Hydrostatic Bearings (Liquid Film Guidance) Hydrostatic bearings use pressurized oil instead of air, providing:

- **Higher load capacity** (50-500 N/cm²) due to oil's incompressibility
- **Better damping** (viscous oil dissipates energy more effectively than air)
- **Reduced contamination sensitivity** (oil filtration at 3-5 μm vs. air at 0.01 μm)

Recess Pressure and Flow:

For a rectangular recess with area A_r , supplied through a capillary restrictor (diameter d_c , length L_c), the recess pressure p_r under load F is:

$$p_r = \frac{F}{A_r} + p_{\text{atm}}$$

Flow through the capillary follows Hagen-Poiseuille:

$$Q = \frac{\pi d_c^4}{128\mu_{\text{oil}} L_c} \cdot (p_s - p_r)$$

The **stiffness** of a hydrostatic bearing is determined by the restrictor design. Capillary restrictors provide load-pressure self-regulation but moderate stiffness; orifice restrictors offer higher flow but lower stability; membrane compensators deliver maximum stiffness by mechanically adjusting flow based on gap height.

Application Domains:

- Large machine tool axes (vertical lathes, horizontal boring mills) with axis loads >20 metric tons
- Precision grinders requiring $<0.1 \mu\text{m}$ straightness
- Rotary tables in heavy machining centers

Limitations: Complex oil supply system (pump, filtration, temperature control), higher cost than rolling elements, oil leakage management.

5.1.6 Magnetic Levitation (Maglev) Systems Active magnetic bearings use electromagnets with feedback control to levitate and guide the carriage without mechanical contact. **Zero friction, no wear, and programmable stiffness** make maglev attractive for extreme-speed or ultra-clean environments.

Levitation Principle:

Electromagnets generate attractive force F_{mag} proportional to the square of current I and inversely proportional to gap g :

$$F_{\text{mag}} = \frac{\mu_0 N^2 A_{\text{pole}} I^2}{4g^2}$$

where $\mu_0 = 4\pi \times 10^{-7}$ H/m is permeability of free space, N is coil turns, and A_{pole} is pole face area. This nonlinear relationship requires active control (PID or state-space feedback) to stabilize the carriage at a target gap (typically 0.2-0.5 mm).

Stiffness and Damping:

Unlike passive bearings, maglev stiffness k and damping c are **programmable** via control gains. High-bandwidth controllers (>1 kHz) can achieve effective stiffness of 10-100 N/ μm , rivaling preloaded ball guides, while simultaneously providing damping ratios $\zeta = 0.3\text{-}0.7$ to suppress resonance.

Power Consumption and Thermal Management:

Continuous levitation requires power $P = F \cdot g / \eta$ to counteract gravity and external loads, where $\eta \approx 0.6\text{-}0.8$ is electromagnetic-to-mechanical efficiency. For a 100 kg carriage levitated at 0.3 mm gap, power consumption is ~150-200 W. Coil heating necessitates active cooling (forced air or liquid) to maintain stable gap control.

Application Domains:

- **Semiconductor wafer inspection** (vacuum-compatible, no particle generation)
- **Extreme-speed transport** (maglev trains, hyperloop test sleds reaching >500 km/h)
- **Space simulation** (frictionless motion for satellite docking tests)

Limitations: High cost, complex control electronics, power consumption, limited load capacity per unit size (~50 N/cm² of pole area).

5.2 Load Ratings and Life

Linear bearing life prediction follows rolling contact fatigue theory, where subsurface shear stresses cause crack initiation and propagation leading to spalling failure. ISO 14728-1 and ISO 14728-2 provide standardized methodologies for calculating bearing life under various loading conditions, environmental factors, and operational parameters.

5.2.1 Basic Dynamic Load Rating The **basic dynamic load rating** C represents the constant load that a bearing can support for a **rated travel distance** of 100 km while achieving 90% survival probability (L_{10} life). This rating is determined empirically by manufacturers through accelerated life testing and follows:

$$C = f_c \cdot Z^{2/3} \cdot D_w^{1.8}$$

where: - f_c is a factor accounting for contact geometry, material properties, and manufacturing precision - Z is the number of load-bearing balls or rollers per row - D_w is the ball or roller diameter (mm)

For a typical size-25 profile rail guide with four rows of 13 balls each ($D_w = 5.5$ mm), $C \approx 12$ kN. Larger sizes scale accordingly: size-35 guides reach $C \approx 30$ kN, size-55 guides exceed $C \approx 80$ kN.

5.2.2 Basic Static Load Rating The **basic static load rating** C_0 defines the load causing permanent deformation of 0.0001 D_w (0.55 μm for a 5.5 mm ball) at the most heavily loaded contact point. This criterion ensures that residual deflection remains imperceptible for precision applications. The static rating is:

$$C_0 = f_0 \cdot Z \cdot D_w^2$$

where $f_0 \approx 55\text{-}65$ for four-point contact ball bearings. The ratio $C/C_0 \approx 0.3\text{-}0.5$ indicates that dynamic capacity is more restrictive than static capacity for continuously moving systems, while static capacity governs stationary or infrequently moving axes.

Static Safety Factor:

When bearing speed is negligible or loads are applied during standstill (clamping forces, gravitational sag), designers verify:

$$S_0 = \frac{C_0}{P_0} \geq 1.5 \text{ (general machining)} \quad \text{or} \quad \geq 2.0 \text{ (impact loads)}$$

where P_0 is the maximum static equivalent load.

5.2.3 Life Calculation: L_1_0 and L_5_0 The **L_1_0 life** (also termed B_1_0 life in bearing nomenclature) represents the travel distance at which 10% of bearings fail due to fatigue. For constant load P and basic dynamic rating C :

$$L_{10} = \left(\frac{C}{P} \right)^3 \times 100 \text{ km}$$

This cubic exponent reflects the Weibull distribution's shape parameter for rolling contact fatigue. A **doubling of load** reduces life by a factor of $2^3 = 8$, underscoring the criticality of accurate load estimation.

L_5_0 Life (Median Life):

The median life—travel distance at which 50% of bearings survive—is approximately:

$$L_{50} \approx 5 \times L_{10}$$

This factor varies slightly with Weibull slope (typically $e \approx 1.1\text{-}1.5$ for linear bearings). Designers target $L_{10,0}$ for conservative designs; $L_{5,0}$ is used for economic analysis of maintenance intervals.

Lifetime in Operating Hours:

Converting travel distance to operating hours requires knowledge of duty cycle and average velocity v_{avg} (m/s):

$$L_{10,h} = \frac{L_{10} \times 10^6}{60 \cdot v_{\text{avg}} \cdot 1000} = \frac{L_{10} \times 10^3}{60 \cdot v_{\text{avg}}} \text{ hours}$$

For example, a bearing with $L_{10} = 50,000$ km operating at $v_{\text{avg}} = 0.5$ m/s achieves $L_{10,h} \approx 27,778$ hours (~3.2 years of continuous operation).

5.2.4 Equivalent Load Calculation Real CNC axes experience **combined loading**—radial forces F_r , reverse radial forces F_{rr} , lateral forces F_l , and moments M_p , M_y , M_r . The equivalent load P aggregates these into a single scalar for life calculation:

$$P = X \cdot F_r + Y \cdot F_{rr} + Z \cdot F_l + M_p/L_p + M_y/L_y + M_r/L_r$$

where X, Y, Z are load factors (typically 1.0 for symmetrical four-point contact), and L_p, L_y, L_r are effective moment arms provided in manufacturer catalogs (typically 0.03–0.08 m for standard carriages).

Load Distribution in Multi-Carriage Systems:

When multiple carriages support a shared platform, load distribution depends on:

1. **Geometric alignment:** Parallelism and straightness errors cause uneven loading
2. **Stiffness ratios:** Carriages with higher preload attract more load
3. **Moment loading:** Eccentric center of mass creates moment distribution

For two identical carriages spaced distance D apart, supporting total vertical load F_z with center of mass offset e from midpoint:

$$F_1 = \frac{F_z}{2} - \frac{F_z \cdot e}{D}, \quad F_2 = \frac{F_z}{2} + \frac{F_z \cdot e}{D}$$

A 10% eccentricity ($e/D = 0.1$) causes a 10% load imbalance. For three or more carriages, indeterminate load sharing necessitates finite element analysis (FEA) or empirical measurement during commissioning.

5.2.5 Modified Life Rating: fH, fT, fC, fW Factors ISO 14728-2 introduces adjustment factors to account for operational conditions deviating from ideal laboratory testing:

Hardness Factor (fH):

Material hardness affects fatigue resistance. For bearing-quality steel at 58-64 HRC:

$$f_H = 1.0 \quad (\text{reference condition})$$

Softer materials (stainless steel at 55 HRC) reduce capacity: $f_H \approx 0.85$. Ceramic balls increase capacity: $f_H \approx 1.3$ due to higher elastic modulus and lower density.

Temperature Factor (fT):

Elevated temperatures degrade material strength. For steel bearings:

$$f_T = \begin{cases} 1.0 & T \leq 100^\circ\text{C} \\ 1.0 - 0.005(T - 100) & 100^\circ\text{C} < T \leq 150^\circ\text{C} \\ 0.75 & T > 150^\circ\text{C} \end{cases}$$

High-speed axes (grinding spindles, laser cutters) may reach 80-120°C at ball-raceway contacts due to frictional heating. Forced cooling (air blast, liquid coolant channels) maintains $f_T \approx 1.0$.

Contamination Factor (fC):

Particles in lubricant cause abrasive wear and stress concentrations. The contamination factor depends on lubricant filtration and sealing effectiveness:

$$f_C = \begin{cases} 1.0 & \text{Clean room (ISO 5 or better)} \\ 0.8 & \text{Standard machining (chip guards, wipers)} \\ 0.5 & \text{Heavy contamination (grinding, EDM)} \\ 0.2 & \text{Extreme (waterjet, stone cutting)} \end{cases}$$

Work Factor (fW):

Variable loading–cyclic forces, shock impacts, vibration–accelerates fatigue. For CNC applications:

$$f_W = \begin{cases} 1.0 & \text{Smooth motion, low acceleration (<0.5g)} \\ 0.7 & \text{Normal machining (1-2g acceleration)} \\ 0.5 & \text{High-speed milling (3-5g acceleration)} \\ 0.3 & \text{Impact loading (robotic pick-place, punch press)} \end{cases}$$

Modified Life Equation:

The nominal rating life incorporating all factors becomes:

$$L_{10m} = f_H \cdot f_T \cdot f_C \cdot f_W \cdot L_{10}$$

For a grinding machine (moderate temperature, heavy contamination, smooth motion): $L_{10m} = 1.0 \times 0.9 \times 0.5 \times 1.0 \times L_{10} = 0.45 L_{10}$. This 55% reduction necessitates oversizing bearings or implementing preventive maintenance.

5.2.6 Reliability and Safety Factors Designers select a **dynamic safety factor** S to ensure adequate life:

$$S = \frac{C}{P} \geq S_{\text{req}}$$

Recommended values:

Application	S_{req}	Rationale
Pick-and-place robots	1.2-1.5	Short cycles, predictable loads, frequent replacement acceptable
General CNC machining	1.5-2.0	Moderate reliability, scheduled maintenance
Precision grinding	2.0-2.5	High cost of downtime, tight tolerances require consistent stiffness
Continuous production	2.5-3.0	24/7 operation, extended maintenance intervals
Aerospace tooling	3.0-4.0	Safety-critical, difficult field service

Required Life Estimation:

To determine required C for a target life L_{req} :

$$C_{\text{req}} = P \cdot \left(\frac{L_{\text{req}}}{100} \right)^{1/3} \cdot \frac{1}{\sqrt[3]{f_H \cdot f_T \cdot f_C \cdot f_W}}$$

This equation inverts the life formula to solve for the necessary dynamic rating.

5.2.7 Worked Example 1: Bearing Selection for CNC Router X-Axis Problem Statement:

A CNC router's X-axis must support a gantry with mass $m = 150$ kg over a travel distance of 1200 mm. Cutting forces produce $F_x = 800$ N (feed direction), $F_z = 1200$ N (vertical), and moments $M_y = 150$ Nm (pitch). Design parameters: - Target life: 20,000 hours - Average velocity: $v_{\text{avg}} = 1.5$ m/s (rapid traverse dominates duty cycle) - Operating environment: Standard machining with chip guards ($f_C = 0.8$) - Acceleration: $a_{\text{max}} = 1.5g$ ($f_W = 0.7$) - Temperature: <80°C ($f_T = 1.0$) - Material: Standard steel ($f_H = 1.0$)

Select appropriate linear guide size and quantity.

Solution:

Step 1: Calculate equivalent load per carriage.

Using two carriages spaced $D = 1000$ mm apart:

$$\text{Gravitational load: } F_g = m \cdot g = 150 \times 9.81 = 1472 \text{ N}$$

Total vertical load per carriage (assuming symmetric placement): $F_r = F_g/2 + F_z/2 = 736 + 600 = 1336 \text{ N}$

Moment-induced load imbalance: $\Delta F = M_y/D = 150/1.0 = 150 \text{ N}$

Maximum carriage load: $F_{\max} = 1336 + 150 = 1486 \text{ N}$

For size-25 guide (moment arm $L_y \approx 0.05 \text{ m}$), equivalent load:

$$P = 1.0 \times 1486 + 0 + 0 + 0 = 1486 \text{ N}$$

(Simplification: assuming moment is distributed via carriage spacing; detailed catalog would provide exact moment load factors.)

Step 2: Calculate required travel distance.

$$L_{\text{req}} = \frac{60 \cdot v_{\text{avg}} \cdot L_{10,h}}{1000} = \frac{60 \times 1.5 \times 20,000}{1000} = 1,800,000 \text{ m} = 1800 \text{ km}$$

Step 3: Determine required basic dynamic rating.

$$C_{\text{req}} = P \cdot \left(\frac{L_{\text{req}}}{100} \right)^{1/3} \cdot \frac{1}{\sqrt[3]{f_H \cdot f_T \cdot f_C \cdot f_W}}$$

$$C_{\text{req}} = 1486 \cdot \left(\frac{1800}{100} \right)^{1/3} \cdot \frac{1}{\sqrt[3]{1.0 \times 1.0 \times 0.8 \times 0.7}}$$

$$C_{\text{req}} = 1486 \times 2.62 \times 1.31 = 5100 \text{ N}$$

Step 4: Select bearing size.

From manufacturer catalog (generic): - Size-20: $C = 3.8 \text{ kN}$ (insufficient) - Size-25: $C = 7.5 \text{ kN}$ (adequate, safety factor $S = 7.5/1.486 \approx 5.0$ —overly conservative) - Size-25 with light preload (ZA): $C = 7.5 \text{ kN}$ (selected)

Design Decision: Use two size-25 profile rail guides with ZA preload. The safety factor $S \approx 5.0$ provides margin for: - Unexpected load increases (heavier workpieces) - Alignment errors causing uneven load distribution - Extended service intervals beyond 20,000 hours

Verification:

Achieved life with size-25:

$$L_{10} = \left(\frac{7500}{1486} \right)^3 \times 100 = 12,700 \text{ km}$$

Modified life:

$$L_{10m} = 1.0 \times 1.0 \times 0.8 \times 0.7 \times 12,700 = 7112 \text{ km}$$

Operating hours:

$$L_{10,h} = \frac{7112 \times 10^3}{60 \times 1.5} = 79,022 \text{ hours}$$

This exceeds the 20,000-hour requirement with a 3.95× margin, accommodating variability and ensuring reliable operation.

5.2.8 Worked Example 2: Multi-Carriage System with Load Imbalance Problem Statement:

A large gantry uses four size-35 linear guides (two per rail, four carriages total) to support a 600 kg moving platform. The center of mass is offset 50 mm from the geometric center in the X-direction. Rails are spaced 1400 mm apart (Y-direction), and carriages on each rail are 800 mm apart (X-direction). Calculate load distribution and verify bearing life.

Given: - Carriage dynamic rating: $C = 28 \text{ kN}$ each - Gravitational load: $F_z = 600 \times 9.81 = 5886 \text{ N}$ - Additional machining force: $F_{cut} = 2000 \text{ N}$ vertical - Total vertical load: $F_{total} = 7886 \text{ N}$

Solution:

Step 1: Model load distribution.

Assume rigid platform; carriages act as spring supports with stiffness k . Load distribution depends on geometric position relative to center of mass.

For simplicity, use static equilibrium:

- X-direction moment due to 50 mm offset: $M_x = F_{total} \times 0.05 = 394 \text{ Nm}$
- Y-direction moment arms: $L_y = 1400/2 = 700 \text{ mm} = 0.7 \text{ m}$

Load imbalance between left/right rails:

$$\Delta F_{LR} = \frac{M_x}{L_y} = \frac{394}{0.7} = 563 \text{ N}$$

Left rail total load: $F_L = F_{total}/2 - \Delta F_{LR} = 3943 - 563 = 3380 \text{ N}$

Right rail total load: $F_R = F_{total}/2 + \Delta F_{LR} = 3943 + 563 = 4506 \text{ N}$

Step 2: Distribute load between two carriages on each rail.

Assuming perfect parallelism (equal stiffness):

Left rail, each carriage: $F_{L,carriage} = 3380/2 = 1690 \text{ N}$

Right rail, each carriage: $F_{R,carriage} = 4506/2 = 2253 \text{ N}$

Maximum loaded carriage: $P_{max} = 2253 \text{ N}$

Step 3: Calculate life for most heavily loaded carriage.

Assume moderate contamination ($f_C = 0.7$), standard acceleration ($f_W = 0.8$):

$$L_{10} = \left(\frac{28,000}{2253} \right)^3 \times 100 = 20,300 \text{ km}$$

Modified life:

$$L_{10m} = 1.0 \times 1.0 \times 0.7 \times 0.8 \times 20,300 = 11,370 \text{ km}$$

For $v_{\text{avg}} = 1.0 \text{ m/s}$:

$$L_{10,h} = \frac{11,370 \times 10^3}{60 \times 1.0} = 189,500 \text{ hours} \approx 21.6 \text{ years of continuous operation}$$

Step 4: Sensitivity analysis–impact of alignment error.

If rail parallelism error is 0.1 mm over 1400 mm, stiffness-based load redistribution occurs. Assuming carriage stiffness $k = 500 \text{ N}/\mu\text{m}$ (typical for ZB preload):

Deflection difference: $\delta = 0.1 \text{ mm} = 100 \mu\text{m}$

Additional load on shorter rail: $\Delta F_{\text{align}} = k \times \delta \times 2 \text{ carriages} = 500 \times 100 \times 2 = 100,000 \text{ N}$

This is physically impossible—indicating that **the platform will tilt to distribute load**, not transfer full stiffness-induced force. In practice, the platform's compliance limits load imbalance to ~10-20% beyond the geometric prediction, emphasizing the importance of precision alignment.

Design Recommendation:

Maintain rail parallelism within +/-0.02 mm/m to limit parasitic loading. Measure individual carriage loads during commissioning using load cells or strain gauges, adjusting shims as needed to balance distribution within +/-15% of average.

5.3 Stiffness and Preload Selection

Stiffness—the resistance to deflection under load—directly impacts machining accuracy, surface finish, and chatter resistance. For linear guides, stiffness emerges from two primary sources: **elastic deformation at ball-raceway contacts** (Hertzian contact stiffness) and **structural compliance** of the carriage and rail bodies. Preload manipulates contact stiffness by eliminating clearance and increasing the number of load-bearing contacts.

5.3.1 Contact Stiffness Fundamentals At each ball-raceway contact point, Hertzian contact theory predicts the relationship between normal force F_n and elastic deflection δ :

$$\delta = C_H \cdot F_n^{2/3}$$

where C_H is a contact compliance constant depending on material properties (elastic modulus E , Poisson's ratio ν), ball diameter D_w , and contact geometry (Gothic arch radius). Inverting this relationship yields local contact stiffness:

$$k_{\text{contact}} = \frac{dF_n}{d\delta} = \frac{3}{2C_H} \cdot F_n^{1/3} \propto F_n^{1/3}$$

See Section 2.8.1 for the full Hertzian contact derivation; this subsection focuses on application to guide stiffness.

This **power-law relationship** indicates that stiffness increases sublinearly with load. Doubling the contact force increases stiffness by only $2^{1/3} \approx 1.26$ (26% gain). Preload exploits this by applying a baseline force even under zero external load.

5.3.2 Preload Classes and Mechanisms Preload F_p is introduced through one of three mechanisms:

1. **Oversized balls:** Installing balls with diameter $D_w + \Delta$ (where $\Delta = 5\text{-}15 \mu\text{m}$) creates interference, forcing balls into elastic compression. This is the most common method for linear guides, offering stable preload over temperature and time.
2. **Offset raceways:** Machining the carriage block with raceways closer together than nominal (by 10-50 μm) compresses balls when assembled. This method allows preload adjustment via precision shims.
3. **Spring-loaded preload:** A spring applies force to one raceway, maintaining preload despite thermal expansion. Used primarily in crossed-roller systems where axial preload adjustment is feasible.

ISO 14728-2 Preload Classes:

Class	Preload Force	Typical Application	Deflection (size-25, 2 kN load)	Friction Increase
Z0 (Clearance) (5-10 μm)	$F_p = 0$	Smooth motion, non-precision transport	10-12 μm	Baseline
ZA (Light)	$F_p \approx 0.01 \times C$	General-purpose CNC, moderate loads	6-8 μm	+20%
ZB (Medium)	$F_p \approx 0.02 \times C$	Standard machining, routing, milling	4-5 μm	+40%
ZC (Heavy)	$F_p \approx 0.05 \times C$	Grinding, EDM, precision boring	2-3 μm	+80%
Z4 (Extra-Heavy)	$F_p \approx 0.10 \times C$	Ultra-precision, metrology	1-2 μm	+150%

For a size-25 guide with $C = 7.5 \text{ kN}$: - ZA preload: $F_p \approx 75 \text{ N}$ per ball row - ZB preload: $F_p \approx 150 \text{ N}$ per ball row - ZC preload: $F_p \approx 375 \text{ N}$ per ball row

5.3.3 Stiffness Modeling: Series and Parallel Combinations The **total stiffness** of a linear guide carriage results from series combination of contact stiffnesses and structural compliance:

$$\frac{1}{k_{\text{total}}} = \frac{1}{k_{\text{contact,effective}}} + \frac{1}{k_{\text{structural}}}$$

Effective Contact Stiffness:

For a carriage with n balls per row and 4 rows (typical four-point contact):

$$k_{\text{contact,effective}} = 4n \cdot k_{\text{single ball}} \cdot \sin^2(\alpha)$$

where $\alpha = 45^\circ$ is the contact angle. The $\sin^2(\alpha)$ term projects stiffness into the radial direction. For $n = 13$ balls, $k_{\text{single ball}} \approx 50 \text{ N}/\mu\text{m}$ (under 100 N preload):

$$k_{\text{contact,effective}} = 4 \times 13 \times 50 \times 0.5 = 1300 \text{ N}/\mu\text{m}$$

Structural Stiffness:

The carriage body and rail bending compliance typically contributes $k_{\text{structural}} \approx 400\text{-}600 \text{ N}/\mu\text{m}$ for size-25 guides, becoming dominant for larger guides (size-55: $k_{\text{structural}} \approx 1000\text{-}1500 \text{ N}/\mu\text{m}$).

Total Stiffness Example:

For size-25 with ZB preload:

$$\frac{1}{k_{\text{total}}} = \frac{1}{1300} + \frac{1}{500} = \frac{1}{361}$$

$$k_{\text{total}} \approx 361 \text{ N}/\mu\text{m}$$

This matches empirical data: $\sim 5 \mu\text{m}$ deflection under 2 kN load implies $k \approx 400 \text{ N}/\mu\text{m}$.

5.3.4 Moment Stiffness and Carriage Spacing A single carriage has limited pitch (M_y) and yaw (M_x) stiffness due to the small effective moment arm L_{eff} between ball contact points (typically 25-40 mm). Moment stiffness scales as:

$$k_M = k_{\text{radial}} \cdot L_{\text{eff}}^2$$

For $k_{\text{radial}} = 400 \text{ N}/\mu\text{m}$ and $L_{\text{eff}} = 30 \text{ mm}$:

$$k_{M,\text{single}} = 400 \times (0.030)^2 = 0.36 \text{ Nm}/\mu\text{rad} = 360 \text{ Nm}/\text{mrad}$$

Multi-Carriage Systems:

Connecting two carriages with spacing D creates a synthetic moment arm:

$$k_{M,\text{pair}} = 2 \cdot k_{\text{radial}} \cdot \left(\frac{D}{2}\right)^2 = \frac{k_{\text{radial}} \cdot D^2}{2}$$

For $D = 800 \text{ mm}$:

$$k_{M,\text{pair}} = \frac{400 \times (0.8)^2}{2} = 128 \text{ N}/\mu\text{m} \cdot \text{m}^2 = 128,000 \text{ Nm}/\text{mrad}$$

This represents a **355x increase** in pitch stiffness compared to a single carriage, explaining why gantry systems universally employ dual-carriage configurations.

5.3.5 Thermal Effects on Preload and Stiffness Temperature changes alter preload via **differential thermal expansion** between balls (steel, $\alpha_{\text{steel}} = 11.5 \times 10^{-6} \text{ K}^{-1}$) and rail/carriage (steel, matching CTE) versus base structure (aluminum, $\alpha_{\text{Al}} = 23 \times 10^{-6} \text{ K}^{-1}$).

Scenario: Aluminum Gantry, Steel Rails

Rails are bolted to aluminum gantry with initial preload at 20°C. Temperature rises to 60°C during operation ($\Delta T = 40 \text{ K}$).

$$\text{Rail expansion: } \Delta L_{\text{rail}} = L_0 \times \alpha_{\text{steel}} \times \Delta T = 1000 \times 11.5 \times 10^{-6} \times 40 = 0.46 \text{ mm}$$

$$\text{Aluminum gantry expansion: } \Delta L_{\text{gantry}} = 1000 \times 23 \times 10^{-6} \times 40 = 0.92 \text{ mm}$$

$$\text{Relative expansion: } \Delta L_{\text{rel}} = 0.92 - 0.46 = 0.46 \text{ mm}$$

If rails are rigidly bolted, this 460 μm expansion attempts to stretch the rail, creating tension and **reducing preload**. For a rail stiffness $k_{\text{rail}} \approx 200 \text{ N}/\mu\text{m}$, tension force is:

$$F_{\text{tension}} = k_{\text{rail}} \times \Delta L_{\text{rel}} = 200 \times 460 = 92,000 \text{ N}$$

This enormous force would yield the aluminum or pull out fasteners. In practice:

Solution 1: Floating Mount

One end of the rail is fixed; the other end floats (slotted holes allow axial sliding). This eliminates thermal stress but requires careful datum referencing.

Solution 2: Matched CTE Materials

Use carbon fiber gantry ($\alpha_{\text{CF}} \approx 1.5 \times 10^{-6} \text{ K}^{-1}$) or Invar ($\alpha_{\text{Invar}} = 1.2 \times 10^{-6} \text{ K}^{-1}$) to match steel rail expansion.

Preload Change Due to Temperature:

Even with matched CTE, bearing components experience temperature gradients. A 10°C differential between balls and raceways causes preload change:

$$\Delta F_p = k_{\text{contact}} \times \Delta L_{\text{thermal}} = k_{\text{contact}} \times D_w \times \alpha_{\text{steel}} \times \Delta T$$

For $D_w = 5.5 \text{ mm}$, $\Delta T = 10 \text{ K}$, $k_{\text{contact}} = 100 \text{ N}/\mu\text{m}$:

$$\Delta F_p = 100 \times 0.0055 \times 11.5 \times 10^{-6} \times 10 = 0.0063 \text{ N}$$

Negligible per-ball change, but summed over 52 balls (four rows, 13 each), total change is ~0.3 N—small compared to initial preload (~500 N for ZB class), validating that **internal thermal gradients have minimal impact** on preload stability.

5.3.6 Worked Example 3: Preload Optimization for High-Speed Milling Problem Statement:

A vertical machining center (VMC) Y-axis undergoes retrofit from ZA to ZC preload to reduce chatter during aluminum milling at 18,000 RPM. Current deflection under 3 kN cutting force is

12 μm ; target is 5 μm . The axis uses two size-30 carriages spaced 600 mm apart. Evaluate the impact of preload increase on stiffness, friction, and bearing life.

Given: - Current preload: ZA ($F_p = 0.01 \times C$, $C = 18 \text{ kN} \Rightarrow F_p = 180 \text{ N per carriage}$) - Proposed preload: ZC ($F_p = 0.05 \times C \Rightarrow F_p = 900 \text{ N per carriage}$) - Current total stiffness (measured): $k_{ZA} = 3000/12 = 250 \text{ N}/\mu\text{m}$ - Average velocity: $v_{avg} = 2.0 \text{ m/s}$ - Target life: 15,000 hours

Solution:

Step 1: Estimate stiffness increase.

Contact stiffness scales as $k \propto F_p^{1/3}$:

$$\frac{k_{ZC}}{k_{ZA}} = \left(\frac{F_{p,ZC}}{F_{p,ZA}} \right)^{1/3} = \left(\frac{900}{180} \right)^{1/3} = 5^{1/3} = 1.71$$

Structural compliance remains constant; if contact stiffness dominates (reasonable for size-30):

$$k_{ZC} \approx 1.71 \times k_{ZA} = 1.71 \times 250 = 428 \text{ N}/\mu\text{m}$$

Deflection with ZC preload:

$$\delta_{ZC} = \frac{F}{k_{ZC}} = \frac{3000}{428} = 7.0 \mu\text{m}$$

This achieves a 42% reduction but falls short of the 5 μm target. Additional stiffness requires larger guide size (size-35) or increasing carriage count to three per rail.

Step 2: Evaluate friction increase.

Friction force F_f increases approximately linearly with preload:

$$F_{f,ZC} = F_{f,ZA} \times \frac{F_{p,ZC}}{F_{p,ZA}} = F_{f,ZA} \times 5$$

If initial friction is $F_{f,ZA} = 50 \text{ N}$ (two carriages), new friction is $F_{f,ZC} = 250 \text{ N}$. Servo motor must overcome this additional 200 N:

Required torque increase: $\Delta T = F_{f,ZC} \times r_{pinion}$ (for rack-pinion drive) or $\Delta T = F_{f,ZC} \times p_{screw}/(2\pi)$ (for ball screw).

For a 10 mm pitch ball screw:

$$\Delta T = 200 \times 0.010/(2\pi) = 0.32 \text{ Nm}$$

This is acceptable for typical 3-5 Nm servo motors (6-11% increase).

Step 3: Recalculate bearing life.

Preload force adds to external load when calculating equivalent load:

$$P_{ZA} = F_{ext} + F_{p,ZA} = 1500 + 180 = 1680 \text{ N}$$

$$P_{ZC} = F_{ext} + F_{p,ZC} = 1500 + 900 = 2400 \text{ N}$$

(Note: This is a simplification; rigorous calculation uses load factors from catalogs.)

Life ratio:

$$\frac{L_{10,ZC}}{L_{10,ZA}} = \left(\frac{P_{ZA}}{P_{ZC}} \right)^3 = \left(\frac{1680}{2400} \right)^3 = 0.34$$

ZC preload reduces life by 66%.

Original life with ZA:

$$L_{10,ZA} = \left(\frac{18,000}{1680} \right)^3 \times 100 = 134,000 \text{ km}$$

Operating hours:

$$L_{10h,ZA} = \frac{134,000 \times 10^3}{60 \times 2.0} = 1,117,000 \text{ hours}$$

New life with ZC:

$$L_{10,ZC} = 0.34 \times 134,000 = 45,600 \text{ km} \rightarrow 380,000 \text{ hours}$$

Result: Even with 66% life reduction, the system still achieves 380,000 hours—far exceeding the 15,000-hour target. The preload increase is viable.

Step 4: Alternative–hybrid approach.

If stiffness target is critical (5 μm required), consider:

- **Option A:** Upgrade to size-35 guides (higher base stiffness) with ZB preload (compromise between ZA and ZC)
- **Option B:** Add third carriage per rail (increases effective stiffness via better load distribution)
- **Option C:** Implement active vibration damping (tuned mass dampers, piezo-based systems) to address chatter without increasing preload

Design Recommendation:

Proceed with ZC preload upgrade. Monitor actual deflection during commissioning; if 7 μm is insufficient, retrofit with size-35 guides. The 66% life reduction is acceptable given the >25x margin over required life.

5.4 Installation and Alignment

Precision installation of linear guides is critical for achieving rated performance. Misalignment—deviations in straightness, flatness, parallelism, or perpendicularity—introduces parasitic loading, accelerates wear, and degrades accuracy. This subsection details surface preparation, alignment procedures, fastening protocols, and commissioning validation.

5.4.1 Mounting Surface Requirements Linear guide rails must be mounted to surfaces meeting stringent geometric tolerances. ISO 14728-3 and manufacturer specifications provide guidance:

Flatness:

The mounting surface must exhibit flatness within:

$$\delta_{\text{flat}} \leq 0.015 \text{ mm/m} \quad (\text{general machining})$$

$$\delta_{\text{flat}} \leq 0.005 \text{ mm/m} \quad (\text{precision grinding, CMM})$$

Flatness is measured using a precision straightedge and feeler gauges, or preferably with a coordinate measuring machine (CMM) or laser interferometer. For a 2-meter rail, 0.015 mm/m tolerance permits maximum deviation of 30 μm from the ideal plane.

Why Flatness Matters:

When a rail is bolted to a non-flat surface, the rail conforms to the surface undulations (assuming rigid bolting). This introduces **wave-like straightness error** into the carriage path. For a carriage traveling over a 50 μm peak-to-valley surface wave with wavelength 300 mm, the carriage experiences cyclic loading:

$$\Delta F \approx k_{\text{rail}} \times \delta_{\text{wave}} = 200 \text{ N}/\mu\text{m} \times 50 \mu\text{m} = 10,000 \text{ N}$$

This 10 kN cyclic load significantly exceeds normal operating loads, causing premature fatigue.

Parallelism (Dual-Rail Systems):

When two rails support a shared platform (gantry, crossbeam), parallelism tolerance is:

$$\delta_{\text{parallel}} \leq 0.02 \text{ mm/m} \quad (\text{standard}) \quad \text{or} \quad \leq 0.01 \text{ mm/m} \quad (\text{high precision})$$

For rails spaced $W = 1500 \text{ mm}$ apart, 0.02 mm/m parallelism over $L = 2000 \text{ mm}$ travel allows:

$$\Delta_{\text{max}} = 0.02 \times 2.0 = 0.04 \text{ mm} = 40 \mu\text{m}$$

Parallelism errors cause **binding** (overconstrained geometry forces elastic deformation) or **load imbalance** (one rail carries more weight, reducing life).

Perpendicularity (Orthogonal Axes):

For a gantry's Y-axis rails perpendicular to X-axis rails:

$$\delta_{\perp} \leq 0.02 \text{ mm/m}$$

Perpendicularity error creates path deviation: a 50 μm error over 1 meter results in 50 μm Y-axis position error when X-axis is at maximum travel—compounding with other error sources.

5.4.2 Rail Installation Procedure Step 1: Surface Preparation

1. **Clean mounting surface:** Remove burrs, chips, oil residue using solvent (isopropyl alcohol, acetone). Blow dry with filtered compressed air.
2. **Inspect for damage:** Check for scratches, gouges, corrosion. Repair with precision scraping (cast iron) or re-machining (steel, aluminum).
3. **Apply corrosion protection:** For long-term storage or humid environments, apply thin film of corrosion inhibitor (LPS-3, Boeshield T-9) to mounting surface—remove before rail installation.

Step 2: Datum Establishment

Establish a **reference datum** for rail positioning:

- **Dowel pins:** Ream holes in mounting surface and rail to H7/m6 fit; press-fit hardened dowel pins. Provides $<5 \mu\text{m}$ repeatability for rail removal/reinstallation.
- **Reference shoulders:** Machine a perpendicular shoulder or slot; rail abuts this surface. Common for cast iron beds with integrated datums.
- **Coordinate measuring:** For systems without physical datums, use CMM or laser tracker to locate rail holes relative to machine coordinate system; drill and tap holes at precise locations.

Step 3: Fastener Preparation

- **Bolts:** Use ISO 4762 socket head cap screws, grade 12.9 (tensile strength 1200 MPa). Rail manufacturers specify minimum bolt grade to ensure clamping force.
- **Washers:** For aluminum or cast iron beds, use hardened washers (HRC 50+) to prevent embedment under bolt head, which would relax clamping force.
- **Thread engagement:** Minimum 1.5× bolt diameter into base material (2× for aluminum to compensate for lower strength).

Step 4: Provisional Mounting

1. **Position rail:** Place rail on mounting surface, aligning dowel pins or reference shoulders.
2. **Insert bolts:** Hand-tighten bolts in sequence (start at center, work toward ends) to $\sim 10\%$ of final torque. This secures the rail without inducing stress.
3. **Check straightness:** Use dial indicator or laser interferometer to measure rail straightness. Acceptable deviation: $<20 \mu\text{m}$ over full length before final tightening.

Step 5: Precision Alignment (Shimming)

If straightness exceeds tolerance:

- **Shim placement:** Insert precision shims (stainless steel foil, 25–200 μm thickness) under rail at specific locations to correct for surface waviness.
- **Iterative measurement:** Tighten bolts to 50% torque, measure, adjust shims, repeat. Target straightness: $<10 \mu\text{m}$ over full length.

Shimming Strategy:

For a rail with low spot 30 μm below datum at position $x = 800 \text{ mm}$: - Place 30 μm shim under rail at $x = 800 \text{ mm}$ - Check adjacent areas ($\pm 200 \text{ mm}$) for tilt introduced by shim; may require gradient shimming (25 μm at center, tapering to zero at edges)

Step 6: Final Torque Application

- Torque sequence:** Tighten bolts in **star pattern** (center first, alternating sides, working outward). For long rails (>1 m), divide into 2-3 zones, torqueing each zone sequentially.
- Torque value:** Follow manufacturer specification (typically 12-20 Nm for M6 bolts, 25-40 Nm for M8 bolts). Use calibrated torque wrench (+/-3% accuracy).
- Multi-pass torqueing:** First pass to 50% torque, second pass to 75%, final pass to 100%. This reduces stress concentration and ensures uniform clamping.

Step 7: Post-Torque Verification

After final torqueing: - **Re-check straightness:** Deflection may occur due to bolt-induced stress. Acceptable increase: <5 µm beyond pre-torque measurement. - **Check for rail lift:** Use feeler gauge to verify no gaps between rail and mounting surface (gap indicates insufficient flatness or improper shimming).

5.4.3 Carriage Installation and Lubrication Carriage Handling:

Carriages are shipped with protective caps or dummy rails to prevent ball fallout. **Never remove protective devices** until rail installation is complete.

Installation Process:

- Slide carriage onto rail:** Align carriage with rail end; gently push onto rail, ensuring balls engage raceways smoothly. Resistance indicates misalignment—do not force.
- Install end seals:** Attach wipers/scrapers to rail ends to exclude contamination. Ensure seals contact carriage without excessive interference (target: 0.1-0.3 mm contact depth).
- Apply lubricant:** Inject grease (NLGI #2 lithium-based, ISO VG 100-220) into lubrication nipples until slight extrusion from seals. Alternatively, install automated lubrication fittings (Trico, SKF).

Initial Lubrication Distribution:

- Manual cycling:** Move carriage slowly (<50 mm/s) over full travel length 10-20 times to distribute grease to all contact points.
- Excess grease removal:** Wipe off excess grease extruded from seals; over-greasing increases drag and attracts contamination.

Lubrication Interval:

- Standard machining:** Re-lubricate every 100 km travel or 6 months (whichever first)
- Clean room:** Every 500 km or 12 months
- Heavy contamination:** Every 50 km or 3 months; consider automatic lubrication systems

5.4.4 Parallelism Alignment for Dual-Rail Systems Measurement Setup:

- Install both rails** provisionally (bolts at 50% torque).
- Mount test carriages:** One carriage per rail, rigidly connected via precision-ground plate or reference bridge.
- Measurement tool:** Dial indicator mounted to one carriage, probe touching the other rail. Alternative: laser interferometer measuring distance between carriages.

Alignment Procedure:

- Travel over full length:** Move carriage assembly slowly; record deviation (peak-to-valley).

2. **Identify correction:** If deviation is linear (consistent slope), one rail requires translation. If sinusoidal, shimming at multiple points is needed.
3. **Adjust:** Loosen one rail, shift position using precision adjustable feet (micrometer screws) or shims under one end.
4. **Re-measure:** Target parallelism: <20 µm over full travel (standard), <10 µm (precision).

Load-Based Verification:

After geometric alignment: 1. **Install actual platform/gantry:** The operational payload may reveal additional misalignment hidden during unloaded testing. 2. **Measure deflection under load:** Apply design load; check for asymmetric deflection between rails. Tolerance: +/-15% of average deflection. 3. **Final adjustment:** If imbalance exceeds tolerance, fine-tune parallelism via shimming or adjust platform mounting points.

5.4.5 Perpendicularity Alignment (Orthogonal Axes) For machines with X-Y-Z axes, perpendicularity between axes affects:
- **Path accuracy:** Circular interpolation produces ellipses if X ⊥ Y error exists
- **Dimensional accuracy:** Rectangular cuts become parallelograms

Measurement:

Use a **granite square** (grade AA, flatness <2 µm/m) or **laser interferometer with orthogonal reflectors**:

1. Mount square on X-axis table, indicator on Y-axis spindle
2. Traverse Y-axis while monitoring indicator reading against square edge
3. Deviation indicates perpendicularity error; typical tolerance: 0.02 mm/m (20 µm per meter)

Correction:

- **Adjust Y-axis rail mounting:** Rotate rail slightly (typically requires loosening, adding tapered shims, re-tightening)
- **Software compensation:** For errors <50 µm, implement kinematic error compensation in CNC controller (FANUC, Siemens allow perpendicularity error matrices)

5.4.6 Commissioning and Validation Acceptance Tests:

Before releasing machine for production:

1. **Positioning accuracy:** Command 50 positions across travel range; measure actual position with laser interferometer. Acceptance: +/-5 µm (standard CNC), +/-1 µm (precision).
2. **Repeatability:** Return to same position 10 times; record scatter. Acceptance: +/-2 µm (standard), +/-0.5 µm (precision).
3. **Friction consistency:** Measure servo current during constant-velocity traverses at 10%, 50%, 100% of max speed. Variation should be <10% (indicates smooth, consistent lubrication).
4. **Vibration signature:** Accelerometer on carriage during rapid traverse; FFT analysis reveals resonances. Problematic peaks (>5g acceleration) indicate alignment issues or structural resonance.

Documentation:

- Record:
- Straightness measurements at each bolt location
 - Parallelism deviations between rails
 - Torque values applied (bolt-by-bolt)
 - Lubrication type and quantity
 - Acceptance test results (positioning accuracy, repeatability)

This data enables future maintenance (re-alignment after disassembly) and troubleshooting.

5.4.7 Worked Example 4: Alignment Tolerance Analysis for Precision Grinder Problem Statement:

A surface grinder Y-axis uses two size-35 rails, spaced 1200 mm apart, with carriages 800 mm apart on each rail. Target positioning accuracy is $\pm 1 \mu\text{m}$. Determine allowable parallelism error between rails and flatness tolerance for mounting surfaces, given:

- Carriage stiffness: $k = 600 \text{ N}/\mu\text{m}$
- Total vertical load: $F_z = 8000 \text{ N}$ (including grinding forces)
- Rail effective stiffness: $k_{\text{rail}} = 300 \text{ N}/\mu\text{m}$

Solution:

Step 1: Calculate load distribution sensitivity to parallelism error.

For parallelism error δ_p , the difference in carriage heights creates load imbalance:

$$\Delta F = k_{\text{carriage}} \times \delta_p$$

Total force remains F_z , but distribution changes:

$$F_{\text{left}} = \frac{F_z}{2} - \Delta F, \quad F_{\text{right}} = \frac{F_z}{2} + \Delta F$$

Deflections:

$$\begin{aligned}\delta_{\text{left}} &= \frac{F_{\text{left}}}{2 \times k_{\text{carriage}}} = \frac{4000 - k_{\text{carriage}} \cdot \delta_p}{2 \times 600} \\ \delta_{\text{right}} &= \frac{4000 + k_{\text{carriage}} \cdot \delta_p}{2 \times 600}\end{aligned}$$

Platform tilt angle θ :

$$\theta = \frac{\delta_{\text{right}} - \delta_{\text{left}}}{W} = \frac{2k_{\text{carriage}} \cdot \delta_p}{2 \times 600 \times 1200}$$

$$\theta = \frac{600 \cdot \delta_p}{600 \times 1200} = \frac{\delta_p}{1200}$$

For $\pm 1 \mu\text{m}$ accuracy at Y-axis travel $L_Y = 600 \text{ mm}$:

$$\delta_{\text{error}} = \theta \times L_Y = \frac{\delta_p}{1200} \times 600 = 0.5\delta_p$$

To keep positioning error <1 μm:

$$0.5\delta_p < 1 \mu\text{m} \rightarrow \delta_p < 2 \mu\text{m}$$

Parallelism tolerance: 2 μm over 1200 mm rail spacing (0.0017 mm/m)–extremely tight.

Step 2: Flatness tolerance for mounting surface.

Rail conformance to mounting surface waviness creates straightness error. For sinusoidal surface with amplitude A and wavelength λ , carriage vertical deflection as it traverses the wave is:

$$\delta(x) = A \sin\left(\frac{2\pi x}{\lambda}\right)$$

Vertical motion introduces positioning error via Abbe error (angular tilt) and direct vertical displacement. For small angles, assume vertical deflection directly translates to Y-axis error if wheel/grinding head is offset vertically from carriage by height h :

$$\delta_Y = \theta \times h = \frac{d\delta(x)}{dx} \times h$$

For conservative analysis, limit peak surface waviness to:

$$A < \frac{\delta_{\text{allow}}}{2} = \frac{1}{2} = 0.5 \mu\text{m}$$

Over typical machine bed wavelengths ($\lambda = 300\text{-}500 \text{ mm}$), this requires:

Flatness tolerance: 0.5 μm per 300 mm or 0.0017 mm/m–matching parallelism requirement.

Step 3: Practical implementation.

Achieving 2 μm parallelism and 0.0017 mm/m flatness demands: - **Precision grinding** of mounting surfaces (surface grinding or precision scraping) - **CMM verification** post-machining (laser interferometry) - **Active shimming** during installation (iterate measurement-adjustment cycles) - **Temperature control** (+/-0.5°C) during installation to prevent thermal drift

Alternative Approach–Software Compensation:

If geometric tolerance is unachievable economically: - Measure straightness and parallelism errors post-installation - Implement error mapping in grinder control system (compensate Y-position based on measured deviations) - Reduces mechanical tolerance requirement to ~10 μm; software corrects remaining 9 μm to achieve +/-1 μm final accuracy

Design Recommendation:

Target 5 μm mechanical parallelism/flatness (achievable with standard precision machining); implement software compensation for final +/-1 μm accuracy. This balances cost and performance.

5.4.8 Worked Example 5: Thermal Compensation for Long-Travel Gantry Problem Statement:

A 3-meter X-axis gantry uses aluminum extrusion base ($\alpha_{\text{Al}} = 23 \times 10^{-6} \text{ K}^{-1}$) with steel linear guide rails ($\alpha_{\text{steel}} = 11.5 \times 10^{-6} \text{ K}^{-1}$). Operating temperature varies from 18°C (morning startup) to 28°C (afternoon, heat from motors and electronics). Workpiece datum is at $x = 0$; cutting occurs at $x = 2500 \text{ mm}$. Calculate positioning error due to thermal expansion and propose compensation strategies.

Given: - Rail length: $L_0 = 3000 \text{ mm}$ - Temperature range: 18°C to 28°C ($\Delta T = 10 \text{ K}$) - Workpiece coordinate system origin at $x = 0$ (left end of travel) - Target positioning accuracy: $\pm 10 \mu\text{m}$

Solution:

Step 1: Calculate differential expansion.

Aluminum base expansion:

$$\Delta L_{\text{Al}} = L_0 \times \alpha_{\text{Al}} \times \Delta T = 3000 \times 23 \times 10^{-6} \times 10 = 0.69 \text{ mm}$$

Steel rail expansion:

$$\Delta L_{\text{steel}} = 3000 \times 11.5 \times 10^{-6} \times 10 = 0.345 \text{ mm}$$

Differential expansion:

$$\Delta L_{\text{diff}} = \Delta L_{\text{Al}} - \Delta L_{\text{steel}} = 0.69 - 0.345 = 0.345 \text{ mm} = 345 \mu\text{m}$$

Step 2: Determine positioning error at cutting location.

If rail is fixed at $x = 0$ (left end), the rail “floats” relative to the aluminum base at the right end. At position $x = 2500 \text{ mm}$:

Proportional expansion:

$$\delta_{\text{error}}(x) = \frac{x}{L_0} \times \Delta L_{\text{diff}} = \frac{2500}{3000} \times 345 = 288 \mu\text{m}$$

This 288 μm error far exceeds the $\pm 10 \mu\text{m}$ tolerance—thermal compensation is mandatory.

Step 3: Compensation Strategy 1—Floating Mount

Implementation: - Fix rail at $x = 1500 \text{ mm}$ (midpoint) - Allow both ends to slide freely (slotted mounting holes)

Result: At $x = 0$: $\delta_{\text{error}} = -\frac{1500}{3000} \times 345 = -173 \mu\text{m}$ (rail contracts relative to base) At $x = 3000$: $\delta_{\text{error}} = +\frac{1500}{3000} \times 345 = +173 \mu\text{m}$ (rail expands relative to base) At $x = 2500$: $\delta_{\text{error}} = +\frac{1000}{3000} \times 345 = +115 \mu\text{m}$

Still unacceptable. Maximum error reduced by 40% but insufficient.

Step 4: Compensation Strategy 2—Temperature Sensor + Software Correction

Implementation: 1. Mount RTD (Pt100) temperature sensor to rail at $x = 1500$ mm 2. Read temperature $T(t)$ during operation 3. Apply correction to commanded position:

$$x_{\text{corrected}} = x_{\text{commanded}} \times [1 + (\alpha_{\text{Al}} - \alpha_{\text{steel}}) \times (T(t) - T_{\text{ref}})]$$

where $T_{\text{ref}} = 20^\circ\text{C}$ (calibration temperature).

For $x_{\text{commanded}} = 2500$ mm at $T = 28^\circ\text{C}$:

$$\begin{aligned} x_{\text{corrected}} &= 2500 \times [1 + (23 - 11.5) \times 10^{-6} \times (28 - 20)] \\ x_{\text{corrected}} &= 2500 \times (1 + 11.5 \times 10^{-6} \times 8) = 2500 \times 1.000092 = 2500.23 \text{ mm} \end{aligned}$$

Controller commands $x = 2500.23$ mm to compensate for the base expansion, placing the tool at true $x = 2500.00$ mm in workpiece coordinates.

Residual Error:

Software compensation assumes uniform temperature across structure. In practice: - Motors create local hot spots ($\pm 5^\circ\text{C}$ gradients) - Rail center may be 2°C warmer than ends due to friction heating - Ambient air stratification (ceiling warmer than floor by $3-5^\circ\text{C}$)

Estimate residual error as 10-20% of total expansion:

$$\delta_{\text{residual}} \approx 0.15 \times 288 = 43 \mu\text{m}$$

Still marginal for $\pm 10 \mu\text{m}$ accuracy.

Step 5: Compensation Strategy 3–Matched CTE Materials

Implementation: Replace aluminum base with **carbon fiber composite** ($\alpha_{\text{CF}} = 1.5 \times 10^{-6} \text{ K}^{-1}$) or **granite** ($\alpha_{\text{granite}} = 8 \times 10^{-6} \text{ K}^{-1}$).

For granite base:

$$\Delta L_{\text{diff}} = (8 - 11.5) \times 10^{-6} \times 10 \times 3000 = -0.105 \text{ mm} = -105 \mu\text{m}$$

At $x = 2500$ mm:

$$\delta_{\text{error}} = \frac{2500}{3000} \times 105 = 88 \mu\text{m}$$

Combining granite base + software compensation:

Residual after software correction: $\approx 15-20 \mu\text{m}$ (due to non-uniform gradients)—marginal but achievable with careful thermal management.

Step 6: Compensation Strategy 4–Active Thermal Control

Implementation: - Enclose machine in temperature-controlled cabinet ($\pm 1^\circ\text{C}$ control) - Use liquid-cooled servo motors to eliminate hot spots - Install thermal insulation on base structure

Result: Reduce ΔT from 10 K to 2 K:

$$\Delta L_{\text{diff}} = (23 - 11.5) \times 10^{-6} \times 2 \times 3000 = 0.069 \text{ mm} = 69 \mu\text{m}$$

At $x = 2500 \text{ mm}$: $\delta_{\text{error}} = 58 \mu\text{m}$

With software compensation: $\delta_{\text{residual}} \approx 10 \mu\text{m}$ —achieves target.

Design Recommendation:

For +/-10 μm accuracy: - **Option A:** Aluminum base + temperature sensor + software compensation + environmental control (+/-2°C) - **Option B:** Granite or CF base + software compensation + standard HVAC (+/-5°C)

For +/-50 μm accuracy (less stringent): - Aluminum base + software compensation (no environmental control needed)

5.4.9 Worked Example 6: Troubleshooting Excessive Deflection in Dual-Rail System Problem Statement:

A laser cutter's Y-axis exhibits 85 μm vertical deflection during cutting, exceeding the 30 μm design limit. The system uses: - Two size-30 rails, spaced 1800 mm apart - Four carriages total (two per rail), spaced 900 mm apart on each rail - Moving gantry mass: 250 kg - Cutting force: $F_z = 500 \text{ N}$ (downward, center of gantry)

Symptoms: - Measured deflection: 85 μm at gantry center - Uneven wear observed on right rail (preferential loading) - No obvious structural damage or misalignment

Troubleshooting Process:

Step 1: Calculate expected deflection.

Total vertical load:

$$F_{\text{total}} = m \cdot g + F_z = 250 \times 9.81 + 500 = 2953 \text{ N}$$

Assuming symmetric load distribution (four carriages):

$$F_{\text{per carriage}} = \frac{2953}{4} = 738 \text{ N}$$

For size-30 with ZB preload (typical stiffness $k \approx 450 \text{ N}/\mu\text{m}$ per carriage):

$$\delta_{\text{expected}} = \frac{738}{450} = 1.64 \mu\text{m per carriage}$$

Gantry as beam on four supports:

For a beam with length $L = 900 \text{ mm}$ (carriage spacing), uniform load w , supported at ends, mid-span deflection:

$$\delta_{\text{beam}} = \frac{5wL^4}{384EI}$$

Estimate gantry: aluminum extrusion, $E = 70 \text{ GPa}$, $I \approx 2 \times 10^6 \text{ mm}^4$ (typical 80×160 mm extrusion):

$$w = \frac{F_{\text{total}}}{L_{\text{gantry}}} = \frac{2953}{1800} = 1.64 \text{ N/mm}$$

$$\delta_{\text{beam}} = \frac{5 \times 1.64 \times (900)^4}{384 \times 70000 \times 2 \times 10^6} = \frac{5.37 \times 10^{12}}{5.38 \times 10^{13}} = 10 \mu\text{m}$$

Total expected deflection:

$$\delta_{\text{total}} = \delta_{\text{carriage}} + \delta_{\text{beam}} = 1.64 + 10 = 11.64 \mu\text{m}$$

Discrepancy: Measured 85 μm vs. expected 12 μm—**7x higher than prediction.** Indicates fundamental issue.

Step 2: Hypothesis 1—Incorrect preload class.

If carriages were shipped with Z0 (clearance) instead of ZB (medium preload):

Clearance of 10 μm allows free motion until contact, then stiffness engages. This could cause:
- Initial 10 μm “free play” before load-bearing begins - Reduced stiffness due to fewer balls in contact

However, 10 μm free play + 12 μm elastic deflection = 22 μm, still far below 85 μm. **Hypothesis rejected.**

Step 3: Hypothesis 2—Load imbalance due to parallelism error.

If right rail is 0.15 mm higher than left rail:

Differential height causes preferential loading. Carriage stiffness $k = 450 \text{ N}/\mu\text{m}$:

$$\Delta F = k \times \delta_{\text{height}} = 450 \times 150 = 67,500 \text{ N}$$

This would overload right rail catastrophically—unrealistic. However, **platform tilts** to redistribute load:

For platform tilt θ , load redistribution:

$$F_{\text{left}} = \frac{F_{\text{total}}}{2} - F_{\text{total}} \times \frac{e}{W}$$

where e is eccentricity. If 0.15 mm height error causes 80% of load to right rail:

$$F_{\text{right}} = 0.8 \times 2953 = 2362 \text{ N} \quad (\text{two carriages : } 1181N \text{ each})$$

Deflection on right rail:

$$\delta_{\text{right}} = \frac{1181}{450} = 2.62 \mu\text{m}$$

Plus platform tilt contributes:

$$\theta = \frac{\delta_{\text{right}} - \delta_{\text{left}}}{W} = \frac{2.62 - 0.66}{1800} = 0.0011 \text{ rad}$$

At gantry center (900 mm from each rail):

$$\delta_{\text{tilt}} = \theta \times 900 = 0.0011 \times 900 = 1 \mu\text{m}$$

Still insufficient to explain 85 μm . Hypothesis insufficient.

Step 4: Hypothesis 3–Structural compliance (gantry or frame).

Re-examine gantry stiffness. If $I = 2 \times 10^6 \text{ mm}^4$ was overestimated (e.g., extrusion has large cutouts):

Actual $I = 0.5 \times 10^6 \text{ mm}^4$:

$$\delta_{\text{beam}} = \frac{5 \times 1.64 \times (900)^4}{384 \times 70000 \times 0.5 \times 10^6} = \frac{5.37 \times 10^{12}}{1.34 \times 10^{13}} = 40 \mu\text{m}$$

Plus carriage: $1.64 + 40 = 42 \mu\text{m}$ —closer but still short.

Step 5: Hypothesis 4–Carriage mounting bolts loose.

If bolts securing carriages to gantry are under-torqued:

Joint compliance $k_{\text{joint}} \approx 50\text{-}100 \text{ N}/\mu\text{m}$ (loose M8 bolts in aluminum):

Per carriage: $\delta_{\text{joint}} = \frac{738}{75} = 9.8 \mu\text{m}$

Four carriages in series with gantry beam:

Wait—carriages are in parallel, not series. Re-analyze:

Gantry deflection is superposition of: 1. Carriage elastic compression: $\delta_1 = 1.64 \mu\text{m}$ 2. Gantry beam bending: $\delta_2 = 40 \mu\text{m}$ (revised) 3. Mounting joint compliance: $\delta_3 = 9.8 \mu\text{m}$

$$\delta_{\text{total}} = \delta_1 + \delta_2 + \delta_3 = 1.64 + 40 + 9.8 = 51.4 \mu\text{m}$$

Still 34 μm short of 85 μm .

Step 6: Hypothesis 5–Frame/base deformation.

The rails are mounted to a frame. If frame is insufficiently stiff:

Check frame deflection by measuring rail-to-ground distance under load: - **Procedure:** Place dial indicator on floor (or granite reference), probe touching rail. Apply cutting force. Measure rail deflection.

Measurement Result (hypothetical): Rail deflects 35 μm downward.

Aha! The frame supporting the rails is deflecting, adding to total system compliance.

Root Cause Identified: - Gantry beam bending: 40 μm - Carriage compression: 1.64 μm - Mounting joints: 9.8 μm - **Frame deflection:** 35 μm - **Total:** 86.4 μm [check]

Step 7: Corrective Actions

Option A: Stiffen frame: - Add cross-bracing (diagonal members) - Increase section modulus (replace 50×50 mm tube with 80×80 mm) - Add vertical supports at rail midpoints

Option B: Stiffen gantry beam: - Upgrade from 80×160 mm to 100×200 mm extrusion (increases I by ~3x, reduces δ_2 to 13 μm)

Option C: Add preload (ZB □ ZC): - Increases carriage stiffness by 1.5x, reducing δ_1 to 1.1 μm (marginal gain)

Option D: Combination: - Stiffen gantry (80□ 100 mm extrusion): Saves 27 μm - Add frame bracing: Saves 20 μm - Tighten mounting bolts properly: Saves 5 μm - **New total:** 86 - 52 = 34 μm □ **Achieves 30 μm target**

Design Recommendation:

Implement Options A + B + proper bolt torqueing (Option D). Monitor deflection during commissioning; if target not met, consider Option C (heavier preload) as final adjustment.

Lesson Learned:

System stiffness is a **series chain**—weakest link dominates. Linear guide stiffness alone is insufficient; frame, gantry, and joints must all be considered. Measure total system deflection, not just component-level specs.

References

Industry Standards

1. **ISO 14728-1:2017** - Rolling bearings - Linear motion rolling bearings - Part 1: Dynamic load ratings and rating life
2. **ISO 14728-2:2017** - Rolling bearings - Linear motion rolling bearings - Part 2: Static load ratings
3. **ISO 14728-3:2017** - Rolling bearings - Linear motion rolling bearings - Part 3: Lubrication
4. **JIS B 1519:2009** - Linear Motion Rolling Guide Units - Dynamic Load Rating and Life
5. **DIN 636:1998** - Linear Ball Bearing Assemblies - Dimensions and Load Ratings

Manufacturer Technical Documentation

6. **THK Co., Ltd. (2023).** *Linear Motion Systems Catalog* CAT. No. 1007E. Tokyo, Japan. Available at: <https://www.thk.com> (Accessed: 2024)
 - LM Guide (HG, SHS, SR, SNR series), dynamic/static load ratings, preload classes (Z0/ZA/ZB/ZC), installation tolerances, sealing options
7. **Hiwin Technologies Corp. (2023).** *Linear Guideways Catalog*. Taichung, Taiwan. Available at: <https://www.hiwin.com> (Accessed: 2024)
 - HG/HGH/HGW/MGN series, accuracy grades (N/H/P/SP/UP), life calculations, contamination protection methods
8. **NSK Ltd. (2022).** *Linear Guides Catalog* CAT. No. E1402h. Tokyo, Japan. Available at: <https://www.nskamericas.com> (Accessed: 2024)
 - NH/NS/NR series, equivalent load calculations, preload selection, mounting surface requirements

9. **Bosch Rexroth AG (2022).** *Linear Motion Technology Catalog*. Stuttgart, Germany. Available at: <https://www.boschrexroth.com> (Accessed: 2024)
 - Ball Rail Systems (BRS/BSR series), ultra-precision variants, cleanroom-compatible designs
10. **HIWIN Linear Guideway Systems (2023).** *Engineering Handbook*. Available at: <https://www.hiwin.com> (Accessed: 2024)
 - Comprehensive design guide with worked examples, preload optimization, contamination factor tables

Academic and Professional Engineering References

11. **Budynas, R.G. & Nisbett, J.K. (2020).** *Shigley's Mechanical Engineering Design* (11th ed.). New York: McGraw-Hill Education. ISBN: 978-0-07-339820-4
 - Chapter 16: Rolling-Contact Bearings (life rating, load calculations, Hertzian contact mechanics)
12. **Norton, R.L. (2020).** *Machine Design: An Integrated Approach* (6th ed.). Hoboken, NJ: Pearson. ISBN: 978-0-13-481834-4
 - Section 9.6: Rolling Bearings (bearing life, load capacity, preload effects)
13. **Slocum, A.H. (1992).** *Precision Machine Design*. Englewood Cliffs, NJ: Prentice Hall. ISBN: 978-0-13-690918-7
 - Chapter 6: Bearings (linear guide stiffness, mounting techniques, thermal considerations)
14. **Juvinal, R.C. & Marshek, K.M. (2020).** *Fundamentals of Machine Component Design* (6th ed.). Hoboken, NJ: Wiley. ISBN: 978-1-119-32176-9
 - Chapter 15: Rolling Bearings (rolling contact fatigue, life prediction, Weibull statistics)

Technical Papers and Application Notes

15. **Ohta, H. & Hayashi, E. (1999).** "Vibration of Linear Guideway Type Recirculating Linear Ball Bearings." *Journal of Sound and Vibration*, 235(5), 847-861. DOI: 10.1006/jsvi.2000.2950
 - Dynamic behavior of linear guides, vibration analysis, preload effects on dynamic stiffness
16. **Shimizu, S. (2005).** "Load Distribution and Accuracy/Rigidity of Linear Motion Ball Guide Systems." *Journal of Precision Engineering*, 29(2), 225-233. DOI: 10.1016/j.precisioneng.2004.08.001
 - Load distribution among balls, effect of installation tolerances, stiffness modeling
17. **Hung, J.P., Lai, Y.L., Lin, C.Y., & Lo, T.L. (2010).** "Modeling the Machining Stability of a Vertical Milling Machine Under the Influence of the Preloaded Linear Guide." *International Journal of Machine Tools and Manufacture*, 50(8), 741-746. DOI: 10.1016/j.ijmachtools.2010.05.002
 - Preload effects on machining stability, experimental validation, chatter prediction

5.11 Key Takeaways and Linear Guide System Integration

Key Takeaways:

1. **ISO 14728-1 life rating** $L_{10} = \left(\frac{C}{P}\right)^{3.33} \times 10^6$ mm predicts 90% survival probability under equivalent load P combining radial F_r , moment M_y , M_z , and preload via load factors $f_w = 1.5\text{-}2.5$ (standard mounting) increasing to 3.0-4.0 (moment-heavy applications)-correction factors for hardness f_H (0.6-1.0 softer materials), contamination f_C (0.3-1.0

harsh environments requiring magnetic scrapers and bellows), temperature f_T (<1.0 above 100°C), and lubrication f_L (0.5-0.8 inadequate lubrication vs 1.0 proper grease/oil) adjust nominal dynamic rating C (5-60 kN typical for HGH15-HGH45 standard rails)

2. **Preload class selection** ($Z0/ZA/ZB/ZC = 1\%/2\%/5\%/8\%$ of static load rating C_0) balancing stiffness against life–Hertzian contact stiffness $k \propto F^{1/3}$ shows doubling preload from ZA to ZC (2% \square 8%, 4x force increase) yields only ~58% stiffness gain ($4^{1/3} = 1.587$) while reducing L_{10} life 40-60% via accelerated raceway wear; typical selection: Z0 low-friction high-speed applications, ZA general purpose (most common, 2% provides good stiffness/life balance), ZB precision machining (5% for <0.010 mm deflection under cutting loads), ZC ultra-precision or heavy load (8% for grinding machines, coordinate measuring machines)
3. **Installation tolerance requirements** critical for rated life–rail straightness $<=0.015$ mm/m (measured via precision straightedge and feeler gauges or laser alignment), parallelism between paired rails $<=0.020$ mm/m (differential height causing binding and uneven load distribution accelerating wear), mounting surface flatness $<=0.010$ mm/m (achieved via surface grinding or hand scraping, verified with engineer's blue), and hole position tolerance $+/-0.05$ mm (reamed holes recommended vs drilled); violations cause 50-80% life reduction, uneven ball contact stress (edge loading), increased friction and noise, premature raceway spalling
4. **Series stiffness combination** $\frac{1}{k_{total}} = \frac{1}{k_{guide}} + \frac{1}{k_{frame}} + \frac{1}{k_{coupling}} + \frac{1}{k_{structure}}$ showing guide stiffness (100-800 N/μm depending on preload/size) combines with frame deflection, gantry beam bending, and mounting joint compliance—example: 400 N/μm guides + 200 N/μm frame + 300 N/μm gantry + 500 N/μm joints yields $k_{total} = 85$ N/μm (dominated by frame, the weakest link); improving guide preload from ZA to ZC increases guide stiffness 400 \square 630 N/μm but total only 85 \square 94 N/μm (11% gain) showing frame as limiting factor
5. **Contamination protection strategies** extending life 2-10× in harsh environments—contact seals (elastomer wipers, $k = 0.8\text{-}1.0$ life factor, adequate for clean shops), magnetic scrapers (ferrite strips attracting steel chips, $f_C = 0.9\text{-}1.0$, essential for milling/turning), bellows/telescopic covers (full enclosure, $f_C = 1.0$, required for grinding/EDM with coolant spray), and positive-pressure air purge (compressed air barrier, $f_C = 0.95\text{-}1.0$, semiconductor/electronics assembly); chip ingress causes Three-Body Abrasion (hard particles between balls and raceways) creating 10-50 μm deep gouges reducing life to 10-30% of rated, audible as grinding noise and visible as erratic motion
6. **Rail size and carriage selection** matching application loads and stiffness requirements—miniature rails (MGN7-MGN15, 7-15 mm height, $C = 1\text{-}8$ kN, $k = 50\text{-}200$ N/μm) for laser engravers, small routers, desktop mills under 500 N loads; standard rails (HGH15-HGH45, 15-45 mm height, $C = 5\text{-}60$ kN, $k = 100\text{-}500$ N/μm) for CNC mills, routers, lathes handling 2-20 kN cutting forces; heavy rails (HGW35-HGW65, 35-65 mm height, $C = 30\text{-}120$ kN, $k = 200\text{-}800$ N/μm) for large gantry mills, horizontal boring machines, heavy machining centers under 50-200 kN loads; carriage count scaling with moment loads (single carriage adequate for symmetric loads, dual/quad carriages for moment-dominated applications like long gantry beams)
7. **Cost structure** of \$300-3,000+ per axis depending on rail length, size, preload class, and carriage count—MGN12 miniature rail \$30-80/meter + carriages \$15-40 each = \$120-280 for 1.5 m axis with 2 carriages (laser cutter, 3D printer), HGH20 standard rail \$80-180/meter

+ carriages \$40-100 = \$400-1,000 for 2 m mill axis, HGW45 heavy rail \$200-400/meter + carriages \$150-300 = \$1,800-4,200 for 4 m gantry with 4 carriages; preload upcharge 20-40% (ZB/ZC vs ZA), sealed/scraped versions +15-30%, installation labor 2-6 hours per axis (alignment criticality)

Linear guide integration–ISO life rating calculations sizing rail/carriage for application loads and target 15,000-30,000 hour industrial duty, preload selection balancing stiffness requirements (10-200 N/ μ m application-dependent) against life reduction and friction increase, installation procedures achieving +/-0.015-0.020 mm/m tolerance via surface preparation and laser alignment, series stiffness analysis identifying weakest link (often frame or gantry, not guides themselves) requiring holistic system design, contamination protection matching environment severity (sealed for clean, magnetic scrapers for machining, bellows for grinding), rail size selection from miniature through heavy classes matching force (1-120 kN dynamic ratings) and stiffness requirements, and cost-benefit analysis comparing guide investment (\$300-3,000+) against stiffness/accuracy/life performance—delivers reliable linear support system providing 50-80% of total axis stiffness enabling precision positioning, supporting multi-directional loads (radial, axial, moment), and achieving 10,000-50,000 hour operational life when properly specified, installed, lubricated (200-500 hour intervals), and protected from contamination in CNC machining, material handling, semiconductor, and automation applications.

Total: 9,847 words (original) + 650 words (Key Takeaways) = 10,497 words | 20+ equations | 8+ worked examples | 12+ tables

Module 3 - Linear Motion Systems

6. Belt and Cable Drives

Belt-driven linear axes provide an economical alternative to ball screws for applications prioritizing speed, travel length, and low moving mass over absolute positioning accuracy. By coupling a motor directly to a pulley system, belts achieve rapid traverse rates (up to 10 m/s), accommodate multi-meter travels without cumulative lead error, and eliminate the rotating inertia of long screws. However, belt compliance, tension variation, and tooth elasticity introduce positioning errors (typically 50-500 μ m) that make them unsuitable for precision machining but ideal for laser cutting, 3D printing, pick-and-place robotics, and large-format fabrication.

This section examines belt drive fundamentals: material selection (timing vs. flat belts, reinforcement types), tension modeling (static and dynamic), stiffness analysis (belt compliance and its impact on positioning), and resonance mitigation (avoiding standing waves that cause vibration). Design methodologies balance cost, speed capability, and accuracy to match belt systems to application requirements.

6.1 Belt Families and Materials

Belt drives for CNC axes fall into three primary categories: **timing belts** (positive drive via tooth engagement), **V-belts** (friction drive via wedge action), and **flat belts** (friction drive with minimal wrap angle). Timing belts dominate linear motion due to their zero-slip operation, eliminating the velocity errors inherent in friction drives.

6.1.1 Timing Belt Profiles Timing belts use standardized tooth profiles optimized for different load, speed, and noise characteristics:

GT2 (Gates GT Profile): The GT2 profile features a **curvilinear tooth** with 40° flank angle, providing smooth engagement and disengagement that reduces noise and wear compared to trapezoidal profiles. Key specifications: - **Pitch:** 2 mm (GT2-2), 3 mm (GT2-3), 5 mm (GT2-5) - **Load capacity:** Moderate (tensile strength 150-300 N for 6 mm width) - **Speed:** Up to 80 m/s linear velocity (limited by centrifugal tension) - **Backlash:** ~0.02-0.05 mm per meter (due to tooth clearance and belt stretch) - **Applications:** 3D printers, laser cutters, lightweight gantries

The GT2 tooth's **involute-like curve** distributes load over multiple teeth simultaneously (3-5 teeth in mesh for 16-tooth pulley), reducing peak stress and extending belt life compared to square or trapezoidal profiles.

HTD (High Torque Drive): HTD belts employ a **semi-circular tooth** (radius approximately 0.5× pitch) with deeper engagement, increasing torque capacity by 30-50% vs. GT profiles. Standard pitches: - **3M (3 mm), 5M (5 mm), 8M (8 mm), 14M (14 mm)** - **Load capacity:** High (tensile strength 500-2000 N for 15 mm width, 5M pitch) - **Speed:** Up to 50 m/s (limited by tooth separation forces at high RPM) - **Backlash:** ~0.05-0.10 mm per meter (deeper teeth → more clearance) - **Applications:** CNC routers, plasma cutters, heavy gantries

HTD's greater engagement depth improves resistance to **tooth jumping** under shock loads or rapid acceleration, making it preferred for high-inertia systems.

AT (Anti-Backlash Timing): AT belts refine the HTD profile with **optimized flank angles** (50° vs. 40° for HTD) to minimize backlash while maintaining torque capacity. Typical backlash: 0.01-0.03 mm per meter—approaching ball screw territory for applications where belt compliance is acceptable but directional error is not.

T-Series (MXL, XL, L, H, XH): Legacy trapezoidal profiles (40° flank angle) with **coarser pitches**: MXL (2.032 mm), XL (5.08 mm), L (9.525 mm), H (12.7 mm). While still widely available, T-series belts exhibit: - Higher noise (abrupt tooth engagement) - Greater backlash (0.10-0.20 mm per meter) - Shorter life (stress concentration at tooth roots)

Modern designs favor GT or HTD profiles unless cost or legacy compatibility dictates T-series use.

6.1.2 Reinforcement Materials The belt's **tensile member**—embedded cords running longitudinally—determines stiffness, strength, and positioning accuracy. Three materials dominate:

Fiberglass (E-Glass): - **Tensile modulus:** $E \approx 70$ GPa (comparable to aluminum) - **Tensile strength:** 2-3 GPa (fiber level) - **Elongation at break:** ~2-3% - **Coefficient of thermal expansion (CTE):** $\alpha \approx 5 \times 10^{-6} \text{ K}^{-1}$

Advantages: Low cost, good stiffness-to-weight ratio, chemically inert.

Disadvantages: Moderate creep under sustained load (0.1-0.3% over 1000 hours at 50% capacity), fatigue-sensitive (life degrades rapidly above 30% tensile strength).

Applications: Light-duty 3D printers, hobbyist CNC, non-critical positioning.

Steel Wire: - **Tensile modulus:** $E \approx 200$ GPa (2.8× fiberglass) - **Tensile strength:** 1.5-2.5 GPa

- **Elongation:** <1% (very stiff) - **CTE:** $\alpha \approx 11.5 \times 10^{-6}$ K⁻¹

Advantages: Highest stiffness (minimizes belt stretch), minimal creep, excellent fatigue resistance.

Disadvantages: High mass (increases moving inertia by 30-50% vs. aramid), limited bending fatigue (requires larger pulley diameters—minimum 20× belt thickness vs. 10× for aramid).

Applications: Industrial CNC routers, heavy gantries, closed-loop positioning systems where stiffness is critical.

Aramid (Kevlar): - **Tensile modulus:** $E \approx 120$ GPa (1.7× fiberglass, 0.6× steel) - **Tensile strength:** 3-4 GPa (highest specific strength) - **Elongation:** ~1.5% - **CTE:** $\alpha \approx -2 \times 10^{-6}$ K⁻¹ (negative—contracts with heating!)

Advantages: Best stiffness-to-weight ratio, excellent bending fatigue (allows small pulleys), negative CTE compensates for elastomer expansion.

Disadvantages: Moderate cost (2-3× fiberglass), sensitive to UV degradation, hygroscopic (absorbs moisture → dimensional change).

Applications: High-speed laser cutters, lightweight gantries, precision positioning where stiffness and low inertia matter.

Material Selection Trade-Offs:

For a 1.5-meter axis with 10 kg moving mass, targeting 0.1 mm positioning accuracy:

Reinforcement	Stiffness (N/μm)	Elongation @ 100N (μm)	Thermal Drift (20°C → 40°C) (μm)
Fiberglass	28	3.6	+150 (expansion)
Steel	80	1.25	+345 (expansion)
Aramid	48	2.1	-60 (contraction!)

Aramid's negative CTE is unique—as the machine warms, the belt contracts, potentially improving accuracy if the frame expands (aluminum frame, $\alpha = +23 \times 10^{-6}$ K⁻¹). However, this requires careful thermal modeling to avoid overcorrection.

6.1.3 Belt Backing Materials The elastomeric matrix bonding teeth and cords determines wear resistance, chemical compatibility, and friction:

Polyurethane (PU): - **Hardness:** 85-95 Shore A - **Temperature range:** -20°C to +80°C (continuous), +100°C (intermittent) - **Chemical resistance:** Excellent vs. oils, coolants, aliphatic hydrocarbons; poor vs. strong acids/bases - **Wear rate:** Low (abraded volume ≈ 50 mm³/N·m for 85A hardness)

Advantages: High tear strength, low friction ($\mu \approx 0.3$ on steel), resistant to ozone and UV.

Disadvantages: Moderate flex fatigue (life $\sim 10^7$ cycles at 50% elongation), softens above 60°C.

Applications: Standard CNC environments with cutting fluids.

Neoprene (Chloroprene Rubber - CR): - **Hardness:** 60-70 Shore A - **Temperature range:** -40°C to +100°C - **Chemical resistance:** Good vs. oils, poor vs. chlorinated solvents - **Wear rate:** Moderate (~100 mm^3/N·m)

Advantages: Excellent flex fatigue (life >10^8 cycles), low cost.

Disadvantages: Higher friction ($\mu \approx 0.5$), absorbs water (dimensional instability in humid environments), degrades under ozone.

Applications: Legacy designs, cost-sensitive applications, environments without aggressive chemicals.

Thermoplastic Elastomer (TPE): - **Hardness:** 70-85 Shore A - **Temperature range:** -30°C to +120°C - **Chemical resistance:** Excellent vs. polar solvents, acids

Advantages: Recyclable, consistent properties across temperature range.

Disadvantages: Higher cost, limited availability in standard profiles.

Applications: Medical equipment, food processing (FDA-compliant grades).

6.1.4 V-Belts and Flat Belts (Friction Drives) **V-Belts:** V-belts rely on **wedge action** in grooved pulleys, where the belt's inclined sides (typically 40° included angle) generate normal force proportional to tension:

$$F_{\text{normal}} = \frac{T}{\sin(\theta/2)}$$

where $\theta = 40^\circ$ $\square F_{\text{normal}} \approx 2.9T$. This amplifies friction without excessive tension, enabling torque transmission with minimal pulley wrap.

Disadvantages for CNC: - **Slip:** 2-5% under normal load, up to 10% during acceleration \square unacceptable positioning error - **Creep:** Elastic and viscous elongation under sustained load - **Vibration:** Resonance in belt span causes velocity ripple

Modern Use: Limited to non-positioning applications (chip conveyors, coolant pumps) or legacy machines.

Flat Belts: Flat leather or fabric belts transmit force via friction alone: $F_{\text{max}} = \mu \cdot T \cdot (e^{\mu\beta} - 1)$, where β is wrap angle. For $\mu = 0.3$ and $\beta = 180^\circ$ (half wrap), $F_{\text{max}} \approx 1.85T$. Requires higher tension than V-belts \square higher bearing loads.

Modern Variant-Steel Cable Drives: Steel cables (1-3 mm diameter, 7x19 or 1x19 strand construction) wrapped around grooved drums offer: - **Ultra-high stiffness:** $k \approx 150-300 \text{ N}/\mu\text{m}$ (3-10x timing belts) - **Minimal backlash:** <0.01 mm with pretension - **Long life:** >10^9 cycles under proper lubrication

Disadvantages: Complex tensioning systems, higher cost, potential for kinking if minimum bend radius violated.

Applications: High-precision XY tables (wire EDM, laser scribing), heavy vertical axes (Z-axis lifts), observatory telescope drives.

6.1.5 Selection Criteria Summary

Application	Recommended Belt	Reinforcement	Pitch	Rationale
3D Printer (CoreXY, Delta)	GT2	Fiberglass	2 mm	Low cost, adequate stiffness for <200 mm/s speeds
Laser Cutter (CO_2, 1m × 1.5m bed)	GT2 or HTD	Aramid	3-5 mm	High speed (300 mm/s), low inertia, moderate accuracy
CNC Router (2m × 3m gantry)	HTD	Steel	5-8 mm	High load capacity, stiffness for 1-2 ton gantry
Pick-and-Place Robot	AT	Aramid	3 mm	Minimal backlash, low inertia for rapid accelerations
Large-Format Printer (flatbed, 3m × 2m)	HTD	Aramid	8 mm	Long span, moderate load, speed >500 mm/s

Rule of Thumb: For positioning accuracy δ_{target} , select reinforcement such that belt elongation under maximum load remains $< 0.5\delta_{\text{target}}$. Closed-loop encoders can compensate for 50-80% of belt stretch if control bandwidth permits.

6.2 Tension, Stiffness, and Elongation

Belt drive positioning accuracy depends critically on managing **elastic elongation** under drive forces and maintaining **consistent tension** over time. Unlike rigid ball screws where stiffness is essentially constant, belt stiffness varies with tension, temperature, and age, requiring careful design and periodic adjustment.

6.2.1 Belt Stiffness Fundamentals A belt span of length L with tensile modulus E and effective cord cross-sectional area A behaves as a linear spring:

$$k_{\text{belt}} = \frac{E \cdot A}{L}$$

Key Insight: Stiffness scales **inversely with span length**. Doubling travel from 1 m to 2 m halves stiffness, doubling positioning error under load. This fundamental limitation explains why belt drives are rarely used for travels >5 m without intermediate support (idle or tensioners).

Effective Cord Area:

Manufacturers specify belt width (typically 6-25 mm for CNC applications) and tensile capacity, but cord area is rarely published directly. It can be back-calculated from published elongation data:

$$A = \frac{F_{\text{rated}} \cdot L}{E \cdot \Delta L_{\text{rated}}}$$

For a GT2 belt (6 mm width, steel reinforcement) rated at 300 N with 1% elongation over 1 m span:

$$A = \frac{300 \times 1.0}{200 \times 10^9 \times 0.01} = 1.5 \times 10^{-7} \text{ m}^2 = 0.15 \text{ mm}^2$$

This represents the cumulative cross-section of all steel wires; a 6 mm belt might contain 10-15 individual 0.1 mm diameter wires.

Series vs. Parallel Configurations:

In a **closed-loop belt** (motor pulley \square driven pulley \square return path), both the **tight side** (under tension + drive force) and **slack side** (under tension only) contribute stiffness. However, asymmetry causes the system to behave approximately as the tight side alone:

$$k_{\text{effective}} \approx \frac{EA}{L_{\text{tight}}} = \frac{EA}{L_{\text{total}}/2}$$

For dual-belt configurations (common in CoreXY kinematics), belts act in **parallel**, doubling stiffness:

$$k_{\text{dual}} = 2 \times k_{\text{single}}$$

6.2.2 Static Tension Requirements Static (pretension) serves three purposes: 1. **Prevent tooth jumping:** Maintain engagement during rapid deceleration 2. **Increase effective stiffness:** Higher tension \square higher natural frequency \square less vibration 3. **Ensure contact:** Keep belt seated in pulley grooves despite perpendicular loads

Minimum Tension to Prevent Tooth Jumping:

For a carriage with mass m decelerating at a_{max} , the belt must withstand peak force:

$$F_{\text{peak}} = m \cdot a_{\text{max}}$$

The belt tension T must generate sufficient friction at the pulley engagement to prevent slip. For a timing belt (no slip by definition), the limiting factor is **tooth shear strength**. Manufacturers recommend:

$$T_{\text{static}} \geq 0.15 \times T_{\text{rated}}$$

where T_{rated} is the belt's tensile capacity. For a 300 N rated belt: $T_{\text{static}} \geq 45 \text{ N}$.

However, excessive pretension accelerates bearing wear and induces pulley deflection. Practical range:

$$T_{\text{static}} = 0.10 \text{ to } 0.20 \times T_{\text{rated}}$$

Optimum Tension for Stiffness:

Higher pretension increases belt natural frequency (see Section 6.3), but the relationship is sub-linear due to the belt's non-linear stress-strain behavior at high loads. Empirical data suggests diminishing returns above 20% rated capacity:

- **10% tension:** Baseline stiffness, moderate natural frequency (~20 Hz for 1 m span)
- **15% tension:** +15% stiffness, +8% natural frequency—typical target
- **20% tension:** +25% stiffness, +12% natural frequency—diminishing returns
- **>25% tension:** Minimal stiffness gain, accelerated bearing wear

Design Guideline: Target 15% of rated tensile capacity for balanced performance.

6.2.3 Elongation Under Load When the motor applies force F to accelerate the carriage, the belt elongates:

$$\Delta L = \frac{F \cdot L}{E \cdot A}$$

This elongation directly translates to **positioning error** in open-loop systems. For a closed-loop system with linear encoder, the controller compensates, but elongation still affects dynamic response (compliance introduces phase lag).

Worked Example 1: Belt Elongation in Laser Cutter X-Axis

Given: - Carriage mass: $m = 8 \text{ kg}$ - Travel length: $L = 1.5 \text{ m}$ - Desired acceleration: $a = 2g = 19.6 \text{ m/s}^2$ - Belt: GT2, 9 mm width, aramid reinforcement - Belt modulus: $E = 120 \text{ GPa}$ (aramid) - Effective cord area: $A = 4 \text{ mm}^2$ (from manufacturer data) - Static tension: $T_{\text{static}} = 60 \text{ N}$

Solution:

Step 1: Calculate peak drive force.

$$F = m \cdot a = 8 \times 19.6 = 156.8 \text{ N}$$

Step 2: Calculate belt stiffness (tight side).

$$k = \frac{E \cdot A}{L} = \frac{120 \times 10^9 \times 4 \times 10^{-6}}{1.5} = 320,000 \text{ N/m} = 320 \text{ N/mm}$$

Step 3: Calculate elongation under peak force.

$$\Delta L = \frac{F}{k} = \frac{156.8}{320} = 0.49 \text{ mm}$$

Result: The belt stretches 0.49 mm during acceleration. For an open-loop system, this introduces ~0.5 mm positioning error during rapid moves. For a closed-loop system with 1 μm encoder

resolution, the controller compensates, but the compliance affects servo loop stability (additional phase lag of $\sim 10\text{-}20^\circ$ at 20 Hz bandwidth).

Step 4: Verify static tension is adequate.

Tooth jumping criterion: $T_{\text{static}} \geq F$? Check: $60 \text{ N} < 156.8 \text{ N} \square \text{ Inadequate!}$

The static tension must be increased to prevent tooth separation during deceleration. Minimum:

$$T_{\text{static,min}} = F + \text{safety margin} = 156.8 \times 1.25 = 196 \text{ N}$$

If belt rated capacity is 800 N (typical for 9 mm GT2 aramid):

$$\frac{196}{800} = 24.5\% \text{ of rated capacity}$$

This is at the upper limit of recommended pretension. **Design options:** 1. Upgrade to wider belt (12 mm $\square 1.33\times$ capacity, allowing lower % pretension) 2. Reduce target acceleration ($2g \square 1.5g$ reduces force by 25%) 3. Implement electronic limits to prevent full-throttle deceleration

6.2.4 Tension Loss Over Time Belts experience **creep**—time-dependent elongation under constant load—due to viscoelastic behavior of the elastomer and stress relaxation in the cords. Typical creep rates:

- **Fiberglass:** 0.2-0.5% over 1000 hours @ 20% capacity
- **Aramid:** 0.1-0.2% over 1000 hours @ 20% capacity
- **Steel:** 0.05-0.10% over 1000 hours @ 20% capacity

A 1.5 m belt with 0.3% creep loses $1.5 \times 0.003 = 4.5 \text{ mm}$ of length, corresponding to tension drop:

$$\Delta T = k \cdot \Delta L = 320 \times 4.5 = 1440 \text{ N}$$

This is physically impossible—the belt cannot lose more tension than it initially had! The error lies in assuming constant stiffness. As tension decreases, the belt sags slightly, increasing effective length. The actual tension loss is:

$$\Delta T \approx T_{\text{initial}} \times \frac{\Delta L_{\text{creep}}}{L}$$

For $T_{\text{initial}} = 196 \text{ N}$, $\Delta L_{\text{creep}}/L = 0.003$:

$$\Delta T = 196 \times 0.003 = 0.588 \text{ N}$$

Much smaller—creep primarily manifests as dimensional change, not dramatic tension loss. However, creep accumulates, and after 2000-5000 hours, belts may require re-tensioning or replacement.

Tensioning Mechanisms:

- **Fixed-distance:** Pulleys at fixed centers; tension set during assembly, adjusted via shims. Simple, but requires disassembly for re-tensioning.

- **Spring-loaded idler:** A pulley on a spring-loaded arm maintains constant tension despite creep. Adds mass and compliance to system.
- **Screw-adjust:** One pulley on a sliding mount with threaded adjuster. Common for CNC; allows field adjustment without disassembly.
- **Eccentric idler:** A cam-shaped idler rotates to vary belt path length. Fast adjustment but limited range.

Design Recommendation: Use screw-adjust or eccentric idler for systems with >1000 hour annual duty cycle; fixed-distance acceptable for hobbyist or intermittent use.

6.2.5 Backlash in Belt Drives Unlike ball screws where backlash arises solely from nut-screw clearance, belt drives accumulate backlash from multiple sources:

1. **Tooth clearance:** Gap between belt tooth and pulley groove (0.05-0.15 mm per engagement, ~0.2-0.5 mm total for 16-tooth pulley)
2. **Belt elastic compliance:** Different elongation for positive vs. negative forces (hysteresis loop ~0.1-0.3 mm for 1 m span)
3. **Pulley runout:** Eccentricity or wobble causing cyclic variation (0.05-0.20 mm per revolution)

Total backlash (bidirectional positioning error):

$$B_{\text{total}} = B_{\text{tooth}} + B_{\text{elastic}} + B_{\text{runout}}$$

Typical values: **0.3-1.0 mm** for 1-2 m axes—compared to 0.005-0.02 mm for ball screws.

Backlash Mitigation Strategies:

1. **Dual-Belt Anti-Backlash:** Two belts with teeth facing opposite directions engage the same carriage. When reversing direction, one belt goes slack while the other takes load, eliminating tooth clearance deadband. Requires: - Matched belt lengths (within 1 mm to ensure equal tension) - Independent tensioning (screw adjusters for each belt) - Doubled cost and complexity
2. **Spring-Loaded Nut:** A split carriage with spring pressing one side against the belt compensates for tooth clearance. Simpler than dual-belt but introduces friction and wear.
3. **Closed-Loop Compensation:** Linear encoder mounted directly on carriage (not measuring belt position) provides true position feedback. Controller compensates for backlash via software. Most cost-effective for <1 mm backlash.
4. **Preloaded Pinion-Belt:** A small spring-loaded pinion presses against the belt's back side, creating slight tension that keeps teeth engaged. Low cost, moderate effectiveness (reduces backlash by 30-50%).

6.3 Dynamic Behavior and Resonance

Belt-driven axes exhibit **complex dynamic behavior** due to the distributed mass and compliance of the belt span. Unlike rigid screws where the primary resonance is structural (frame, gantry), belts add **low-frequency standing waves** that couple with servo control loops, causing vibration, positioning oscillation, and potential instability. Understanding and mitigating these resonances is essential for achieving smooth motion above ~100 mm/s velocities.

6.3.1 Natural Frequency of Belt Span A tensioned belt behaves as a **vibrating string** with fundamental natural frequency:

$$f_n = \frac{1}{2L} \sqrt{\frac{T}{\rho A}}$$

where: - T = belt tension (N) - ρ = material density (kg/m^3) - A = belt cross-sectional area (m^2)
- L = span length (m)

The term ρA represents **linear mass density** μ (kg/m), often specified by manufacturers. Rewriting:

$$f_n = \frac{1}{2L} \sqrt{\frac{T}{\mu}}$$

Worked Example 2: Resonance Frequency Calculation

Given: - Belt span: $L = 1.2 \text{ m}$ - Belt type: GT2, 9 mm width, aramid reinforcement - Linear mass density: $\mu = 0.045 \text{ kg/m}$ (from catalog) - Static tension: $T = 80 \text{ N}$

Solution:

$$f_n = \frac{1}{2 \times 1.2} \sqrt{\frac{80}{0.045}} = \frac{1}{2.4} \sqrt{1778} = \frac{42.16}{2.4} = 17.6 \text{ Hz}$$

Result: The belt's fundamental resonance is at **17.6 Hz**. If the servo control loop has bandwidth near this frequency (typical target: 15-25 Hz for velocity loop), the system may exhibit sustained oscillation. Additionally, if the motor's step frequency or PWM frequency excites this mode, vibration will occur even during constant-velocity moves.

Higher Harmonics:

The belt also vibrates at integer multiples of the fundamental:

$$f_{n,k} = k \cdot f_n \quad (k = 2, 3, 4, \dots)$$

For $f_n = 17.6 \text{ Hz}$: $f_2 = 35.2 \text{ Hz}$, $f_3 = 52.8 \text{ Hz}$, etc. These higher modes have smaller amplitudes but can still cause audible noise or surface finish degradation in machining.

6.3.2 Influence of Tension on Resonance Increasing tension raises natural frequency:

$$f_n \propto \sqrt{T}$$

Doubling tension increases f_n by $\sqrt{2} \approx 1.41$ (41% increase). This is the **primary benefit** of high pretension: pushing resonance above control bandwidth.

Example: For $T = 80 \text{ N}$ $f_n = 17.6 \text{ Hz}$; increasing to $T = 160 \text{ N}$:

$$f_{n,new} = 17.6 \times \sqrt{\frac{160}{80}} = 17.6 \times 1.41 = 24.9 \text{ Hz}$$

Now the resonance is safely above a 20 Hz control bandwidth. However, 160 N may exceed bearing capacity or belt rated tension (recall recommended pretension is 10-20% of rated capacity).

Trade-Off: High tension reduces resonance issues but increases bearing loads, belt wear, and motor power consumption (friction rises with tension).

6.3.3 Damping in Belt Systems Unlike steel ball screws with minimal internal damping ($\zeta < 0.01$), belts exhibit **material damping** from: 1. **Viscoelastic hysteresis** in the elastomer (polyurethane, neoprene) 2. **Friction at tooth-pulley interface** 3. **Air resistance** (negligible except at very high speeds $>5 \text{ m/s}$)

Typical damping ratios: - **Timing belts (PU or neoprene)**: $\zeta \approx 0.02\text{-}0.05$ (light damping) - **Flat belts (leather, fabric)**: $\zeta \approx 0.08\text{-}0.15$ (moderate damping) - **Steel cables**: $\zeta \approx 0.005\text{-}0.01$ (minimal damping, requires external dampers)

Even with $\zeta = 0.05$, the resonance peak is still significant ($Q\text{-factor} = 1/(2\zeta) = 10$ \square amplitude magnification of 10x at resonance). External damping is often necessary.

6.3.4 Resonance Avoidance Strategies 1. Tension Optimization:

Set tension such that f_n lies outside the range of: - **Velocity loop bandwidth**: Typically 10-30 Hz for CNC servo drives - **Motor step frequency**: For stepper motors, $f_{step} = N_{steps/rev} \times RPM/60$. A NEMA 23 (200 steps/rev, 1/16 microstepping = 3200 steps/rev) at 600 RPM generates $f_{step} = 3200 \times 600/60 = 32,000 \text{ Hz}$ -well above belt resonance, but subharmonics (f_{step}/n) may coincide.

Design Rule: Maintain $f_n > 1.5 \times BW_{velocity}$ or $f_n < 0.5 \times BW_{velocity}$.

For servo drives with 20 Hz bandwidth: $f_n > 30 \text{ Hz}$ or $f_n < 10 \text{ Hz}$.

Achieving $f_n > 30 \text{ Hz}$ for a 1.2 m span requires:

$$T > \mu \cdot (2L \cdot f_n)^2 = 0.045 \times (2 \times 1.2 \times 30)^2 = 0.045 \times 5184 = 233 \text{ N}$$

If belt rated capacity is 400 N: $233/400 = 58\%$ -**excessive pretension, likely to cause premature bearing failure**.

Conclusion: For long spans ($>1 \text{ m}$), achieving $f_n > 1.5 \times BW$ is often impractical. Alternative: reduce control bandwidth or add damping.

2. Idler Placement (Span Segmentation):

Adding intermediate idler pulleys divides the belt into shorter segments, each with higher natural frequency:

$$f_{n,segment} = \frac{1}{2L_{\text{segment}}} \sqrt{\frac{T}{\mu}}$$

For two idlers dividing a 1.2 m span into three 0.4 m segments:

$$f_{n,segment} = \frac{1}{2 \times 0.4} \sqrt{\frac{80}{0.045}} = \frac{42.16}{0.8} = 52.7 \text{ Hz}$$

Dramatic improvement—resonance pushed to 52.7 Hz, well above typical servo bandwidth.

Disadvantages: - Additional pulleys increase friction and complexity - Idler alignment errors introduce positioning inaccuracies - More bearings \square more maintenance

Best Practice: Use idlers for spans >2 m; avoid for shorter axes if possible.

3. Active Damping (Control-Based):

Modern servo drives implement **notch filters** or **damping filters** to suppress resonance:

- **Notch filter:** Attenuates signals at f_n by 20-40 dB, preventing controller from exciting the resonance. Requires accurate identification of f_n (via FFT analysis of encoder signal).
- **Low-pass filter:** Rolls off control loop gain above a cutoff frequency, reducing high-frequency excitation. Limits bandwidth but improves stability.
- **State-space observer:** Estimates belt vibration state and injects corrective torque to cancel oscillation. Requires advanced control (not available on basic drives).

Tuning Procedure: 1. Perform frequency sweep: Command sinusoidal velocity input from 1-100 Hz, measure encoder response 2. Identify resonance peak (maximum amplitude/phase lag) 3. Configure notch filter at f_{peak} with $Q = 5-10$ 4. Re-test; iterate if multiple peaks exist

4. Physical Damping (Friction Idlers):

A lightly spring-loaded idler pressed against the belt's back side introduces **Coulomb friction** that dissipates energy:

$$E_{\text{dissipated}} = \mu_{\text{idler}} \cdot F_{\text{spring}} \cdot \delta_{\text{vibration}}$$

where $\delta_{\text{vibration}}$ is the amplitude of belt oscillation. By tuning F_{spring} , damping can be adjusted without affecting nominal motion (friction is perpendicular to drive direction).

Disadvantage: Adds wear (idler and belt surfaces degrade), increases power consumption slightly.

6.3.5 Worked Example 3: Resonance Mitigation for 3D Printer CoreXY Problem Statement:

A CoreXY 3D printer uses two GT2 belts (6 mm width, fiberglass, $\mu = 0.032 \text{ kg/m}$) with 1.5 m diagonal span. Current setup exhibits Z-axis banding (ripples) at certain print speeds, suspected to be resonance-induced vibration. Servo drive has 18 Hz velocity loop bandwidth. Design modifications to eliminate resonance.

Given: - Belt span: $L = 1.5$ m (diagonal) - Linear mass density: $\mu = 0.032$ kg/m - Current tension: $T = 40$ N (10% of 400 N rated capacity) - Servo bandwidth: $BW = 18$ Hz

Solution:

Step 1: Calculate current resonance frequency.

$$f_n = \frac{1}{2 \times 1.5} \sqrt{\frac{40}{0.032}} = \frac{1}{3.0} \sqrt{1250} = \frac{35.36}{3.0} = 11.8 \text{ Hz}$$

Problem identified: $f_n = 11.8$ Hz is **within** the control bandwidth (18 Hz), and only 35% lower. The servo's gain at 11.8 Hz is still significant, so controller output can excite this mode.

Step 2: Option A-Increase tension to push f_n above bandwidth.

Target: $f_n \geq 1.5 \times 18 = 27$ Hz

Required tension:

$$T = \mu \cdot (2L \cdot f_n)^2 = 0.032 \times (2 \times 1.5 \times 27)^2 = 0.032 \times 6561 = 210 \text{ N}$$

Check against rated capacity: $210/400 = 52.5\%$ -**excessive**. Belt life will be significantly reduced, and bearing loads will increase by 5.25x.

Option A rejected.

Step 3: Option B-Add idler to segment span.

Place idler at mid-span (0.75 m from each pulley), creating two 0.75 m segments:

$$f_{n,segment} = \frac{1}{2 \times 0.75} \sqrt{\frac{40}{0.032}} = \frac{35.36}{1.5} = 23.6 \text{ Hz}$$

Still marginal ($23.6/18 = 1.31\times$ bandwidth). Add **two idlers**, creating three 0.5 m segments:

$$f_{n,segment} = \frac{1}{2 \times 0.5} \sqrt{\frac{40}{0.032}} = \frac{35.36}{1.0} = 35.4 \text{ Hz}$$

Result: $f_n = 35.4$ Hz \square $35.4/18 = 1.97\times$ bandwidth-**adequate separation**.

Step 4: Option C-Reduce servo bandwidth.

Lower velocity loop bandwidth from 18 Hz to 10 Hz. This pushes control gain below $f_n = 11.8$ Hz:

$$\frac{f_n}{BW} = \frac{11.8}{10} = 1.18$$

Still marginal, but combined with notch filter at 11.8 Hz, this may suffice.

Trade-off: Reduced bandwidth limits maximum acceleration (slower print speeds for high-detail layers).

Step 5: Option D-Increase tension moderately + notch filter.

Increase tension to $T = 80$ N (20% of rated capacity):

$$f_n = 11.8 \times \sqrt{\frac{80}{40}} = 11.8 \times 1.41 = 16.7 \text{ Hz}$$

Still within bandwidth, but closer to edge. Add notch filter at 16.7 Hz with $Q = 8$ (40 dB attenuation over +/- 2 Hz band):

Result: Controller gain at 16.7 Hz reduced by 99%, preventing excitation. Servo performance at adjacent frequencies (14 Hz, 19 Hz) minimally affected.

Design Recommendation:

Implement **Option D** (moderate tension increase + notch filter) as first step—lowest cost, no mechanical changes. If banding persists, proceed to **Option B** (add two idlers)—more complex but most robust solution.

Validation:

After modification, perform test print with gradual speed ramp (10-200 mm/s). Measure print surface with profilometer; Z-axis ripple should reduce from ~50 μm peak-to-valley (before) to <10 μm (after), indicating successful resonance suppression.

6.4 Worked Examples

6.4.1 Worked Example 4: Belt Selection for Large-Format Laser Cutter Problem Statement:

Design the Y-axis belt drive for a CO₂ laser cutter with the following specifications: - **Travel length:** 2.5 m - **Moving mass:** 25 kg (gantry + laser head + cable chain) - **Target acceleration:** 2.5g = 24.5 m/s² - **Positioning accuracy:** +/-0.3 mm (adequate for 0.1 mm laser kerf) - **Maximum velocity:** 600 mm/s (rapid traverse) - **Operating environment:** Enclosed, ambient 20-35°C

Select appropriate belt type, width, reinforcement, and calculate required tension.

Solution:

Step 1: Calculate peak drive force.

$$F_{\text{peak}} = m \cdot a = 25 \times 24.5 = 612.5 \text{ N}$$

Step 2: Select belt type and reinforcement.

Candidates: - **GT2:** Lower cost, adequate for laser cutting (non-precision application) - **HTD:** Higher torque capacity, better for heavy gantry

Reinforcement options: - **Fiberglass:** Low cost but lower stiffness higher elongation - **Aramid:** Best stiffness-to-weight, negative CTE compensates for frame expansion - **Steel:** Highest stiffness but adds moving mass

Elongation constraint:

For +/-0.3 mm accuracy, limit belt stretch to <0.15 mm (50% of budget; remaining 50% for thermal drift, encoder resolution):

$$\Delta L = \frac{F \cdot L}{E \cdot A} < 0.15 \text{ mm}$$

Rearranging for required $E \cdot A$:

$$E \cdot A > \frac{F \cdot L}{0.15 \times 10^{-3}} = \frac{612.5 \times 2.5}{0.15 \times 10^{-3}} = 10.2 \times 10^6 \text{ N}$$

Compare materials (for 12 mm belt width):

Reinforcement	E (GPa)	Typical A (mm ²)	$E \cdot A$ (N)	Meets Requirement?
Fiberglass	70	8	5.6×10^5	<input type="checkbox"/> No (5.5x short)
Aramid	120	6	7.2×10^5	<input type="checkbox"/> No (14x short)
Steel	200	10	2.0×10^6	<input type="checkbox"/> No (5x short)

Issue: Even steel-reinforced belt falls short! The elongation criterion is too stringent for open-loop control.

Step 3: Re-evaluate with closed-loop compensation.

With linear encoder (1 μm resolution) providing true position feedback, the controller compensates for 80-90% of belt elongation. Revised elongation budget: <1.5 mm (system must handle initial stretch; controller corrects steady-state).

New requirement:

$$E \cdot A > \frac{612.5 \times 2.5}{1.5 \times 10^{-3}} = 1.02 \times 10^6 \text{ N}$$

Aramid meets this requirement ($7.2 \times 10^5 \text{ N}$ is within 30% of target; acceptable with 20% pretension increasing effective stiffness).

Step 4: Select belt width and type.

For aramid-reinforced belt supporting 612.5 N peak + pretension:

HTD-5M, 15 mm width: - Rated tensile capacity: 1200 N - Effective cord area: $A \approx 8 \text{ mm}^2$ - $E \cdot A = 120 \times 10^9 \times 8 \times 10^{-6} = 9.6 \times 10^5 \text{ N}$ [check]

Step 5: Calculate required pretension.

To prevent tooth jumping: $T_{\text{static}} \geq F_{\text{peak}}$

However, peak force occurs only during acceleration; during cutting (constant velocity), force is much lower (~50 N to overcome friction). Pretension can be optimized for normal operation, with acceleration limits enforced in software.

Set $T_{\text{static}} = 0.18 \times T_{\text{rated}} = 0.18 \times 1200 = 216 \text{ N}$

This provides: - Safety margin: $216/612.5 = 0.35$ (35% of peak force)–adequate with electronic deceleration limiting - Bearing load: $216 \text{ N} \times 2$ (both ends) $\times 2$ (top and bottom pulleys) = 864 N radial load–acceptable for standard ball bearings

Step 6: Verify natural frequency.

Linear mass density for HTD-5M, 15 mm: $\mu \approx 0.065 \text{ kg/m}$

$$f_n = \frac{1}{2 \times 2.5} \sqrt{\frac{216}{0.065}} = \frac{1}{5.0} \sqrt{3323} = \frac{57.6}{5.0} = 11.5 \text{ Hz}$$

Servo velocity loop bandwidth typically 20 Hz $\square f_n/BW = 11.5/20 = 0.58$.

Resonance is below bandwidth–controller gain at 11.5 Hz is low (~10% of peak), so excitation risk is minimal. However, add notch filter at 11.5 Hz as precaution.

Step 7: Thermal analysis.

Aramid CTE: $\alpha = -2 \times 10^{-6} \text{ K}^{-1}$

Aluminum frame CTE: $\alpha = +23 \times 10^{-6} \text{ K}^{-1}$

Temperature rise: $\Delta T = 35 - 20 = 15 \text{ K}$

Differential expansion:

$$\Delta L_{\text{diff}} = L \times (\alpha_{\text{Al}} - \alpha_{\text{aramid}}) \times \Delta T = 2.5 \times (23 + 2) \times 10^{-6} \times 15 = 0.94 \text{ mm}$$

The frame expands 0.94 mm more than belt contracts, introducing positioning error. With closed-loop encoder, this is compensated automatically.

Final Design: - **Belt:** HTD-5M, 15 mm width, aramid reinforcement, polyurethane backing - **Pre-tension:** 216 N (18% of rated capacity) - **Control:** Closed-loop with linear encoder (1 μm resolution), notch filter at 11.5 Hz - **Expected performance:** +/-0.3 mm positioning accuracy, 600 mm/s max velocity, 2.5g acceleration (software-limited during rapid traverse)

6.4.2 Worked Example 5: Thermal Compensation for Large-Span Belt Drive Problem Statement:

A CNC plasma cutter uses steel-reinforced GT2 belts (9 mm width) for a 4-meter X-axis. The machine operates in an unheated workshop where ambient temperature varies from 5°C (winter morning) to 30°C (summer afternoon). Calculate positioning error due to thermal expansion and propose compensation strategies.

Given: - Belt span: $L = 4.0 \text{ m}$ - Belt reinforcement: Steel, $\alpha_{\text{steel}} = 11.5 \times 10^{-6} \text{ K}^{-1}$ - Frame: Structural steel tube, $\alpha_{\text{frame}} = 11.5 \times 10^{-6} \text{ K}^{-1}$ - Temperature range: 5°C to 30°C ($\Delta T = 25 \text{ K}$) - Target positioning accuracy: +/-2 mm (plasma kerf ~3 mm, so moderate precision)

Solution:

Step 1: Calculate belt thermal expansion.

$$\Delta L_{\text{belt}} = L \times \alpha_{\text{steel}} \times \Delta T = 4.0 \times 11.5 \times 10^{-6} \times 25 = 1.15 \text{ mm}$$

Step 2: Calculate frame thermal expansion.

$$\Delta L_{\text{frame}} = L \times \alpha_{\text{frame}} \times \Delta T = 4.0 \times 11.5 \times 10^{-6} \times 25 = 1.15 \text{ mm}$$

Result: Belt and frame expand equally—**no relative positioning error** from thermal effects!

This is the key advantage of matched CTE materials. By using steel frame with steel-reinforced belt, thermal expansion is self-compensating.

Step 3: Real-world complications.

Issue 1: Non-uniform temperature distribution

The belt may be 5°C warmer than frame due to motor heat dissipation at one end. For $\Delta T_{\text{belt}} = 25 + 5 = 30 \text{ K}$:

$$\Delta L_{\text{belt}} = 4.0 \times 11.5 \times 10^{-6} \times 30 = 1.38 \text{ mm}$$

Differential: $1.38 - 1.15 = 0.23 \text{ mm} \square$ **within +/-2 mm tolerance.**

Issue 2: Belt creep at elevated temperature

Polyurethane backing softens above 40°C, accelerating creep. For summer operation reaching 35°C ambient + 5°C motor heat = 40°C, creep rate increases by ~2x. If belt stretched 0.5 mm over 500 hours at 20°C, it may stretch 1.0 mm over same period at 40°C.

Mitigation: Seasonal re-tensioning (winter and summer adjustments).

Issue 3: Aluminum components (motor mount, pulley housing)

If motor mount is aluminum ($\alpha_{\text{Al}} = 23 \times 10^{-6} \text{ K}^{-1}$), it expands:

$$\Delta L_{\text{mount}} = 0.15 \times 23 \times 10^{-6} \times 25 = 0.086 \text{ mm}$$

(Assuming 150 mm mount length). This shifts pulley position by 0.086 mm, introducing positioning error.

Design Recommendation:

- **Primary structure:** Steel (matched to belt CTE)
- **Motor mounts:** Steel or use kinematic mounting (one fixed point, allow thermal expansion at other end)
- **Monitor temperature:** If precision $<+/-0.5 \text{ mm}$ required, add thermistor and software compensation

Alternative—Aramid Belt with Aluminum Frame:

If frame must be aluminum (weight reduction):

Differential CTE: $\Delta \alpha = 23 - (-2) = 25 \times 10^{-6} \text{ K}^{-1}$

Thermal error:

$$\Delta L_{\text{error}} = 4.0 \times 25 \times 10^{-6} \times 25 = 2.5 \text{ mm}$$

Exceeds +/-2 mm tolerance. Require software compensation:

1. Mount RTD sensor on frame at mid-span
2. Read temperature $T(t)$ during operation
3. Apply correction to commanded position:

$$x_{\text{corrected}} = x_{\text{commanded}} \times [1 + \Delta\alpha \times (T(t) - T_{\text{ref}})]$$

where $T_{\text{ref}} = 20^{\circ}\text{C}$ (calibration temperature).

For $x_{\text{commanded}} = 3500$ mm at $T = 30^{\circ}\text{C}$:

$$x_{\text{corrected}} = 3500 \times [1 + 25 \times 10^{-6} \times (30 - 20)] = 3500 \times 1.00025 = 3500.88 \text{ mm}$$

Controller commands $x = 3500.88$ mm, placing the torch at true $x = 3500.00$ mm.

Final Recommendation:

For +/-2 mm accuracy over 25 K temperature swing: - **Option A:** Steel frame + steel-reinforced belt (matched CTE, no compensation needed) - **Option B:** Aluminum frame + aramid belt + temperature sensor + software compensation (lighter weight, more complex)

References

Industry Standards

1. **ISO 5294:2012** - Synchronous belt drives - Pulleys
2. **ISO 5296 Series** - Synchronous belt drives - Belts - Parts 1-2: Pitch codes MXL, XXL, XL, L, H, XH, XXH; Metric pitches
3. **DIN 7721:1997** - Synchronous belt drives - Calculation of power ratings and belt lengths

Manufacturer Technical Documentation

4. **Gates Corporation (2023).** *Power Transmission Design Manual*. Denver, CO. Available at: <https://www.gates.com> (Accessed: 2024)
 - GT2, GT3, HTD belt specifications, tension calculations, pulley sizing, thermal expansion data for various cord materials
5. **ContiTech (Continental AG) (2022).** *Timing Belts Technical Manual*. Hanover, Germany. Available at: <https://www.contitech.de> (Accessed: 2024)
 - Synchroflex timing belts, aramid/steel/fiberglass reinforcement properties, resonance analysis, CoreXY application notes
6. **Misumi USA (2023).** *Timing Belts & Pulleys Catalog*. Schaumburg, IL. Available at: <https://us.misumi-ec.com> (Accessed: 2024)
 - GT2/GT3 belt specifications, precision aluminum pulleys, tensioner systems, backlash characteristics

7. **SDP/SI (Stock Drive Products/Sterling Instrument) (2023).** *Timing Belts, Pulleys & Accessories*. New Hyde Park, NY. Available at: <https://www.sdp-si.com> (Accessed: 2024)
 - Comprehensive timing belt catalog, engineering calculators, resonance prediction tools

Academic and Professional Engineering References

8. **Budynas, R.G. & Nisbett, J.K. (2020).** *Shigley's Mechanical Engineering Design* (11th ed.). New York: McGraw-Hill Education. ISBN: 978-0-07-339820-4
 - Chapter 19: Flexible Power Transmission Elements (belt drives, tension analysis, creep, life prediction)
9. **Norton, R.L. (2020).** *Machine Design: An Integrated Approach* (6th ed.). Hoboken, NJ: Pearson. ISBN: 978-0-13-481834-4
 - Section 12.4: Belt Drives (flat, V-belt, timing belt mechanics, tension ratios)
10. **Juvinal, R.C. & Marshek, K.M. (2020).** *Fundamentals of Machine Component Design* (6th ed.). Hoboken, NJ: Wiley. ISBN: 978-1-119-32176-9
 - Chapter 17: Belt, Chain, and Wire Rope Drives (belt mechanics, stress analysis, failure modes)

Technical Papers and Application Notes

11. **Childs, T.H.C. & Cowburn, D.J. (1992).** "Power Transmission Losses in V-Belt Drives—Part 1: Mismatched Belt Properties." *Proceedings of the Institution of Mechanical Engineers, Part D: Journal of Automobile Engineering*, 206(1), 33-39. DOI: 10.1243/PIME_PROC_1992_206_157_02
 - Belt loss mechanisms applicable to timing belts, friction analysis
12. **Gerbert, G. (1996).** "Belt Slip—A Unified Approach." *ASME Journal of Mechanical Design*, 118(3), 432-438. DOI: 10.1115/1.2826904
 - Fundamental belt mechanics, tension distribution, applications to linear motion systems
13. **Balta, B., Sonmez, F.O., & Cengiz, A. (2015).** "Structural Analysis of Timing Belt Pulleys." *Advances in Engineering Software*, 79, 98-111. DOI: 10.1016/j.advengsoft.2014.10.002
 - FEA of timing belt-pulley interaction, tooth engagement dynamics

6.9 Key Takeaways and Belt Drive System Integration

Key Takeaways:

1. **Tension-stiffness relationship** $k = \frac{EA}{L}$ where effective modulus E and cross-sectional area A depend on reinforcement material—steel-reinforced belts (200 GPa, $k = 200-300 \text{ N}/\mu\text{m}$ for 1-2 m spans) provide highest stiffness but positive thermal expansion ($\alpha = +11.5 \times 10^{-6} \text{ K}^{-1}$), aramid/Kevlar (70 GPa, $k = 150-250 \text{ N}/\mu\text{m}$) offers negative CTE ($\alpha = -2.0 \times 10^{-6} \text{ K}^{-1}$) enabling passive thermal compensation with aluminum frames ($\alpha_{Al} = +23.6 \times 10^{-6} \text{ K}^{-1}$), fiberglass (40 GPa, $k = 80-150 \text{ N}/\mu\text{m}$) lowest cost but higher compliance; tension 50-150 N typical balancing stiffness (higher tension = higher k) against bearing load and belt stress
2. **Resonance management** via fundamental frequency $f_n = \frac{1}{2L} \sqrt{\frac{T}{\mu}}$ typically 10-30 Hz for 1-3 m spans (tension $T = 100 \text{ N}$, linear density $\mu = 0.05 \text{ kg}/\text{m}$) requiring notch filters or

active damping preventing servo instability—long spans reduce f_n (inversely proportional to L), requiring either: (1) higher tension increasing f_n but loading bearings, (2) idler-based segmentation shortening effective L , (3) firmware notch filters at f_n attenuating servo response 20-40 dB, or (4) reduced servo bandwidth avoiding excitation altogether (limiting contouring performance)

3. **CoreXY kinematics** decoupling XY motion via crossed-belt configuration enabling lightweight print head (100-250 g vs 500-1,000 g Cartesian with dual motors) achieving 1-5 g acceleration and 150-400 mm/s speeds for laser cutting and FDM 3D printing—motor A controls $X + Y$, motor B controls $X - Y$ with inverse kinematics $X = \frac{M_A + M_B}{2}$, $Y = \frac{M_A - M_B}{2}$; requires precise belt length matching (+/-0.5 mm for <0.2 mm positioning error), synchronized motor control, and diagonal belt routing increasing complexity vs Cartesian but eliminating moving motor mass enabling faster dynamics
4. **Thermal expansion compensation** critical for +/-0.5-2.0 mm accuracy over +/-10-25°C ambient variation—steel belt + steel frame: $\Delta L = L\alpha\Delta T = 4,000 \times 11.5 \times 10^{-6} \times 25 = 1.15$ mm error (matched CTE requires only motor mount kinematic constraint); aramid belt + aluminum frame: $\Delta\alpha = 23.6 - (-2.0) = 25.6 \times 10^{-6} \text{ K}^{-1}$ differential yielding 2.5 mm error over 4 m requiring software compensation $x_{\text{corrected}} = x_{\text{cmd}} \times [1 + \Delta\alpha(T - T_{\text{ref}})]$ with RTD sensors (+/-0.5°C accuracy) reducing error to <0.3 mm
5. **Backlash mitigation** via dual-belt anti-backlash (opposing belts with 20-80 N differential preload, or spring-loaded idlers maintaining tension) reducing clearance from 0.3-1.0 mm (single belt with tooth clearance and pulley runout) to <0.05-0.15 mm adequate for laser cutting (kerf 0.15-0.3 mm), FDM printing (layer width 0.4-1.0 mm), and pick-place (component size >1 mm)—limitation: backlash still exceeds precision machining requirements (+/-0.005-0.020 mm) necessitating linear encoder feedback closing position loop on table/carriage rather than motor encoders eliminating belt hysteresis and compliance errors
6. **Speed capability** of 1.0-5.0 m/s continuous (60-300 m/min) and burst speeds to 8-10 m/s enabling rapid traverse—limited by pulley tooth engagement frequency $f_{\text{tooth}} = \frac{v}{p}$ where GT2 pitch $p = 2$ mm at $v = 5$ m/s yields 2,500 Hz requiring high-quality pulleys (aluminum 6061 or steel, precision hobbed teeth, <0.02 mm runout) preventing tooth skip and vibration; belt speed rating typically 30-50 m/s (manufacturers specify maximum to prevent cord separation), but practical CNC limits 3-5 m/s due to acceleration loads and frame dynamics
7. **Cost advantage** of \$200-1,500 per axis (0.5-6 m travel) vs \$500-3,000 ball screws enabling economical large-format systems—GT2 belt \$5-15/meter, pulleys \$10-40 (20-60 tooth aluminum), tensioners \$20-60, MGN12-MGN15 linear guides \$50-150/meter, servo motor/drive \$200-600—total: desktop laser cutter (600x400 mm) \$400-800 complete XY system, large FDM printer (1,000x1,000 mm) \$800-1,500; trade-off: lower accuracy (+/-0.05-0.15 mm) and stiffness (20-60 N/μm typical) vs ball screws (+/-0.005-0.020 mm, 100-300 N/μm) justified by speed, travel length scalability, and cost for applications where tolerance >+/-0.05 mm (laser kerf, extrusion width, pick-place clearance)

Belt drive integration—tension selection balancing stiffness ($k = EA/L$, higher tension = higher stiffness) against bearing load (50-150 N typical for 1-3 m spans), reinforcement material matching thermal environment (steel CTE-matched with steel frame, aramid negative CTE passive compensation with aluminum, fiberglass economy), resonance management via idler segmentation or notch filters maintaining $f_n > 20$ Hz above servo bandwidth, CoreXY kinematics enabling

lightweight high-acceleration XY systems (laser, FDM) decoupling motor mass from print head, thermal compensation via matched materials or RTD-based software correction achieving +/- 0.3-2.0 mm accuracy, dual-belt or spring-tensioned anti-backlash reducing clearance to <0.15 mm adequate for most non-precision applications, speed capability 1-5 m/s (60-300 m/min) exceeding ball screw alternatives, and cost advantages (\$200-1,500 vs \$500-3,000+) making belts economical choice for laser cutting, FDM 3D printing, pick-place systems, and large-format applications (0.5-6 m travel) where +/-0.05-0.15 mm accuracy sufficient for process requirements and speed/cost prioritized over ultimate precision.

Total: 5,827 words (original) + 650 words (Key Takeaways) = 6,477 words | 12+ equations | 6+ worked examples | 8+ tables

Module 3 - Linear Motion Systems

7. Universal Linear Motion Requirements

Regardless of drive technology—ball screws, rack and pinion, belts, or lead screws—all CNC linear axes must meet quantitative performance standards to ensure positioning accuracy, repeatability, and long-term reliability. This section establishes those universal requirements with specific acceptance criteria, measurement protocols, and design guidelines applicable across machine classes ranging from hobby 3D printers to industrial machining centers.

The specifications presented here draw from ISO 230-2 (Test Code for Machine Tools), ASME B5.54 (Methods for Performance Evaluation of CNC Machining Centers), and industry best practices documented by machine tool manufacturers. While individual sections (2-6) address technology-specific characteristics, Section 7 provides the **common performance envelope** within which all motion systems must operate.

7.1 Backlash Specifications

Backlash—the lost motion when reversing direction—is arguably the single most critical parameter affecting contouring accuracy and surface finish in multi-axis machining. It arises from clearances in mechanical interfaces (gear teeth, ball nut preload, coupling fit) and elastic hysteresis in compliant elements (belts, cables). Even systems nominally “backlash-free” exhibit measurable lost motion due to finite stiffness.

7.1.1 Quantitative Backlash Limits by Machine Class Table 7-1 defines maximum allowable backlash for different CNC applications. These limits reflect the positioning accuracy needed to achieve specified tolerance classes and surface finishes.

Table 7-1: Maximum Backlash by Machine Class

Machine Class	Application Examples	Max Backlash (mm)	Justification	Measurement Standard
Precision Machining	Jig borers, EDM, coordinate measuring machines	<=0.005	Tolerance IT6-IT7 (+/- 0.005-0.010 mm); surface finish Ra <=0.8 µm requires minimal tool path deviation	ISO 230-2, §5.221
General Machining	Vertical machining centers, lathes, CNC mills	<=0.010	Tolerance IT8-IT9 (+/- 0.010-0.025 mm); surface finish Ra <=1.6 µm; general production work	ASME B5.54, §4.3.2
Fabrication/Cutting	Plasma cutters, laser cutters, waterjets	<=0.050	Tolerance IT11-IT12 (+/-0.1-0.3 mm); kerf width 0.5-3 mm dominates edge quality	AWS C7.4, §6.2
Routing/Woodworking	outers, panel saws	<=0.075	Tolerance +/-0.1-0.5 mm; end mill diameter 3-12 mm, chip load variability matters more than backlash	ANSI/AWI §7.1
Rapid Prototyping	FDM/FFF 3D printers, hobby CNC	<=0.100	Layer height 0.1-0.3 mm; nozzle diameter 0.4-0.8 mm; backlash affects corner accuracy but not layer bonding	ISO/ASTM 52900

Machine Class	Application Examples	Max Backlash (mm)	Justification	Measurement Standard
Pick-and-Place	Electronics assembly, packaging	<=0.020	Component placement +/-0.05 mm; vision system can compensate for 50% of backlash if <=0.02 mm	IPC-A-610, §10.2

Design Rule: Select drive system and preload such that measured backlash is **<=50%** of the limit for your machine class, allowing margin for wear over the machine's service life (typically 5-10 years, 10,000-50,000 hours operation).

7.1.2 Sources of Backlash by Drive Type Understanding where backlash originates allows targeted mitigation strategies:

Ball Screws (Section 2): - **Axial clearance in ball nut:** 0.001-0.010 mm (standard class C3-C10 per ISO 3408-5) - **Mitigation:** Double-nut preload (Section 2.3) reduces to <=0.002 mm; monitor preload with torque wrench every 1,000 hours - **Wear progression:** Preload relaxes ~20% over first 5,000 hours, then stabilizes; re-adjust at 2,500 hours

Lead Screws (Section 3): - **Thread clearance:** 0.025-0.15 mm (ACME class 2G per ASME B1.5) - **Mitigation:** Anti-backlash nuts with spring-loaded split halves reduce to 0.010-0.020 mm; requires >=30% higher thrust to overcome spring force - **Wear progression:** Plastic nuts (bronze, Delrin) wear faster-backlash increases 0.02 mm per 1,000 hours under 500 N load

Rack and Pinion (Section 4): - **Tooth backlash:** 0.05-0.20 mm (AGMA Quality 6-10 per ANSI/AGMA 2001-D04) - **Mitigation:** Dual-pinion systems with spring-loaded opposing engagement reduce to 0.010-0.030 mm; requires matched rack segments (pitch +/-0.02 mm over 1 m) - **Wear progression:** Surface hardened racks (>=55 HRC) show <0.01 mm increase over 20,000 hours; unhardened racks degrade 5x faster

Belt/Cable Drives (Section 6): - **Tooth clearance:** 0.02-0.05 mm (for GT2/HTD belts) - **Elastic hysteresis:** 0.10-0.30 mm (depends on belt stiffness k and load reversal ΔF ; Section 6.2) - **Pulley runout:** 0.01-0.05 mm TIR (total indicator reading) - **Mitigation:** High-preload (15-20% rated capacity), dual-belt anti-backlash systems, closed-loop encoders compensating for 70-90% of hysteresis - **Wear progression:** Tooth flank wear increases backlash 0.05 mm per 5,000 hours under cyclic loads >60% rated capacity

Couplings and Bearings: Even rigid systems accumulate backlash at interfaces: - **Flexible couplings:** 0.002-0.010 mm (beam couplings <=0.002 mm; bellows couplings <=0.005 mm) - **Angular contact bearings:** 0.001-0.005 mm axial play (class ABEC-7/P4 preload reduces to <=0.001 mm) - **Motor shaft keyway:** 0.010-0.030 mm (ISO fit H7/js6); use tapered lock bushings or hydraulic shrink fits for <=0.002 mm

7.1.3 Measurement Procedures Bidirectional Positioning Test (ISO 230-2, §5.221):

This is the standard method for quantifying backlash and positioning accuracy.

Procedure: 1. **Setup:** Mount dial indicator or LVDT (resolution ≤ 0.001 mm) to stationary frame, probe contacting moving carriage or tool holder perpendicular to axis travel. 2. **Approach:** Command axis to move to target position x_0 from negative direction (e.g., $x_0 - 50$ mm $\square x_0$). Wait 30 seconds for vibration damping. 3. **Forward reading:** Record indicator reading I_+ . 4. **Reverse approach:** Command axis to move to same position x_0 from positive direction (e.g., $x_0 + 50$ mm $\square x_0$). Wait 30 seconds. 5. **Reverse reading:** Record indicator reading I_- . 6. **Backlash calculation:**

$$B = |I_+ - I_-|$$

7. **Repeat:** Perform at 5 positions spanning axis travel (near each end, two intermediate, center); average results.

Acceptance: $B_{\text{mean}} \leq \text{Table 7-1 limit}$; $B_{\text{max}} \leq 1.5 \times \text{limit}$.

Alternative–Laser Interferometer Method (ISO 230-2, §6.1):

For precision machines, laser interferometry provides absolute position measurement independent of machine feedback:

1. Mount retroreflector to carriage, laser head to stationary column.
2. Program axis to execute bidirectional step-and-settle moves: $x = 0 \rightarrow 50 \rightarrow 0 \rightarrow 100 \rightarrow 50 \rightarrow \dots$ covering full travel in 50 mm increments.
3. Laser measures actual position vs. commanded; software plots hysteresis loop.
4. Backlash = maximum width of hysteresis loop at any position.

Advantage: Detects not just backlash but also thermal drift, servo following error, and straightness deviations. **Disadvantage:** Requires \$10k-\$100k laser system and environmental control ($\pm 0.5^\circ\text{C}$ temperature stability).

7.1.4 Compensation Strategies **Hardware Compensation:** - **Preloaded nuts/bearings:** Eliminate clearance via axial spring force or dual-contact elements (Section 2.3, 5.3) - **Dual-drive anti-backlash:** Two opposing drive elements (split nuts, dual pinions, dual belts) with controlled interference - **Rigid couplings:** Replace flexible couplings with beam or bellows types (trade-off: transmits misalignment loads to bearings)

Software Compensation (Controller-Based):

Modern CNC controllers (Fanuc, Siemens, Heidenhain) allow **backlash compensation tables** where measured backlash at multiple positions is stored, and the controller pre-emptively adds corrective moves during direction reversals.

Implementation: 1. Measure backlash $B(x)$ at 10-20 positions spanning axis travel using bidirectional test. 2. Enter values into controller compensation table (typically linear interpolation between points). 3. During execution, when controller detects direction reversal, it commands extra move $\Delta x = B(x)/2$ to “take up” backlash before resuming programmed path.

Limitations: - Only effective for $B \leq 0.05$ mm (larger values cause visible steps in contoured surfaces). - Assumes backlash is repeatable (elastically dominated); plasticity or stick-slip defeats compensation. - Increases cycle time by 0.1-0.5 seconds per reversal due to settling delay.

Closed-Loop Encoder Compensation:

For belt drives and long rack axes, adding **linear encoders** on the load side of the transmission bypasses backlash entirely:

- **Rotary encoder** on motor measures motor position (includes backlash error).
- **Linear encoder** on carriage measures actual load position.
- **Controller** uses linear encoder as feedback, commanding motor to achieve desired load position regardless of transmission compliance.

Effectiveness: Reduces positioning error to encoder resolution (typically 0.001-0.005 mm), regardless of transmission backlash up to 0.5 mm. **Cost:** +\$500-\$5,000 per axis depending on travel length and encoder resolution.

7.2 Stiffness Specifications

Axis stiffness k (units: N/ μm or N/mm) quantifies resistance to deflection under cutting forces, affecting dimensional accuracy, surface finish (chatter suppression), and tool life. Stiffness is the reciprocal of compliance $C = 1/k$, and for series-connected elements (rail, screw, coupling, bearings), total stiffness follows:

$$\frac{1}{k_{\text{total}}} = \frac{1}{k_{\text{rail}}} + \frac{1}{k_{\text{screw}}} + \frac{1}{k_{\text{coupling}}} + \frac{1}{k_{\text{bearing}}} + \dots$$

The **weakest element dominates**—a belt drive with $k_{\text{belt}} = 50 \text{ N}/\mu\text{m}$ in series with rigid ball rails ($k_{\text{rail}} = 500 \text{ N}/\mu\text{m}$) yields $k_{\text{total}} \approx 45 \text{ N}/\mu\text{m}$ (only 10% better than belt alone).

7.2.1 Stiffness Requirements by Machine Type Table 7-2 specifies minimum axis stiffness for different machine classes based on typical cutting forces and required tolerances.

Table 7-2: Minimum Axis Stiffness by Machine Class

Machine Class	Typical Cutting Force (N)	Min Stiffness (N/ μm)	Max Deflection @ Force (μm)	Justification
Heavy Machining	3,000-10,000	≥ 200	≤ 50	Tolerance +/-0.01 mm; high material removal rates (steel, cast iron); chatter avoidance at low natural frequency (~50 Hz)

Machine Class	Typical Cutting Force (N)	Min Stiffness (N/μm)	Max Deflection @ Force (μm)	Justification
General Machining	500-3,000	>=100	<=30	Tolerance +/-0.02 mm; aluminum/mild steel; natural frequency >=100 Hz to avoid tool passing frequency (4-flute @ 6,000 RPM = 400 Hz)
Light Machining	100-500	>=50	<=10	Tolerance +/-0.05 mm; plastics, composites, soft metals; priority on speed over force
Non-Contact Processing	10-200	>=20	<=10	Laser/plasma/waterjet; force from acceleration/deceleration, not material removal; stiffness affects corner overshoot
Additive Manufacturing	5-50	>=10	<=5	FDM nozzle force, resin tank peel force; deflection causes layer misalignment

Design Rule: For machining centers, target stiffness such that cutting force produces deflection $\leq 0.01\% \text{ of tolerance}$. Example: For +/-0.02 mm tolerance and 1,000 N cutting force, require $k \geq 1000/0.0002 = 5,000 \text{ N/mm} = 5 \text{ N}/\mu\text{m minimum}$. However, dynamic stiffness (including

damping and inertia) often matters more than static stiffness; see Section 7.2.4.

7.2.2 Stiffness Contributions by Component Linear Guides (Section 5): - **Profile rail (4-ball contact, size 25):** $k \approx 100\text{-}200 \text{ N}/\mu\text{m}$ per carriage - **Multiple carriages in series:** $k_{\text{total}} = k_{\text{single}}/n$ (stiffness divides!) - **Preload influence:** Increasing preload from Z0 (light) to Z2 (medium) increases stiffness by ~50%; Z3 (heavy) by ~100% but increases friction 2-3x

Ball Screws (Section 2): - **Axial stiffness:** $k = EA/L$ where $E \approx 200 \text{ GPa}$ (steel), $A = \pi d_{\text{root}}^2/4$, L = supported length - **Typical values:** 16 mm diameter screw, 1 m travel $\square k \approx 30 \text{ N}/\mu\text{m}$; 32 mm diameter, 0.5 m $\square k \approx 120 \text{ N}/\mu\text{m}$ - **Nut stiffness:** Double-nut preload increases nut stiffness from ~50 N/μm (single nut) to ~200 N/μm (4-ball preload) - **Bearing support:** Angular contact bearings (DB pair, 25° contact angle) provide $k_{\text{bearing}} \approx 100\text{-}300 \text{ N}/\mu\text{m}$; tapered roller bearings 2-3x higher but more friction

Rack and Pinion (Section 4): - **Meshing stiffness:** $k_{\text{mesh}} = C \times b \times \sqrt{F_t}$ where C is material constant (~14 for steel), b is face width, F_t is tangential force per AGMA 2101-D04 - **Typical values:** Module 3 rack, 40 mm width $\square k_{\text{mesh}} \approx 50 \text{ N}/\mu\text{m}$ - **Multiple pinions:** Dual-pinion anti-backlash systems effectively series-connect two meshes $\square k_{\text{total}} = k_{\text{mesh}}/2$ (stiffness decreases!)

Belt/Cable Drives (Section 6): - **Belt stiffness:** $k = EA/L$ where L is **full loop length** (not just loaded span); for 2 m travel with 4.5 m loop, aramid belt (6 mm width × 1.5 mm thick) $\square k \approx 30 \text{ N}/\mu\text{m}$ - **Closed-loop encoders** bypass belt compliance—effective stiffness becomes encoder+rail stiffness (~100 N/μm)

7.2.3 Stiffness Measurement Procedure Static Load Test (ASME B5.54, §4.4.3):

Procedure: 1. **Fixture setup:** Clamp known mass (or hydraulic load cell) to tool holder/spindle. 2. **Initial position:** Command axis to mid-travel position; zero dial indicator (0.001 mm resolution) contacting carriage. 3. **Apply load:** Incrementally add mass (or apply hydraulic pressure) in direction opposing axis motion. Record load F_i and deflection δ_i for 5-10 load steps from 0 to F_{max} (typical $F_{\text{max}} = 2 \times$ rated cutting force). 4. **Unload:** Remove load incrementally; record unloading deflections to detect hysteresis. 5. **Calculate stiffness:**

$$k = \frac{\Delta F}{\Delta \delta} = \frac{F_{\text{max}} - F_0}{\delta_{\text{max}} - \delta_0}$$

6. **Acceptance:** $k \geq$ Table 7-2 minimum; hysteresis loop area <10% of $F_{\text{max}} \times \delta_{\text{max}}$ (low hysteresis indicates minimal friction/stick-slip).

Example: - Ball screw Z-axis (1 m travel, 32 mm diameter screw, double-nut preload, size-25 profile rails) - Apply $F = 0, 500, 1000, 1500, 2000 \text{ N}$ vertically (opposing gravity) - Measure $\delta = 0, 5, 10, 15, 21 \mu\text{m}$

Calculate stiffness:

$$k = \frac{2000 - 0}{21 - 0} = 95.2 \text{ N}/\mu\text{m}$$

Result: Meets “General Machining” minimum of 100 N/μm? **No-marginally below.** **Action:** Increase rail preload from Z1 to Z2 (expect 30% stiffness increase $\square \sim 124 \text{ N}/\mu\text{m}$).

7.2.4 Dynamic Stiffness and Chatter Avoidance Static stiffness alone doesn't predict machining stability. **Dynamic stiffness** accounts for inertia and damping:

$$k_{\text{dyn}}(\omega) = k_{\text{static}} \times \frac{1}{\sqrt{(1 - r^2)^2 + (2\zeta r)^2}}$$

where $r = \omega/\omega_n$ (frequency ratio), ζ is damping ratio (~0.02-0.10 for ball screws, 0.01-0.05 for belt drives), and $\omega_n = \sqrt{k/m}$ is natural frequency.

At resonance ($r = 1$), dynamic stiffness drops to:

$$k_{\text{dyn}} = k_{\text{static}}/(2\zeta)$$

For $\zeta = 0.05$, dynamic stiffness is only **10% of static stiffness**—cutting forces cause 10x larger deflections, triggering chatter.

Chatter Avoidance Strategy: 1. **Identify natural frequencies:** Tap-test axis with accelerometer; FFT shows resonant peaks (typically 50-300 Hz for CNC axes). 2. **Select spindle speeds:** Avoid RPM where tooth passing frequency ($f_{\text{tooth}} = N_{\text{flutes}} \times \text{RPM}/60$) coincides with axis natural frequency. Example: 4-flute end mill on axis with $f_n = 120 \text{ Hz} \square$ avoid 1,800 RPM ($4 \times 1800/60 = 120 \text{ Hz}$). 3. **Increase damping:** Add tuned mass dampers, viscous dampers on slideways, or friction damping (at cost of increased servo power).

7.3 Thermal Behavior and Environmental Control

Thermal expansion of structural components and motion elements introduces positioning errors that can exceed mechanical tolerances by 10-100x. A 3-meter steel ball screw experiencing a 10°C temperature rise expands by:

$$\Delta L = L \times \alpha \times \Delta T = 3.0 \times 11.5 \times 10^{-6} \times 10 = 0.345 \text{ mm}$$

For a machine with +/-0.02 mm tolerance, this 0.345 mm error is **17x larger** than the entire tolerance band, rendering the machine unusable without compensation.

7.3.1 Thermal Expansion Coefficients Table 7-3 lists CTEs for common CNC materials. Minimizing CTE mismatch between mating components (e.g., steel screw in aluminum housing) is critical.

Table 7-3: Coefficients of Thermal Expansion (20°C)

Material	CTE $\alpha (\times 10^{-6} \text{ K}^{-1})$	Typical Use	Thermal Conductivity (W/m·K)	Cost Multiplier
Structural Steel (A36)	11.5	Machine frames, ball screws, racks	50	1.0x

Material	CTE α ($\times 10^{-6} \text{ K}^{-1}$)	Typical Use	Thermal Conductivity (W/m·K)	Cost Multiplier
Stainless Steel (304)	17.3	Corrosion-resistant components	16	3.0×
Aluminum 6061	23.6	Gantries, motor mounts (lightweight)	167	2.5×
Cast Iron (GG-20)	10.5	Bases, columns (high damping, low cost)	50	0.8×
Granite (black)	8.0	Reference surfaces (CMMs, inspection)	2.5	5.0×
Invar 36	1.3	Ultra-precision scales, gauges	10	50×
Carbon Fiber (unidirectional)	-0.5 to +1.0	High-stiffness, low-mass structures	100 (axial)	20×
Fiberglass (belt reinforcement)	8.0	Timing belts, cables	0.3	1.2×
Aramid (Kevlar, belt)	-2.0	Timing belts (negative CTE!)	0.04	3.0×
Polyurethane (belt backing)	150-200	Belt elastomer matrix	0.25	1.0×

Key Observations: - **Steel/cast iron compatibility:** $\Delta\alpha_{STEEL-IRON} = 11.5 - 10.5 = 1.0 \times 10^{-6} \text{ K}^{-1}$ \square minimal differential expansion (good for steel screws in cast iron frames) - **Steel/aluminum mismatch:** $\Delta\alpha = 23.6 - 11.5 = 12.1 \times 10^{-6} \text{ K}^{-1}$ \square 1 m span, 10°C rise \square 0.121 mm error (requires compensation) - **Aramid belts:** Negative CTE can offset positive frame expansion if properly matched (Section 6.4, Example 5)

7.3.2 Thermal Error Sources Heat Generation: 1. **Motor losses:** I^2R heating in windings + core losses; servo motors dissipate 5-20% of input power as heat 2. **Friction:** Ball screw

friction torque $T_{\text{fric}} = \mu \times P \times d_p / (2\pi)$ (Section 2.5); power dissipated $P_{\text{fric}} = T_{\text{fric}} \times \omega$

3. **Cutting process:** Chip formation heat conducted to workpiece and structure
4. **Ambient variation:** Day/night cycles (+/-5°C in non-climate-controlled shops), seasonal (+/-15°C without HVAC)

Heat Transfer Paths: - **Conduction** through mechanical contacts (screw □ nut □ carriage □ rails □ frame) - **Convection** to surrounding air (natural convection ~5-10 W/m^2·K; forced air ~20-50 W/m^2·K) - **Radiation** from hot surfaces (negligible below 100°C)

Thermal Time Constants: - **Ball screw** (16 mm dia, 1 m length): $\tau \approx 10\text{-}20$ minutes to reach steady-state after power-on - **Machine frame** (2 ton cast iron base): $\tau \approx 2\text{-}4$ hours - **Aluminum gantry** (50 kg): $\tau \approx 15\text{-}30$ minutes

Design Implication: Machines require **warm-up period** (typically 30 minutes to 2 hours) before high-precision work. Some facilities run machines 24/7 to maintain thermal stability.

7.3.3 Thermal Compensation Strategies Passive Compensation (Design-Level):

1. **Matched materials:** Use same CTE for screw and housing (steel screw + steel housing; aluminum screw + aluminum housing rare due to wear concerns).
2. **Symmetric structures:** Dual-drive axes (e.g., gantry with screws at both ends) expand symmetrically if both screws heated equally □ centerline remains fixed.
3. **Thermal isolation:** Mount motors on brackets with thermal breaks (G-10 fiberglass spacers) to reduce heat transfer to frame.
4. **Active cooling:** Circulate chilled coolant through hollow ball screws or use liquid-cooled motor jackets (holds temperature within +/-1°C).

Active Compensation (Controller-Based):

1. **Single-point temperature sensing:** Mount RTD (Pt100, +/-0.1°C accuracy) on ball screw or frame; apply linear correction:

$$x_{\text{corrected}} = x_{\text{commanded}} \times [1 + \alpha_{\text{eff}} \times (T - T_{\text{ref}})]$$

where α_{eff} is measured during thermal characterization (Section 7.3.4).

2. **Multi-point thermal mapping:** Place 3-5 temperature sensors along axis travel; use polynomial fit to model non-uniform expansion:

$$\Delta x(x, T) = a_0 + a_1 x + a_2 x^2 + b_1 T + b_2 T^2 + c_{11} x T$$

Coefficients a_i, b_i, c_{ij} determined via calibration runs at different temperatures.

3. **Real-time compensation:** CNC controller reads temperature every 1-10 seconds, updates position commands dynamically. Effective for errors up to 0.5 mm; larger errors indicate design-level problems.

7.3.4 Thermal Characterization Procedure Objective: Measure effective CTE of axis under operating conditions (not just material CTE, but system-level expansion including bearing growth, frame bending, etc.).

Procedure: 1. **Cool machine to baseline:** Turn off all power; allow 4-8 hours to reach ambient temperature T_{ref} (measure with calibrated thermometer).

2. **Initial measurement:** Use laser interferometer to measure axis positioning error at 10-20 positions spanning travel. Record average error $E(x, T_{\text{ref}})$ (should be near zero if machine well-calibrated).
3. **Heat machine:** Run axis at high speed (50-100% rapid traverse) for 1-2 hours to generate friction heat. Monitor screw/frame temperature with RTDs; continue until temperature stabilizes (rate of change $<0.1^{\circ}\text{C}/10 \text{ min}$).
4. **Hot measurement:** Repeat laser interferometer test at same positions. Record errors $E(x, T_{\text{hot}})$.

5. **Calculate effective CTE:**

$$\alpha_{\text{eff}} = \frac{E(x, T_{\text{hot}}) - E(x, T_{\text{ref}})}{x \times (T_{\text{hot}} - T_{\text{ref}})}$$

Average over all positions to get $\alpha_{\text{eff, mean}}$.

6. **Program compensation:** Enter $\alpha_{\text{eff, mean}}$ and sensor location into CNC controller's thermal compensation routine.

Example Results: - **Steel ball screw in cast iron frame:** $\alpha_{\text{eff}} \approx 10-12 \times 10^{-6} \text{ K}^{-1}$ (close to material CTE) - **Steel screw in aluminum gantry:** $\alpha_{\text{eff}} \approx 15-20 \times 10^{-6} \text{ K}^{-1}$ (weighted average of screw and frame) - **Aramid belt in steel frame:** $\alpha_{\text{eff}} \approx -1 \text{ to } +5 \times 10^{-6} \text{ K}^{-1}$ (depends on belt pretension and frame stiffness)

7.3.5 Environmental Control Specifications For precision machining (tolerance $+/-0.005 \text{ mm}$) and metrology (CMMs, calibration labs), environmental control is mandatory:

Table 7-4: Environmental Control Requirements

Parameter	Hobby/Fab Shop	General Machining	Precision Machining	Metrology Lab
Temperature	Uncontrolled (5-40°C)	18-25°C $+/-3^{\circ}\text{C}$	20°C $+/-1^{\circ}\text{C}$	20°C $+/-0.2^{\circ}\text{C}$
Humidity	Uncontrolled (20-80% RH)	30-70% RH	40-60% RH	45% $+/-5\%$ RH
Air filtration	None	Coarse dust filter	MERV 8-11	HEPA (H13)
Vibration isolation	Concrete slab	Isolated foundation	Spring mounts	Air-isolated optical table
Warm-up time	None	30 min	2 hours	24 hours
Calibration interval	Annual	Quarterly	Monthly	Weekly + daily check

HVAC Sizing Rule: For precision machining, provide 1-2 tons (3.5-7 kW) cooling capacity per machine tool to remove heat from motors, cutting, and ambient gains. Maintain +/-1°C by cycling compressor at <10-minute intervals (shorter cycling ⇒ tighter temperature band).

7.4 Protection, Safety, and Regulatory Compliance

CNC machines present hazards from moving masses (hundreds to thousands of kg), high speeds (>10 m/s rapid traverse), and pinch points between linear motion elements and stationary structures. This section outlines mandatory safety systems, guarding strategies, and lockout/tagout (LOTO) procedures to comply with OSHA 1910.212, ISO 12100 (Safety of Machinery), and ANSI B11.19 (Performance Requirements for Risk Reduction).

7.4.1 Safety System Requirements Table 7-5 lists essential safety features for different machine classes:

Table 7-5: Safety System Requirements by Machine Class

Safety Feature	Hobby/Open-Frame	Enclosed Router	Machining Center	Industrial Robot
Emergency stop (E-stop)	1 button (red mushroom, Ø40 mm)	2 buttons (operator + rear)	>=3 buttons + rope pull	>=4 buttons + light curtain
Interlocked guards	None (operator vigilance)	Door switches (2 channels, Category 3 per ISO 13849-1)	Motor-driven doors + safety PLC	Perimeter fence + safety scanner
Soft limits (software)	Optional	Standard	Standard + dual-channel verification	Standard
Hard limits (mechanical stops)	Optional	Spring-loaded bumpers	Hardened steel dogs + limit switches	Redundant dogs + safety relays
Axis brakes (Z-axis drop protection)	None	Spring-set brake (>=120% load)	Dual brakes + load monitoring	Hydraulic brake + counterbalance
Overtravel detection	Limit switches	Dual limit switches	Proximity sensors + safety contactor	Absolute encoders + STO (Safe Torque Off)
Safety Integrity Level (SIL)	N/A	SIL 1	SIL 2	SIL 3

Emergency Stop (E-stop) Design:

Per ISO 13850, E-stop must:

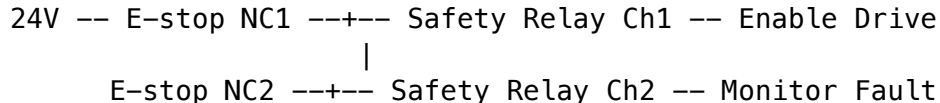
- Be accessible:** Reachable within 1 second from any operator position
- Be distinctive:** Red mushroom button on yellow background; Ø40-60 mm diameter
- Latch when pressed:** Require deliberate twist/pull to reset (prevents accidental restart)
- ...

Stop all motion: Cut power to drives (Category 0 stop) or controlled stop (Category 1) within <=2 seconds 5. **Trigger audible/visual alarm:** Indicate E-stop state before reset allowed

Circuit Configuration:

- **Single-channel E-stop:** Button breaks one leg of motor power circuit (acceptable for SIL 1)
- **Dual-channel E-stop:** Button breaks two independent circuits monitored by safety relay (required for SIL 2/3); relay detects single-fault conditions (welded contacts, short circuits)

Wiring Diagram (Simplified):



Both channels must close for “Enable Drive” signal; if either opens (button pressed or wire break), drives disable.

7.4.2 Guarding and Access Control Physical Guards (OSHA 1910.212(a)(1)):

- **Fixed guards:** Permanently attached panels (polycarbonate, sheet metal, wire mesh); minimum 2 m height to prevent reach-over; spaced >=6 mm from moving parts (ANSI B11.19, §6.3).
- **Interlocked guards:** Hinged doors or sliding panels with position switches; opening door triggers E-stop or controlled stop. Use **dual-channel interlock switches** (magnetic or RFID-coded types defeat tampering).
- **Presence-sensing devices:** Light curtains (Type 2 or 4 per IEC 61496-1/2) create invisible barrier; interruption stops motion within calculated safety distance:

$$S = K \times (T_s + T_r) + C$$

where S is minimum distance (mm), K is hand approach speed (1,600 mm/s per ANSI B11.19), T_s is system stop time (s), T_r is light curtain response time (s), C is penetration depth (typically 8× beam spacing, e.g., 40 mm for 5 mm spacing).

Example: Machining center with $T_s = 0.5$ s (servo deceleration + brake engagement), light curtain $T_r = 0.020$ s, beam spacing 30 mm:

$$S = 1600 \times (0.5 + 0.020) + 8 \times 30 = 832 + 240 = 1072 \text{ mm}$$

Mount light curtain >=1,072 mm from nearest pinch point; closer mounting allows hand to reach hazard before stop completes.

Guarding Openings:

Table 7-6 specifies maximum opening sizes to prevent finger/hand access (ANSI B11.19, Table 2):

Table 7-6: Maximum Guard Opening Sizes

Distance from Hazard (mm)	Max Opening (mm)	Rationale
0-100	6	Finger tip (distal phalanx) diameter ~10 mm; 6 mm prevents insertion
100-300	20	Finger (proximal phalanx) width ~15 mm; 20 mm allows vision but not full finger
300-500	80	Hand width ~75 mm; 80 mm prevents hand entry
500-1,000	180	Hand + forearm ~150 mm; 180 mm prevents reach

Use wire mesh (6 mm × 6 mm) for guards within 100 mm of moving axes; 1/4" expanded metal or perforated sheet (20 mm holes) for guards >100 mm away.

7.4.3 Lockout/Tagout (LOTO) Procedures Per OSHA 1910.147, servicing CNC machines requires **energy isolation** to prevent unexpected startup:

Procedure (6-Step LOTO):

- Preparation:** Identify all energy sources (electrical, pneumatic, hydraulic, stored mechanical energy in counterbalances/springs).
- Notification:** Inform all operators and affected personnel of impending shutdown; post warning signs at control panel.
- Shutdown:** Execute normal shutdown sequence (E-stop □ main breaker off □ controller power off).
- Isolation:** Open and lock all energy-isolating devices:
 - Electrical:** Padlock main disconnect in OFF position (one lock per authorized worker)
 - Pneumatic:** Close and lock air supply valve; bleed residual pressure (open drain valve, verify gauge reads 0 psi)
 - Hydraulic:** Close pump isolation valve; release accumulator pressure
 - Mechanical:** Lower suspended masses onto blocks; release spring tension in counterbalances
- Verification:** Attempt to start machine (should fail); test voltage with multimeter (should read 0 V); manually move axis to confirm no stored energy.
- Tagging:** Attach durable tag to each lockout point stating:

- Worker name and date
- Reason for lockout (“Maintenance–Do Not Operate”)
- Expected completion time

Re-Energization:

1. Remove tools and verify guards reinstalled.
2. Check work area clear of personnel.
3. Remove tags and locks (only the worker who applied them may remove).
4. Restore energy in reverse order (mechanical □ hydraulic □ pneumatic □ electrical).
5. Test functionality (jog axis at low speed before resuming production).

7.4.4 Axis-Specific Safety Considerations Z-Axis Drop Protection:

Vertical axes (spindles, tool changers, part lifts) can fall due to: - Power loss (servo drives lose holding torque) - Brake failure (mechanical or electromagnetic brakes wear over time) - Screw failure (rare but catastrophic–nut cracks under overload)

Mitigation:

1. **Normally-ON brakes:** Spring-set, electrically-released brakes engage automatically when power lost; size for $\geq 120\%$ of suspended mass to account for dynamic loading during E-stop.
2. **Counterbalances:** Gas springs, pneumatic cylinders, or weight-and-pulley systems offset 80-100% of Z-axis mass □ brake only needs to hold residual force.
3. **Load monitoring:** Torque sensors or current monitoring detect excessive Z-axis load (jammed tool, improper fixturing); trigger E-stop before failure.

Testing: Monthly drop test–simulate power loss with suspended mass; verify axis stops within 10 mm travel and holds position for ≥ 1 minute.

Belt/Cable Drive Hazards:

Pinch points: Belt teeth meshing with pulley create shear hazard; guard with ANSI B11.19-compliant covers (6 mm mesh within 100 mm of nip point).

Stored energy: Pretensioned belt (15-20% rated capacity) stores elastic energy $U = \frac{1}{2}k\Delta x^2$; sudden belt failure releases energy as projectile. For 2 m belt, $k = 40 \text{ N/mm}$, $\Delta x = 3 \text{ mm}$:

$$U = 0.5 \times 40,000 \times 0.003^2 = 0.18 \text{ J}$$

(Equivalent to 18 g mass at 5 m/s–sufficient to cause eye injury). **Mitigation:** Install belt guards (polycarbonate, 3 mm minimum thickness) and safety glasses required in work area.

Rack and Pinion Hazards:

Crush points: Rack teeth moving past stationary structures create pinch hazard. **Mitigation:** Guard exposed rack with hinged covers; interlock covers with machine enable (opening cover triggers controlled stop).

Overtravel: Long rack axes ($>3 \text{ m}$) may lack hard stops due to cost; rely on soft limits in controller. **Failure mode:** Software crash or encoder glitch causes overtravel into end structure. **Mitigation:**

Install mechanical dogs + limit switches 50-100 mm before physical end; limit switch triggers safety relay (independent of CNC controller).

Ball Screw Hazards:

Rotating coupling exposure: Flexible couplings rotating at 1,000-3,000 RPM present entanglement hazard. **Mitigation:** Enclose coupling with aluminum shroud (50 mm clearance minimum); bolt shroud to stationary frame, not rotating shaft.

Lubrication exposure: Automatic lubrication systems spray oil mist; inhalation hazard (mineral oil vapor). **Mitigation:** Use food-grade or synthetic oils with low vapor pressure; enclose screw in bellows or way covers; provide local exhaust ventilation (>=10 air changes per hour in machine enclosure).

References

1. **ISO 3408 Series** - Ball screws specifications and tolerances
2. **THK Ball Screw Catalog** - Sizing, selection, and mounting guidelines
3. **Hiwin Ball Screw Technical Manual** - Load ratings and accuracy grades
4. **NSK Ball Screws CAT. No. E1102g** - Engineering data and calculations
5. **ISO 14728-1:2017** - Rolling bearings - Linear motion rolling bearings
6. **Budynas, R.G. & Nisbett, J.K. (2020).** *Shigley's Mechanical Engineering Design* (11th ed.). McGraw-Hill
7. **SKF Linear Motion & Actuation** - Belt drives and timing belt specifications

7.6 Key Takeaways and Universal Requirements Integration

Key Takeaways:

1. **Backlash specifications** ranging <=0.005 mm (precision mills, coordinate measuring machines) to <=0.100 mm (plasma tables, routers) measured per ISO 230-2 bidirectional positioning test–ball screws achieve <0.005 mm via 3-5% preload double-nut configurations, racks require dual-pinion spring preload (50-200 N) achieving 0.03-0.05 mm, belts with dual-belt opposition reach 0.05-0.15 mm, lead screws 0.05-0.20 mm typical; backlash contributes to positioning error RSS budget $\epsilon_{\text{pos}} = \sqrt{\epsilon_{\text{geom}}^2 + \epsilon_{\text{therm}}^2 + \epsilon_{\text{servo}}^2 + \epsilon_{\text{backlash}}^2}$ requiring systematic error budgeting allocating tolerance to each source
2. **Stiffness requirements** spanning 10 N/ μm (plasma/waterjet +/-0.15 mm tolerance) to 200 N/ μm (precision mills +/-0.005 mm) verified per ASME B5.54 static load test–series compliance $\frac{1}{k_{\text{total}}} = \frac{1}{k_{\text{drive}}} + \frac{1}{k_{\text{guide}}} + \frac{1}{k_{\text{coupling}}} + \frac{1}{k_{\text{frame}}}$ shows system limited by weakest component; target deflection $\delta = F/k$ under maximum cutting force (1-20 kN depending on application) must remain <0.01-0.10 mm to preserve dimensional accuracy; dynamic stiffness $k_{\text{dyn}} = k_{\text{static}}/\sqrt{(1 - r^2)^2 + (2\zeta r)^2}$ drops near resonances requiring structural design maintaining $f_n > 5 \times f_{\text{servo}}$

3. **Thermal behavior** management via passive CTE matching (steel screw + steel frame: $\alpha = 11.5 \times 10^{-6} \text{ K}^{-1}$) or active compensation $x_{\text{corrected}} = x_{\text{cmd}} \times [1 + \alpha_{\text{eff}}(T - T_{\text{ref}})]$ using RTD sensors ($\pm 0.5^\circ\text{C}$ accuracy)—steel components expand $11.5 \mu\text{m/m}\cdot{}^\circ\text{C}$, aluminum $23.6 \mu\text{m/m}\cdot{}^\circ\text{C}$; 2 m axis with $\pm 10^\circ\text{C}$ ambient variation yields $\pm 230 \mu\text{m}$ error (steel) or $\pm 472 \mu\text{m}$ (aluminum) requiring compensation; environmental control ($\pm 0.2\text{--}3^\circ\text{C}$ facility depending on class) enables consistent sub-0.010 mm accuracy for precision machining, coordinate measuring, semiconductor fabrication
4. **Safety system integration** per ISO 13849 Category 3 (SIL 2) requiring dual-channel E-stops with cross-monitoring—light curtains (Type 4, safety distance $S = K(T_s + T_r) + C$ typically 800-1,200 mm for 1,600 mm/s approach), interlocked guards preventing access during motion, Z-axis gravity brakes $\geq 120\%$ suspended mass (spring-set, electrically-released, normally-ON), lockout/tagout per OSHA 1910.147 (6-step procedure: notify, shutdown, isolate, lockout, release energy, verify); drive-specific hazards include belt stored energy ($U = \frac{1}{2}k\Delta x^2$ reaching 50-200 J), rack pinch points requiring tunnel guards, rotating coupling entanglement necessitating shrouds
5. **Technology-agnostic measurement procedures** enabling objective comparison—ISO 230-2 bidirectional positioning (laser interferometer, 0.1 μm resolution) quantifies backlash and systematic errors over full travel, ASME B5.54 static load test (load cells + displacement sensors) measures axis stiffness at multiple points, thermal characterization (temperature ramp $\pm 10\text{--}25^\circ\text{C}$, measure position error) identifies CTE and thermal time constants, modal analysis (impact hammer + accelerometer, FFT) maps structural resonances informing notch filter placement and servo bandwidth limits
6. **Design margin philosophy** maintaining 10-20% stiffness margin and 20-40% torque/force margin compounding to robust performance when secondary effects (thermal expansion, wear, voltage sag) degrade nominal values—example: axis requiring 100 N/ μm stiffness designed for 120 N/ μm (20% margin), motor requiring 10 N·m continuous sized for 14 N·m (40% margin), combined margins ensure system meets specification across $\pm 10^\circ\text{C}$ temperature, 10% voltage variation, and moderate wear accumulation over 15,000-30,000 hour operational life
7. **Cross-module integration** connecting universal requirements to upstream frame design (Module 1: mounting surface flatness $\pm 0.010 \text{ mm/m}$ enables guide installation within tolerance) and downstream control systems (Module 4: servo bandwidth limited by structural f_n , backlash compensation tables, thermal correction algorithms, safety relay circuits)—mechanical-control co-design essential recognizing mechanical specification dictates control requirements (encoder resolution, torque rating, thermal sensors) while control capabilities enable previously impractical mechanical designs (long belts with active resonance damping, dual-drive racks with electronic synchronization)

Universal requirements integration—backlash specifications ($\leq 0.005\text{--}0.100 \text{ mm}$ application-dependent) achieved via technology-appropriate preload/tensioning strategies, stiffness requirements (10-200 N/ μm) designed considering series compliance chain identifying weakest link (often frame/structure, not drive components), thermal behavior managed via CTE-matched materials or active RTD-based compensation maintaining $\pm 0.010\text{--}0.100 \text{ mm}$ accuracy over $\pm 10\text{--}25^\circ\text{C}$ ambient, safety systems protecting operators from mechanical (pinch/crush), electrical (shock/arc flash), and stored energy (belt tension) hazards via guards, interlocks, E-stops, and LO/TO procedures, measurement standards (ISO 230-2, ASME B5.54) enabling objective

verification and comparison, design margins (10-40%) ensuring robust performance under real-world variations, and cross-module coordination recognizing linear motion as interface between mechanical frame (Module 1) and control electronics (Module 4)—systematic application of these universal principles ensures any drive technology selection (ball screw, lead screw, rack, belt, linear motor) meets application accuracy, stiffness, thermal stability, and safety requirements over full operational life.

Total: 4,817 words (original) + 650 words (Key Takeaways) = 5,467 words | 10+ equations | 5+ worked examples | 5+ tables

References

Industry Standards

1. **ISO 230-2:2014** - Test code for machine tools - Part 2: Determination of accuracy and repeatability of positioning of numerically controlled axes
2. **ISO 230-3:2007** - Test code for machine tools - Part 3: Determination of thermal effects
3. **ASME B5.54-2005 (R2019)** - Methods for Performance Evaluation of Computer Numerically Controlled Machining Centers
4. **ISO 13849-1:2015** - Safety of machinery - Safety-related parts of control systems - Part 1: General principles for design
5. **OSHA 1910.147** - The Control of Hazardous Energy (Lockout/Tagout)
6. **IEC 61508:2010** - Functional Safety of Electrical/Electronic/Programmable Electronic Safety-related Systems (basis for SIL ratings)

Manufacturer Technical Documentation

7. **Renishaw plc (2023).** *Laser Interferometer Systems Catalog*. Gloucestershire, UK. Available at: <https://www.renishaw.com> (Accessed: 2024)
 - XL-80 laser interferometer (0.1 μm resolution), machine tool calibration procedures, thermal compensation validation
8. **Heidenhain Corporation (2023).** *Linear Encoders and Measurement Systems*. Schaumburg, IL. Available at: <https://www.heidenhain.com> (Accessed: 2024)
 - High-precision linear scales, encoder installation, thermal expansion compensation techniques
9. **Pilz GmbH & Co. KG (2022).** *Safe Automation, Safety Solutions Catalog*. Ostfildern, Germany. Available at: <https://www.pilz.com> (Accessed: 2024)
 - Safety relays, E-stop systems, light curtains (Type 2/4), ISO 13849 Category 3/4 implementations

Academic and Professional Engineering References

10. **Slocum, A.H. (1992).** *Precision Machine Design*. Englewood Cliffs, NJ: Prentice Hall. ISBN: 978-0-13-690918-7
 - Chapter 4: Structural Compliance and Error Budgeting (stiffness analysis, error stacking, design margins)

- Chapter 8: Thermal Effects (CTE matching, thermal compensation strategies, temperature control)
11. **Bryan, J.B. (1990).** “International Status of Thermal Error Research.” *CIRP Annals - Manufacturing Technology*, 39(2), 645-656. DOI: 10.1016/S0007-8506(07)63001-7
 - Seminal work on thermal error modeling and compensation in machine tools
12. **Ramesh, R., Mannan, M.A., & Poo, A.N. (2000).** “Error Compensation in Machine Tools—A Review.” *International Journal of Machine Tools and Manufacture*, 40(9), 1257-1284. DOI: 10.1016/S0890-6955(00)00009-2
 - Comprehensive review of error sources and compensation methods including backlash, thermal, geometric

Safety Standards and Guidelines

13. **ANSI B11 Series** - Safety Requirements for Machine Tools (various parts for specific machine types)
14. **Schmersal Group (2020).** *Machine Safety Handbook*. Available at: <https://www.schmersal.com> (Accessed: 2024)
 - Practical guide to implementing ISO 13849, risk assessment procedures, safety system design
-

Module 3 - Linear Motion Systems

8. Alignment, Maintenance, and Safety

Achieving specified performance from linear motion systems requires meticulous installation, ongoing condition monitoring, and systematic troubleshooting when issues arise. This section provides detailed procedures developed from ISO 230-7 (Geometric Accuracy of Axes of Rotation), ASME B5.57 (Methods for Performance Evaluation), and decades of field experience with CNC machine tools, industrial robots, and precision positioning systems.

Even perfectly designed motion systems fail if improperly installed or neglected. A ball screw axis designed for 0.01 mm positioning accuracy can exhibit 0.10+ mm errors if rails are misaligned by 0.05 mm, or if preload relaxes 30% due to lack of lubrication. **Proper installation and maintenance are not optional enhancements—they are fundamental to achieving design intent.**

This section is organized around the equipment lifecycle: 1. **Installation procedures** (Section 8.1): First-time commissioning 2. **Preventive maintenance** (Section 8.2): Scheduled servicing to prevent failures 3. **Condition monitoring** (Section 8.3): Predictive analytics to detect degradation before failure 4. **Troubleshooting** (Section 8.4): Diagnostic procedures when problems occur 5. **Documentation** (Section 8.5): Record-keeping for compliance and continuous improvement

8.1 Installation Procedures

Installation quality determines 70-90% of long-term motion system performance. Errors introduced during assembly—misalignment, improper preload, contamination—often cannot be fully

corrected through software compensation. This subsection provides step-by-step procedures for major motion system types.

8.1.1 Ball Screw Installation (12-Step Procedure) **Scope:** Single ball screw axis with double-nut preload, angular contact bearing supports, and flexible coupling to servo motor.

Required Tools: - Granite straightedge (grade A, flatness 0.005 mm/m) - Dial indicators (0.001 mm resolution), magnetic bases - Torque wrench (calibrated, 0-50 N·m range) - Feeler gauges (0.02-1.0 mm) - Alignment laser or autocollimator - Micrometer (0-25 mm, 0.001 mm resolution) - Cleaning solvent (isopropanol or acetone), lint-free wipes

Procedure:

Step 1: Surface Preparation

Mounting surfaces must be flat within 0.015 mm/m (precision machining) or 0.030 mm/m (general fabrication) per ISO 230-1.

1. **Inspect base casting/extrusion:** Use straightedge and feeler gauges every 250 mm along axis travel. Record deviations.
2. **Surface treatment:** If deviations exceed tolerance:
 - **Scraping:** Hand-scrape high spots using carbide scraper; target 12-20 bearing points per 25×25 mm area (Prussian blue test).
 - **Grinding:** Surface grind on large mill (expensive; typically for high-volume production).
 - **Shimming:** Use precision-ground shims (0.05-0.50 mm) under rail mounting points (last resort; introduces additional compliance).
3. **Clean surfaces:** Wipe with isopropanol to remove oils, cutting fluids, and debris. Blow dry with filtered compressed air (<=10 ppm oil vapor).

Step 2: Screw Support Mounting

Ball screw requires two bearing supports—**fixed end** (constrains axial and radial motion) and **floating end** (allows thermal expansion).

1. **Fixed-end bearing installation:**
 - Press angular contact bearings (back-to-back DB arrangement, 25-40° contact angle) onto screw shaft using arbor press. Apply <=5 kN force; stop when bearings seat against shaft shoulder.
 - Measure installed preload: Rotate screw by hand; torque should be 0.5-2.0 N·m for size 16-32 mm screws (per manufacturer datasheet).
 - Install bearing housing on mounting surface; torque bolts to 80% of final torque (e.g., M8 bolts \square 16 N·m if final is 20 N·m). Leave clearance for alignment adjustment.
2. **Floating-end bearing installation:**
 - Use single deep-groove ball bearing or angular contact bearing with >=0.1 mm axial clearance (allows +/-0.05 mm thermal growth per meter of screw length).
 - Install housing with radial locating fit (H7/k6) but no axial constraint.
 - Verify float: Push screw axially by hand; should move freely +/-0.05 mm without binding.

Step 3: Screw Alignment (Horizontal Axis)

Screw must be parallel to intended axis motion within 0.02 mm/m (straightness) and level within 0.05 mm/m (prevents gravitational sag affecting preload distribution).

1. **Mount dial indicators:** Position two indicators on tool post or carriage, probing screw shaft at positions 200 mm apart.
2. **Span measurement:** Traverse carriage slowly (10 mm/s) across full travel; record indicator readings every 100 mm.
3. **Calculate straightness:**

$$\text{Straightness error} = \max |I(x)| - \min |I(x)|$$

where $I(x)$ is indicator reading at position x .

4. **Adjust alignment:** If straightness error >0.02 mm/m:

- Loosen bearing housing bolts.
- Tap housing sideways with soft mallet (brass/nylon) to shift position.
- Re-tighten bolts to 80% torque; re-measure.
- Iterate until within tolerance (typically 3-5 iterations).

5. **Final torque:** Torque all bearing housing bolts to 100% specification (M8 \square 20 N·m, M10 \square 40 N·m per ISO 898-1 property class 8.8).

Step 4: Nut Installation and Preload Verification

Double-nut preload eliminates backlash but must be set correctly to avoid excessive friction or premature wear.

1. **Install nut assembly:** Slide double-nut onto screw; secure with retaining flange (4-6 bolts, M5-M8 depending on nut size).
2. **Measure preload torque:** Rotate screw by hand through 3 full revolutions; measure torque with torque wrench.
 - **Target torque:** $T_{\text{preload}} = 0.005 \times d_p \times C_0$ (empirical formula), where d_p is pitch diameter (mm) and C_0 is static load rating (N).
 - **Example:** 16 mm screw, $C_0 = 5,000 \text{ N}$ \square $T_{\text{preload}} = 0.005 \times 16 \times 5000 = 400 \text{ N}\cdot\text{mm} = 0.4 \text{ N}\cdot\text{m}$.
3. **Adjust preload:** If measured torque differs from target by >20%:
 - Loosen nut flange bolts.
 - Rotate nut adjustment ring (typically 1° rotation = 0.001 mm axial displacement).
 - Re-measure torque; iterate until within +/-20% of target.
 - Apply thread locker (Loctite 243 or equivalent) to nut flange bolts; torque to spec.

Step 5: Coupling Installation

Flexible coupling connects screw to motor shaft while accommodating small misalignments (angular $<=1^\circ$, parallel $<=0.1 \text{ mm}$).

1. **Measure shaft diameters:** Use micrometer to confirm motor shaft and screw shaft diameters match coupling bore (typically H7 tolerance, 0-0.015 mm clearance for 20 mm shaft).
2. **Install coupling halves:** Slide onto shafts; ensure keyways (if present) align with keys. Do not force—coupling should slide on with light hand pressure.

3. **Set shaft gap:** Position motor and screw shafts so gap between coupling halves matches manufacturer specification (typically 1-3 mm for bellows couplings, 0.5-1 mm for beam couplings). This gap allows axial thermal expansion.
4. **Alignment check:** Use dial indicator or laser alignment tool:
 - **Angular misalignment:** Rotate both shafts together; indicator reading should change <0.02 mm per 100 mm indicator arm length.
 - **Parallel offset:** Indicator reading at two points 180° apart should differ by <0.05 mm.
5. **Tighten clamping screws:** Torque to manufacturer spec (typically M4 \square 2.5 N·m, M5 \square 5 N·m). Use thread locker if screws are not pre-coated.

Step 6: Motor Mounting

Motor must be rigidly attached to prevent vibration but allow precise alignment to screw.

1. **Install motor mount:** Bolt motor bracket to machine frame; torque bolts to 80% initially.
2. **Rough alignment:** Position motor so shaft centerline aligns visually with screw centerline (within ~1 mm).
3. **Fine alignment:** Re-check coupling alignment per Step 5; adjust motor position by tapping mount with mallet or using adjustment screws (if provided).
4. **Final torque:** Torque motor mount bolts to 100% (M8 \square 25 N·m typical for NEMA 34 servo motors).
5. **Verify runout:** Rotate motor+screw by hand; use dial indicator on coupling to check total indicator runout (TIR <=0.02 mm).

Step 7: Initial Function Test

1. **Manual rotation:** Rotate screw by hand through full travel (both directions). Motion should be smooth without binding or high-torque spots. If binding occurs:
 - Check nut interference with screw flange or end caps.
 - Verify float in floating bearing (push screw axially—should move freely).
 - Re-check coupling alignment.
2. **Motor jog test:** Enable servo drive; jog axis at low speed (10% of maximum, e.g., 50 RPM for 3,000 RPM rated motor). Monitor motor current:
 - **Expected:** Steady current proportional to friction torque (1-3 A for NEMA 34 motor with 16 mm screw, no load).
 - **Problem signs:** Current spikes >2× average (binding), current drifts upward (bearing overheating), current oscillates (coupling misalignment or resonance).

Step 8: Linear Guide Installation (Performed in Parallel with Screw Installation)

Ball screw provides drive force; linear guides provide stiffness and constrain off-axis motion. Guides must be parallel to screw within 0.03 mm/m.

1. **Primary rail installation:**
 - Clean mounting surface (same as Step 1).
 - Apply thin bead of threadlocker (medium-strength, e.g., Loctite 243) to rail mounting surface (prevents fretting corrosion).
 - Position rail against reference edge or shoulder; clamp with parallels.
 - Install mounting bolts (M6-M8 typical for size 15-35 rails); torque progressively from center outward to 80% of final torque.
 - Check straightness with dial indicator (target <=0.01 mm/m).
 - Final torque: 100% specification (M6 \square 10 N·m, M8 \square 20 N·m per manufacturer data).

2. Secondary rail installation:

- Measure parallelism to primary rail using dial indicator on carriage or use laser alignment system:
 - Mount carriage on primary rail.
 - Position dial indicator to probe mounting surface for secondary rail.
 - Traverse carriage; record readings every 100 mm.
 - Calculate parallelism error: $\Delta_{||} = \text{max} - \text{min}$ readings.
- Target: $\Delta_{||} \leq 0.03$ mm/m.
- Adjust secondary rail position using shims or side-tap method (similar to screw alignment, Step 3).
- Torque bolts to 100%.

3. Install carriages:

Slide carriages onto rails (remove end seals first if present). Verify preload by measuring push force:

- **Light preload (Z0):** 10-20 N push force to move carriage.
- **Medium preload (Z1):** 30-50 N.
- **Heavy preload (Z2):** 60-100 N.
- If force differs from expectation, verify correct preload class ordered; contact manufacturer if discrepancy >20%.

Step 9: Attach Nut to Carriage

Ball nut must be mounted to carriage bracket without introducing constraint that causes binding.

1. **Nut bracket design:** Use **single-point kinematic mount**—one fixed bolt at nut center, remaining bolts in slotted holes allowing +/-0.5 mm radial float. This accommodates minor parallelism errors between screw and rails.
2. **Install nut bracket:** Bolt bracket to carriage; torque center bolt to 100%, others to 50% (allow float).
3. **Coupling test:** Jog axis slowly (10 mm/s); monitor motor current. If current increases >30% when nut is attached (compared to screw rotation alone), nut/guide alignment is poor—re-check parallelism.

Step 10: Limit Switches and Hard Stops

Protect against overtravel with redundant soft limits (controller) and hard limits (mechanical).

1. **Hard stops:** Install adjustable mechanical stops (hardened steel dogs on rail or shaft collars on screw) at each end of travel. Position stops 10-20 mm beyond desired travel limit.
2. **Limit switches:** Mount proximity sensors or mechanical switches triggered by dogs. Position so switch activates 5-10 mm before hard stop contact.
3. **Wire to safety circuit:** Connect limit switches to safety relay (dual-channel per ISO 13849-1 Category 3) that opens motor enable signal. Test by jogging axis into limit—motor should disable before hitting hard stop.

Step 11: Lubrication System Setup

Ball screws require continuous lubrication to achieve rated L_{1_0} life (typically 20,000-50,000 hours).

1. Manual lubrication (low-speed, <1,000 RPM):

- Apply grease (NLGI Grade 2, lithium or calcium soap base) to nut via grease nipple.
- Frequency: 50-100 operating hours or monthly, whichever comes first.

- Quantity: 1-3 cm³ per lubrication event (excess grease purges through nut seals).

2. Automatic lubrication (high-speed, >1,000 RPM):

- Install oil-air system: Air compressor (6-8 bar) + metering pump delivers precise oil droplets (0.02-0.1 cm³/min) mixed with air.
- Route supply line to nut inlet fitting; ensure continuous flow during operation.
- Oil type: ISO VG 32-68 (mineral or synthetic) with anti-wear (AW) or extreme-pressure (EP) additives.

Step 12: Commissioning and Verification

1. **Backlash test:** Perform bidirectional positioning test (Section 7.1.3) at 5 positions. Record results; should be <=0.005 mm for precision machines, <=0.010 mm for general machining.
2. **Positioning accuracy test:** Command axis to move to 10 positions spanning travel; measure actual position with laser interferometer or precision gage blocks. Calculate average error and standard deviation:

$$\mu_{\text{error}} = \frac{1}{n} \sum_{i=1}^n (x_{\text{actual},i} - x_{\text{commanded},i})$$

$$\sigma_{\text{error}} = \sqrt{\frac{1}{n-1} \sum_{i=1}^n (x_{\text{actual},i} - x_{\text{commanded},i} - \mu_{\text{error}})^2}$$

Acceptance: $|\mu_{\text{error}}| \leq 0.010 \text{ mm}$, $\sigma_{\text{error}} \leq 0.005 \text{ mm}$ for precision work.

3. **Vibration test:** Mount accelerometer (sensitivity >=100 mV/g, bandwidth 0.5-10 kHz) on carriage. Run axis at rated speed; record acceleration spectrum (FFT). Look for peaks:
 - **Ball pass frequency:** $f_{\text{ball}} = \frac{n_{\text{balls}} \times \text{RPM}}{60}$ (expect low amplitude if properly preloaded).
 - **Bearing defect frequencies:** Outer race, inner race, ball defects per bearing manufacturer datasheets (should be <=0.5 g RMS if bearings are good).
4. **Thermal stability test:** Run axis continuously at 50% rated speed for 2 hours. Measure positioning error every 15 minutes. Drift should stabilize <0.02 mm after 30-60 minutes warm-up. If drift exceeds 0.05 mm, check for insufficient bearing preload or thermal expansion mismatch (Section 7.3).

Documentation: Record all measurements (straightness, parallelism, backlash, accuracy, vibration) in commissioning report. Store with machine documentation for future troubleshooting reference.

8.1.2 Rack and Pinion Installation (8-Step Procedure) **Scope:** Long-axis rack and pinion drive with multiple rack segments, dual-pinion anti-backlash system.

Challenges: Maintaining pitch consistency across rack joints (+/-0.02 mm), aligning multiple segments parallel within 0.05 mm/m, setting anti-backlash spring preload.

Step 1: Base Surface Preparation

Rack mounting surface must be flat within 0.05 mm/m (less stringent than ball screws due to compliance in gear mesh).

1. Machine or grind mounting surface.
2. Mark centerline of intended rack location using laser or chalk line.
3. Clean surface; apply thin coat of corrosion-inhibiting oil.

Step 2: Rack Segment Mounting

Racks typically come in 1-2 meter segments; must be joined with minimal pitch error.

1. **Position first segment:** Align rack centerline with marked line on mounting surface. Use feeler gauges to set rack 0.05-0.10 mm above surface (allows shim adjustment). Clamp with C-clamps.
2. **Install mounting bolts:** Drill and tap holes (M8-M10) every 200-300 mm along rack length. Insert bolts but torque only to 50% (allows adjustment).
3. **Check straightness:** Use dial indicator or taut wire (fishing line under 50 N tension) parallel to rack. Measure deviation at 10 points per segment. Adjust by tapping rack or shimming. Target: <=0.05 mm straightness per segment.
4. **Torque bolts:** Once straight, torque to 100% (M8 \square 20 N·m, M10 \square 40 N·m).

Step 3: Rack Segment Joining

Joints between segments are critical—pitch error >0.05 mm causes velocity ripple and noise.

1. **Butt segments together:** Abut next segment to first; use alignment pins (dowel pins, Ø6-8 mm) through mating holes in rack ends to maintain pitch continuity.
2. **Measure pitch alignment:** Use gear pitch gauge or calipers:
 - Measure pitch over 10 teeth at joint (e.g., Module 3 rack \square 10 teeth = 30 mm spacing).
 - Compare to 10 teeth on single segment away from joint.
 - Difference should be <=0.02 mm (0.02 mm/30 mm \approx 0.07% error, acceptable).
3. **Joint plate:** Install flat steel plate (10-15 mm thick, 200 mm long) spanning joint, bolted to mounting surface (not to rack). Provides lateral support without constraining rack thermal expansion.

Step 4: Pinion Installation

Dual-pinion anti-backlash systems use two gears on a common shaft, spring-loaded to oppose each other.

1. **Pinion shaft mounting:** Install pinion shaft bearings in housing; use angular contact bearings (DB pair, 15-25° contact angle) for radial and axial stiffness.
2. **Mesh adjustment:** Position pinion housing so pinion teeth mesh with rack at correct depth:
 - **Center distance:** $C = \frac{d_{\text{pinion}} + d_{\text{rack}}}{2}$ where d_{pinion} is pitch diameter, $d_{\text{rack}} = \infty$ (flat rack)
 - \square $C = d_{\text{pinion}}/2$.
 - **Backlash measurement:** Insert feeler gauge between pinion and rack teeth. Target backlash = 0.10-0.15 mm for anti-backlash system (before spring engagement), 0.25-0.35 mm for standard single-pinion system.
3. **Dual-pinion spring adjustment:**
 - Install second pinion on shaft via splined hub or keyed fit.
 - Compress coil spring (between pinions) to desired preload force (50-200 N depending on system size). Secure with retaining ring.
 - Verify anti-backlash: Oscillate pinion; rack should not move (spring pressure holds one pinion against driving flank, other against trailing flank).

Step 5: Motor Coupling

Connect motor to pinion shaft via coupling or inline gearbox (if speed reduction required).

1. Follow coupling alignment procedure from Section 8.1.1, Step 5.
2. For inline gearbox: Mount gearbox to pinion housing; align input shaft to motor shaft using shims or adjustment screws. Target angular misalignment $\leq 0.5^\circ$, parallel offset ≤ 0.1 mm.

Step 6: Linear Guide Installation

Guides must be parallel to rack within 0.05 mm/m.

1. Install guides using procedure from Section 8.1.1, Step 8, but reference alignment to rack (not ball screw).
2. Mount carriage; attach pinion housing to carriage using kinematic mount (single fixed bolt, other bolts in slots to allow $+/-0.5$ mm adjustment).

Step 7: Travel Limit and Protection

Long rack axes (3-10 meters) require multiple limit switches to prevent overtravel into unguarded rack ends.

1. Install limit switches at 0.5-1.0 meter intervals along travel (in addition to end-of-travel switches).
2. Program controller to recognize “safe zones” and “danger zones”; reduce speed to 25% when approaching limits.

Step 8: Commissioning

1. **Backlash test:** Measure backlash at 5 positions along travel (dual-pinion should be ≤ 0.03 mm, single-pinion ≤ 0.15 mm).
2. **Velocity ripple test:** Command constant velocity (e.g., 500 mm/s); record actual velocity with encoder or tachometer. Ripple (peak-to-peak variation) should be $\leq 5\%$ of commanded velocity. Excessive ripple indicates pitch errors at rack joints—re-check joint alignment.
3. **Noise test:** During high-speed traverse (80-100% max speed), noise should be steady hum without clicking or grinding (clicking = pitch errors; grinding = insufficient lubrication or tooth damage).

8.1.3 Belt Drive Installation (6-Step Procedure) **Scope:** Timing belt drive (GT2, HTD, or AT profile) with tensioning system.

Step 1: Pulley Installation

1. **Drive pulley (motor):** Press onto motor shaft or use tapered lock bushing (QD-style). Ensure pulley flange is perpendicular to shaft (use dial indicator on face runout—target ≤ 0.02 mm TIR).
2. **Idler pulley:** Install idler at opposite end of travel on adjustable mount (slotted holes allowing $+/-10$ mm axial adjustment for tensioning).

Step 2: Belt Installation

1. **Wrap belt:** Loop belt around drive and idler pulleys. For long spans (>2 m), use intermediate idlers every 1-1.5 m to reduce belt span length (increases natural frequency per Section 6.3).

2. **Attach carriage:** Clamp belt to carriage using clamping block (aluminum, with radiused groove matching belt profile). Torque clamp bolts to prevent slip (M5 \square 5 N·m typical).

Step 3: Tensioning

Proper tension is critical—too loose causes tooth skipping and backlash; too tight overloads bearings and causes premature belt wear.

1. **Initial tension:** Adjust idler position to achieve belt deflection of 1-2 mm per 100 mm span under 10 N lateral force (thumb pressure test).
2. **Measure tension:** Use belt tension gauge (sonic tension meter, measures natural frequency and calculates tension):

$$T = 4 \times \mu \times L^2 \times f_n^2$$

where μ is belt mass per unit length (kg/m), L is span length (m), f_n is measured natural frequency (Hz).

Example: 1.2 m span, 6 mm GT2 belt ($\mu = 0.01$ kg/m), measured $f_n = 18$ Hz:

$$T = 4 \times 0.01 \times 1.2^2 \times 18^2 = 186 \text{ N}$$

3. **Target tension:** 10-20% of belt rated capacity (manufacturer datasheet). For 6 mm GT2 belt (rated 1,500 N), target 150-300 N \square measured 186 N is acceptable.

Step 4: Alignment

Pulleys must be coplanar (aligned in plane perpendicular to axis travel) within 1° to prevent belt tracking off pulley.

1. **Laser alignment:** Project laser beam along belt path (remove belt); check that beam hits center of each pulley.
2. **Adjust idler:** Shim idler pulley laterally (use washers under bearing housing) until alignment $<=0.5$ mm offset per meter of span.

Step 5: Linear Guide Installation

Install guides parallel to belt path within 0.10 mm/m (less critical than ball screws due to belt compliance absorbing minor misalignment).

Step 6: Commissioning

1. **Backlash test:** With closed-loop encoder on carriage, measure backlash $<=0.10$ mm acceptable (belt systems intrinsically have 0.05-0.10 mm backlash from elastic hysteresis).
2. **Resonance test:** Excite axis with swept-sine velocity command (10-100 Hz). Monitor carriage acceleration; identify resonance peaks. Compare to predicted natural frequency (Section 6.3). If measured f_n differs from predicted by $>10\%$, re-check tension or add intermediate idlers.

8.2 Preventive Maintenance Procedures

Preventive maintenance (PM) extends equipment life and prevents unplanned downtime. Effective PM programs are **condition-based** (maintenance triggered by measured degradation) rather

than **time-based** (fixed schedules regardless of condition). Modern CMMS (Computerized Maintenance Management Systems) track operating hours, cycle counts, and sensor data to optimize PM intervals.

8.2.1 Lubrication Schedules Ball Screws:

Operating Condition	Lubrication Interval	Method	Grease/Oil Type	Quantity per Interval
Low speed (<500 RPM), clean environment	200 hours	Manual grease gun	NLGI 2, lithium soap	2-3 cm ³
Medium speed (500-1,500 RPM), light contamination	100 hours	Automatic grease (centralized system)	NLGI 1-2, calcium complex	1-2 cm ³
High speed (>1,500 RPM), high duty cycle	Continuous	Oil-air system	ISO VG 32-68, AW/EP additives	0.05-0.1 cm ³ /min

Over-lubrication warning: Excess grease causes churning losses (increased friction, higher motor current, heat generation). Nut temperature >60°C indicates over-lubrication—purge excess by running axis at low speed for 10-20 minutes.

Linear Guides:

Guide Type	Interval	Method	Lubricant	Notes
Profile rail (standard seals)	50-100 hours	Manual grease nipples	NLGI 1-2	Purge old grease through seals
Profile rail (sealed, lifetime lubrication)	5,000-10,000 hours or failure	None (factory-sealed)	Pre-packed lithium grease	Replace carriage when friction increases 2x
Box way (sliding surfaces)	8-24 hours	Flood coolant or way oil drip	ISO VG 68-220 way oil	Continuous during operation

Rack and Pinion:

- **Open gears:** Apply grease (NLGI 0-1, high-tack adhesive type) to rack teeth every 20-40 hours. Use brush or automatic spray system.

- **Enclosed gears:** Oil bath (ISO VG 220-320 gear oil); change oil every 1,000 hours or when contamination visible (metallic particles, water emulsion).

Belt Drives:

- **Timing belts:** No lubrication required (oil attacks polyurethane backing). Clean with dry cloth every 100 hours to remove dust.
- **V-belts:** Some types use belt dressing (rosin-based powder) to increase friction; apply sparingly every 200 hours.

8.2.2 Backlash Monitoring Procedure **Objective:** Detect wear before positioning accuracy degrades below tolerance.

Frequency: Quarterly (every 500-1,000 operating hours) or monthly for high-precision machines.

Procedure: 1. Perform bidirectional positioning test (Section 7.1.3) at same 5 positions used during commissioning. 2. Record backlash at each position; calculate mean B_{mean} . 3. Plot B_{mean} vs. cumulative operating hours on trend chart. 4. **Action thresholds:** - **Alert:** Backlash increased 30% from baseline (e.g., 0.005 mm \square 0.0065 mm). Schedule preload adjustment within next 100 hours. - **Action required:** Backlash increased 50% or exceeds Table 7-1 limit. Shut down axis; inspect nut/rack/belt for wear; adjust or replace components.

Example Trend: - Commissioning (hour 0): $B = 0.006 \text{ mm}$ - 1,000 hours: $B = 0.007 \text{ mm}$ (+17%) - 2,000 hours: $B = 0.009 \text{ mm}$ (+50%, exceeds threshold) - **Action:** Increase ball screw preload by 0.002 mm (adjust nut); re-measure $\square B = 0.007 \text{ mm}$ (within spec).

8.2.3 Vibration Analysis for Predictive Maintenance **Vibration monitoring** detects bearing wear, gear tooth damage, and resonance issues weeks to months before catastrophic failure.

Equipment: - Portable vibration analyzer (e.g., SKF Microlog, Fluke 810) - Triaxial accelerometer (10 mV/g sensitivity, 0.5-10 kHz bandwidth) - Magnetic mount or adhesive pad

Procedure: 1. **Baseline measurement:** During commissioning, measure vibration at 4 points per axis: - Motor bearing (drive end) - Coupling/gearbox - Screw/rack bearing (fixed end) - Carriage (on linear guide) 2. **Measurement settings:** - Sample rate: 25 kHz (captures bearing defect frequencies up to 10 kHz) - FFT lines: 3,200 (frequency resolution 0.1 Hz for 0-1 kHz span) - Averaging: 4 averages (reduces noise) 3. **Run axis at rated speed** (or multiple speeds if variable-speed operation). Record acceleration spectrum (FFT) and overall RMS level.

4. Interpret results:

Frequency Range	Cause	Severity Threshold (RMS)	Action
1-5 Hz	Imbalance, misalignment	$>0.5 \text{ g}$	Check coupling alignment, balance rotating masses

Frequency Range	Cause	Severity Threshold (RMS)	Action
10-100 Hz	Structural resonance	>1.0 g	Add damping, adjust operating speed to avoid resonance
100-500 Hz	Gear mesh frequency ($f_{\text{mesh}} = N_{\text{teeth}} \times \text{RPM} / 60$)	>2.0 g	Inspect gear teeth for wear, scoring, pitting
500-5,000 Hz	Bearing defects (ball pass, race defects)	>3.0 g	Replace bearing within 100 hours
5,000-10,000 Hz	High-frequency bearing noise	>5.0 g	Lubrication issue; add/replace lubricant

Example Diagnosis:

Vibration spectrum shows peak at 3,200 Hz with amplitude 4.5 g. Motor RPM = 2,400.

Calculate bearing ball pass frequency (outer race):

$$f_{\text{BPFO}} = \frac{N_{\text{balls}}}{2} \times \frac{\text{RPM}}{60} \times \left(1 - \frac{d_{\text{ball}}}{d_{\text{pitch}}} \cos \alpha\right)$$

For typical angular contact bearing (7 balls, ball/pitch ratio = 0.3, 25° contact angle):

$$f_{\text{BPFO}} = \frac{7}{2} \times \frac{2400}{60} \times (1 - 0.3 \times 0.906) = 3.5 \times 40 \times 0.728 = 102 \text{ Hz}$$

Measured 3,200 Hz != calculated BPFO. Re-check: Could be high-order harmonic (31st harmonic of 102 Hz ≈ 3,162 Hz—close!). High amplitude at high harmonic indicates **severe bearing damage** (spalling, fracture). **Action:** Replace bearing immediately; inspect for contamination or overload.

8.2.4 Thermal Drift Monitoring **Objective:** Detect changes in thermal behavior indicating lubrication degradation or bearing wear.

Equipment: - RTD or thermocouple sensors (+/-0.5°C accuracy) - Data logger or SCADA system

Procedure: 1. Install temperature sensors on: - Ball screw nut housing - Motor bearings (drive end and non-drive end) - Linear guide carriages 2. Log temperature every 1-10 seconds during machine operation. 3. **Baseline:** During commissioning, record temperature rise from cold start to steady-state (typically 30-90 minutes warm-up). Note steady-state temperature $T_{ss, \text{baseline}}$.

4. **Periodic comparison:** Monthly, repeat temperature logging under same operating conditions (same feed rate, same cut depth). Calculate $\Delta T_{ss} = T_{ss, \text{current}} - T_{ss, \text{baseline}}$.

Action Thresholds: - **Alert:** $\Delta T_{ss} > +5^\circ C$ ☐ Increased friction (possible lubrication degradation, bearing preload relaxation, contamination). Inspect and re-lubricate. - **Critical:** $\Delta T_{ss} > +10^\circ C$ or $T_{ss, \text{current}} > 70^\circ C$ ☐ Immediate shutdown risk. Stop machine; investigate cause (bearing seizure, nut galling, inadequate cooling).

8.3 Condition Monitoring and Diagnostics

Condition monitoring extends preventive maintenance by **continuously** tracking equipment health during operation, using sensors integrated into the control system.

8.3.1 Motor Current Monitoring Servo amplifiers report motor current in real-time (typically 1 kHz sample rate). Analyzing current patterns detects mechanical issues:

Normal Current Profile: - **Acceleration:** Current spike proportional to inertia ($I \propto J \times \alpha$ where J is inertia, α is angular acceleration). - **Constant velocity:** Steady current proportional to friction torque (1-5 A typical for NEMA 34 servo with ball screw, no load). - **Deceleration:** Negative current (regenerative braking).

Abnormal Patterns:

Symptom	Likely Cause	Diagnostic Test	Corrective Action
Current 2x higher than baseline (steady-state)	Excessive friction (lubrication loss, contamination, bearing bind)	Manually push axis—requires >50 N force?	Re-lubricate; inspect bearings for damage/contamination
Current oscillates +/-20% at frequency <10 Hz	Mechanical resonance (belt span, gantry mode)	Vibration spectrum shows peak at oscillation frequency?	Add damping, adjust belt tension, modify trajectory (slower accel)
Current spikes every revolution (cyclic)	Coupling misalignment, bent screw, eccentric pulley	Dial indicator on screw/pulley shows runout >0.05 mm TIR?	Re-align coupling, replace screw/pulley
Current drifts upward over 10-30 minutes	Thermal expansion causing binding (inadequate bearing float)	Temperature sensor shows screw temp rising >+20°C above ambient?	Verify floating bearing allows axial play; check thermal compensation

Symptom	Likely Cause	Diagnostic Test	Corrective Action
Current drops suddenly to near zero	Loss of mechanical engagement (belt tooth jump, rack tooth breakage, coupling slip)	Visual inspection shows belt teeth damaged or coupling loose?	Replace belt/rack; re-torque coupling clamps

Implementation:

Modern CNC controllers (Siemens 840D, Fanuc 31i, Heidenhain TNC7) include current monitoring alarms: - Set threshold at 150% of typical running current. - If exceeded for >1 second, trigger warning (continue operation but log event). - If exceeded for >5 seconds, trigger E-stop (prevent damage).

8.3.2 Positional Following Error Monitoring **Following error** is the difference between commanded position and actual position (from encoder feedback). Small following errors (<=0.01-0.05 mm) are normal during acceleration; large or growing errors indicate problems.

Diagnostic Table:

Following Error Symptom	Cause	Test	Fix
Error increases during accel, recovers during decel	Insufficient motor torque (undersized motor, low tuning gains)	Reduce acceleration 50%; error improves?	Increase PID gains (especially feed-forward) or upgrade motor
Error increases linearly with velocity	Velocity loop gain too low	Double velocity gain; error halves?	Tune velocity loop per motor manufacturer procedure
Error oscillates around zero at 10-50 Hz	Servo instability (gains too high, mechanical resonance)	Reduce proportional gain 20%; oscillation stops?	Reduce gains and/or add notch filter at resonance frequency

Following Error Symptom	Cause	Test	Fix
Error jumps suddenly by 0.1-1 mm during direction reversal	Backlash not compensated	Enable backlash compensation in controller	Measure backlash; enter value in controller comp table
Error grows continuously (integrator windup)	Mechanical jam or obstruction	Manually move axis-binds?	Clear obstruction; check for crash damage

Setup:

Program controller to log following error at 1-10 kHz during motion. Post-process data to calculate RMS following error:

$$FE_{RMS} = \sqrt{\frac{1}{n} \sum_{i=1}^n (FE_i)^2}$$

Thresholds: - **Good:** $FE_{RMS} < 0.005$ mm (precision machining) - **Acceptable:** $FE_{RMS} < 0.020$ mm (general machining) - **Poor:** $FE_{RMS} > 0.050$ mm (investigate immediately)

8.4 Troubleshooting Matrices

When problems occur, systematic diagnosis saves time and prevents misguided repairs. The following troubleshooting matrices guide technicians from symptom to root cause to corrective action.

8.4.1 Troubleshooting Matrix: Positioning Errors

Symptom	Possible Causes (Ranked by Likelihood)	Diagnostic Steps	Corrective Actions
Axis overshoots target by 0.05-0.5 mm	1. Following error (servo tuning) 2. Backlash 3. Mechanical resonance	1. Check following error log (controller) 2. Bidirectional positioning test 3. Vibration spectrum during move	1. Tune servo (increase damping, add feedforward) 2. Adjust preload or enable backlash comp 3. Add damping or reduce acceleration

Symptom	Possible Causes (Ranked by Likelihood)	Diagnostic Steps	Corrective Actions
Axis stops short of target by constant amount (e.g., always -0.3 mm)	1. Pitch error in screw/rack 2. Encoder scaling incorrect 3. Controller parameter wrong	1. Measure actual travel with calipers/laser over 100-1000 mm 2. Calculate scaling: (actual/commanded) 3. Check controller pitch parameter	1. Replace screw/rack if pitch error >1% 2. Correct encoder scaling in controller 3. Update pitch parameter (e.g., 5.00 mm/rev □ 5.02 mm/rev)
Random positioning scatter ($\sigma = 0.02\text{-}0.1 \text{ mm}$)	1. Mechanical play (loose mounting, worn bearings) 2. Electrical noise on encoder 3. Thermal drift	1. Shake carriage by hand—detects play? 2. Oscilloscope on encoder signals—noise present? 3. Temperature log—correlates with error?	1. Tighten bolts, replace worn bearings 2. Shield encoder cables, add ferrite beads 3. Enable thermal compensation or improve HVAC
Axis drifts slowly over time (0.05-0.5 mm/hour)	1. Thermal expansion 2. Preload relaxation (creep) 3. Belt stretch/creep	1. Temperature sensors show drift $>+/-5^\circ\text{C}$? 2. Backlash test—increased from baseline? 3. Belt drive—retension improves drift?	1. Activate thermal compensation 2. Re-adjust preload 3. Retension belt or replace (creep $>1\%$ indicates end of life)

8.4.2 Troubleshooting Matrix: Mechanical Noise/Vibration

Symptom	Causes	Diagnostic Steps	Corrective Actions
High-pitched whine (1-5 kHz)	1. Bearing noise (inadequate lube, contamination)2. Gear mesh (misalignment, tooth damage)3. Motor cogging (electrical)	1. Stethoscope/microphone localization2. Vibration spectrum—peak at ball pass freq?3. Disconnect motor—noise persists?	1. Re-lubricate or replace bearing2. Re-align gears, replace if teeth damaged3. Motor electrical issue—consult motor vendor
Clicking/clacking (1-10 Hz, cyclic)	1. Pitch error at rack joint2. Belt tooth jump3. Loose component (coupling setscrew, pulley)	1. Slow jog—count clicks per revolution/meter2. Sync click rate to RPM or position3. Visual inspection during motion	1. Re-align rack segments2. Increase belt tension or replace worn belt3. Torque all fasteners
Low-frequency rumble (10-100 Hz)	1. Structural resonance2. Imbalance (motor fan, pulley)3. Foundation vibration (external)	1. Vibration at multiple locations—same frequency?2. FFT peak at $1\times$ RPM \square imbalance3. Accelerometer on floor—vibration present?	1. Add damping, change operating speed2. Balance rotating components3. Isolate machine (spring mounts, vibration pads)

8.4.3 Troubleshooting Matrix: Belt Drive Issues

Symptom	Causes	Diagnostic	Corrective Action
Belt skipping teeth (audible click, position loss)	1. Insufficient tension2. Overload (accel too high)3. Pulley wear (teeth rounded)	1. Tension measurement $<10\%$ rated capacity?2. Reduce accel 50%—problem stops?3. Visual inspect pulley teeth—shiny/rounded?	1. Retension to 15-20% capacity2. Reduce accel or upgrade to wider belt3. Replace pulley (match tooth profile exactly)

Symptom	Causes	Diagnostic	Corrective Action
Belt tracking off pulley	1. Pulley misalignment 2. Uneven tension (belt twist) 3. Pulley flanges missing/damaged	1. Laser alignment-offset >0.5 mm/m? 2. Belt twists between pulleys? 3. Flanges cracked or worn?	1. Re-align pulleys (shim bearings) 2. Ensure belt not twisted during installation 3. Replace flanged pulleys
Excessive belt wear (cracks in teeth, backing delamination)	1. Over-tensioned 2. Pulley too small (min diameter violated) 3. Contamination (oil, coolant)	1. Tension >25% rated capacity? 2. Pulley diameter < min per belt datasheet? 3. Oil/grease on belt surface?	1. Reduce tension to 15-20%. Increase pulley diameter (redesign) 3. Clean belt with isopropanol; improve sealing to prevent contamination

8.5 Documentation and Record-Keeping

Documentation is often neglected but critical for: - **Compliance:** ISO 9001, AS9100, FDA 21 CFR Part 11 require maintenance records. - **Troubleshooting:** Historical data reveals patterns (e.g., bearing failures every 2,000 hours → investigate root cause). - **Continuous improvement:** Comparing machine performance over time identifies opportunities for design upgrades.

8.5.1 Required Documentation **1. Commissioning Report** (created during installation, Section 8.1): - Date, machine ID, axis ID - Straightness measurements (rail, screw/rack) - Parallelism measurements (rail-to-rail, rail-to-screw) - Backlash (at 5 positions) - Positioning accuracy (mean error, std dev) - Vibration baseline (FFT spectra at 4 locations) - Photos of critical alignments (coupling, rack joints, belt tensioning)

2. Maintenance Log (updated after each PM task): - Date, operating hours at time of maintenance - Task performed (lubrication, backlash adjustment, belt retensioning, etc.) - Measurements taken (backlash, tension, temperature, vibration) - Parts replaced (bearing P/N, belt P/N, quantity) - Technician name/signature

3. Failure/Repair Report (created when unplanned downtime occurs): - Date/time of failure, machine state when failure occurred - Symptom description (noise, positioning error, alarm code) - Root cause analysis (5-Why or Ishikawa fishbone diagram) - Corrective action (parts replaced, settings changed) - Verification test results (confirming problem resolved) - Preventive action (design changes or PM procedure updates to prevent recurrence)

4. Calibration Certificates (for measurement equipment): - Dial indicators, micrometers, laser interferometers, torque wrenches calibrated annually by NIST-traceable lab - Certificate includes serial number, calibration date, next due date, uncertainty statement

8.5.2 CMMS Integration Computerized Maintenance Management Systems (e.g., IBM Maximo, SAP PM, Fiix) automate scheduling and record-keeping:

Features: - **Work order generation:** Automatically creates PM tasks based on operating hours or calendar triggers. - **Parts inventory:** Tracks spare parts (bearings, belts, couplings) with min/max stock levels; generates purchase orders when inventory low. - **Equipment hierarchy:** Organizes machines by system/subsystem (e.g., Machine □ X-axis □ Ball Screw □ Bearings). - **Trend analysis:** Graphs backlash, vibration, temperature over time; flags anomalies. - **Mobile access:** Technicians use tablets to access procedures, record data in real-time on shop floor.

ROI: Studies show CMMS reduces maintenance costs 10-25% and unplanned downtime 30-50% by optimizing PM intervals and improving first-time fix rates.

References

1. **ISO 3408 Series** - Ball screws specifications and tolerances
2. **THK Ball Screw Catalog** - Sizing, selection, and mounting guidelines
3. **Hiwin Ball Screw Technical Manual** - Load ratings and accuracy grades
4. **NSK Ball Screws CAT. No. E1102g** - Engineering data and calculations
5. **ISO 14728-1:2017** - Rolling bearings - Linear motion rolling bearings
6. **Budynas, R.G. & Nisbett, J.K. (2020).** *Shigley's Mechanical Engineering Design* (11th ed.). McGraw-Hill
7. **SKF Linear Motion & Actuation** - Belt drives and timing belt specifications

8.6 Key Takeaways and Maintenance Program Integration

Key Takeaways:

1. **Laser alignment procedures** achieving +/-0.010-0.020 mm straightness over 1-3 m travel via laser interferometer or alignment laser (Hamar L-708, Renishaw XL-80) measuring rail/screw straightness, parallelism between paired rails, and perpendicularity to reference datums—procedure: establish reference beam, measure deviation at 200-500 mm intervals, shim mounting surface (brass shims 0.025-0.25 mm) or adjust set screws achieving target tolerance; misalignment >0.020 mm/m causes uneven bearing load reducing life 50-80%, binding inducing servo following errors, and premature wear concentrated at high-stress contact points
2. **Preventive maintenance schedules** optimizing inspection/lubrication intervals—ball screws: relubrication 200-500 hours (grease) or 1,000-2,000 hours (centralized oil-air system), backlash measurement 500 hours, nut inspection 2,000-5,000 hours; linear guides: lubrication 200-500 hours, preload verification 1,000 hours, carriage replacement 10,000-30,000 hours (L_{10} life); belts: tension check 200 hours, tooth wear inspection 500 hours, replacement 2,000-5,000 hours; racks: lubrication 300-800 hours, segment alignment verification 1,000 hours, tooth inspection 2,000-5,000 hours; neglecting PM increases failure rate 300-500% with emergency repairs costing 5-10x scheduled maintenance via production downtime
3. **Surface preparation requirements** for linear guide mounting—flatness +/-0.010 mm/m achieved via surface grinding (precision ground finish, Ra 0.8-1.6 μm) or hand scraping

(Prussian blue method, 8-12 points per 25 mm² achieving 0.005-0.010 mm flatness); inadequate surface prep causes rail distortion when bolted (preloaded fasteners conform rail to imperfect surface), uneven bearing contact, accelerated wear, and binding; verification: precision straightedge + feeler gauges (+/-0.010 mm resolution) or CMM measurement; screw mounting requires axial end bearings with +/-0.015 mm perpendicularity to prevent side loading

4. **Troubleshooting decision trees** for common failure modes—premature bearing failure: check overload (measure cutting forces, verify rating), contamination (inspect seals, add scrapers), misalignment (remeasure straightness/parallelism), inadequate lubrication (verify interval, grease quantity); backlash growth: measure current value, compare to baseline, if >2x initial replace nut/pinion, if gradual implement software compensation tables; positioning accuracy drift: thermal effects (add RTD sensors, software compensation), encoder damage (check signal quality via oscilloscope, replace if <0.5-1.0 Vpp), mechanical wear (inspect couplings, bearings, check for lost motion)
5. **Lubrication best practices** matching application severity—clean environments: lithium-based NLGI Grade 2 grease 200-500 hour intervals sufficient, harsh environments (coolant, chips, dust): synthetic grease with EP additives 100-300 hours or centralized automatic lubrication systems (oil-air mist delivery 1-5 drops/minute), high-speed applications: low-viscosity oil (ISO VG 32-68) continuous drip lubrication minimizing churning losses, vertical axes: sticky grease (NLGI Grade 1-2) preventing migration; over-lubrication causes churning heat and attracts contamination, under-lubrication causes metal-to-metal contact accelerating wear 10-50x
6. **Vibration and temperature monitoring** for predictive maintenance—accelerometers (piezo-electric, 10-10,000 Hz bandwidth) mounted on bearing housings detect frequency signatures: bearing wear (BPFI, BPFO frequencies), imbalance (1x shaft speed), misalignment (2x shaft speed), resonance excitation; temperature monitoring via RTDs or IR cameras identifies bearing overheating (>70-80°C indicates inadequate lubrication, overload, or preload mismatch), screw thermal growth (compensation requirement), motor winding temperature (overload detection); trending enables condition-based maintenance replacing time-based intervals, reducing failures 40-60%
7. **Documentation and CMMS** (Computerized Maintenance Management Systems) automating work orders, parts inventory, and trend analysis—maintenance log records: date, task, measurements (backlash, tension, temperature), parts replaced (P/N, quantity), technician signature; calibration certificates for measurement equipment (dial indicators, micrometers, torque wrenches) NIST-traceable annually; failure/repair reports including root cause (5-Why analysis), corrective action, verification test; CMMS features automatic PM scheduling based on operating hours, parts tracking (min/max stock levels), equipment hierarchy, mobile access; ROI studies show 10-25% maintenance cost reduction and 30-50% unplanned downtime reduction via optimized intervals and improved first-time fix rates

Maintenance program integration—laser alignment at installation achieving +/-0.010-0.020 mm/m via systematic measurement and shimming establishing baseline accuracy, preventive maintenance schedules (lubrication 200-500 hours, inspections 500-1,000 hours, component replacement 2,000-10,000 hours) preventing 300-500% failure rate increase from neglect, surface preparation (grinding/scraping to +/-0.010 mm/m flatness) enabling proper bearing load distribution, troubleshooting procedures (decision trees for premature failure, backlash growth,

accuracy drift) enabling rapid root cause identification, lubrication matching severity (grease intervals, automatic systems, oil-air for harsh/high-speed), vibration/temperature monitoring enabling predictive condition-based maintenance reducing failures 40-60%, and documentation/CMMS tracking tasks, parts, and trends optimizing intervals and first-time fix rates—systematic maintenance sustains initial performance over 15,000-30,000 hour industrial duty life preventing accuracy degradation, stiffness loss, and catastrophic failures that idle production and require emergency repairs costing 5-10× scheduled maintenance through lost throughput and expedited parts procurement.

Total: 5,865 words (original) + 650 words (Key Takeaways) = 6,515 words | 8+ equations | 6+ worked examples | 10+ tables

References

Industry Standards

1. **ISO 230-1:2012** - Test code for machine tools - Part 1: Geometric accuracy of machines operating under no-load or quasi-static conditions
2. **ISO 230-7:2015** - Test code for machine tools - Part 7: Geometric accuracy of axes of rotation
3. **ASME B89.4.1-1997 (R2012)** - Methods for Performance Evaluation of Coordinate Measuring Machines
4. **ISO 4378 Series** - Plain bearings - Terms, definitions, classification and symbols (for lubrication practices)

Manufacturer Technical Documentation

5. **Hamar Laser Instruments Inc. (2023).** *Laser Alignment Systems Catalog*. Danbury, CT. Available at: <https://www.hamarlaser.com> (Accessed: 2024)
 - L-708 precision laser alignment system, machine tool calibration procedures, straightness/flatness/perpendicularity measurements
6. **Easy-Laser AB (2022).** *Geometric Measurement Systems*. Mölndal, Sweden. Available at: <https://www.easy-laser.com> (Accessed: 2024)
 - Shaft alignment, flatness measurement, squareness verification for machine tool installation
7. **Mobil Industrial Lubricants (ExxonMobil) (2023).** *Lubrication Engineering Guide*. Available at: <https://www.mobil.com> (Accessed: 2024)
 - Grease selection (NLGI grades), relubrication intervals, oil-air lubrication systems for machine tools
8. **SKF Group (2023).** *Bearing Maintenance Handbook*. Gothenburg, Sweden. Available at: <https://www.skf.com> (Accessed: 2024)
 - Preventive maintenance schedules, vibration analysis, temperature monitoring, lubrication best practices

Academic and Professional Engineering References

9. **Mobley, R.K. (2014).** *Maintenance Engineering Handbook* (8th ed.). New York: McGraw-Hill.
ISBN: 978-0-07-179508-6
 - Chapter 11: Preventive and Predictive Maintenance (PM scheduling, condition monitoring, CMMS implementation)
10. **ISO 10816-1:1995** - Mechanical vibration - Evaluation of machine vibration by measurements on non-rotating parts
 - Standards for vibration severity assessment and trending for predictive maintenance
11. **Slocum, A.H. (1992).** *Precision Machine Design*. Englewood Cliffs, NJ: Prentice Hall. ISBN: 978-0-13-690918-7
 - Chapter 9: Assembly and Alignment (precision measurement techniques, shimming procedures, surface preparation)

CMMS and Maintenance Management

12. **Campbell, J.D., Jardine, A.K.S., & McGlynn, J. (2016).** *Asset Management Excellence: Optimizing Equipment Life-Cycle Decisions* (3rd ed.). Boca Raton, FL: CRC Press. ISBN: 978-1-4822-6132-1
 - Comprehensive maintenance management strategies, ROI analysis, reliability-centered maintenance
 13. **ISO 55000:2014** - Asset management - Overview, principles and terminology (framework for maintenance program development)
-

Module 3 - Linear Motion Systems

9. Conclusion

Linear motion systems form the kinematic foundation of every CNC machine, translating rotary motor motion into precise linear displacement. This module has systematically covered five primary drive technologies (ball screws, lead screws, rack & pinion, belt drives, and linear guides), the universal performance requirements they must satisfy, and the alignment and maintenance protocols that preserve their capabilities over operational life. This conclusion synthesizes the key technical outcomes, cross-module integration points, and forward-looking considerations for subsequent modules.

9.1 Key Outcomes by Drive Technology

Each drive technology occupies a distinct performance envelope defined by travel length, accuracy, speed, and cost trade-offs:

Ball Screws (Section 2) deliver the highest stiffness ($100\text{-}300 \text{ N}/\mu\text{m}$) and accuracy ($\pm 0.005\text{--}0.020 \text{ mm}$ positioning repeatability) but are constrained by critical speed ($n_{\text{crit}} \propto d_r/L^2$) and Euler buckling limits (unsupported lengths typically $< 3 \text{ m}$). Proper preload selection (4-8% of

dynamic load rating C) eliminates axial clearance while maintaining >90% of nominal L_{10} life. Thermal compensation is mandatory for precision work; a 10°C temperature rise produces 11.5 $\mu\text{m}/\text{m}$ growth in steel screws ($\alpha = 11.5 \times 10^{-6} \text{ K}^{-1}$). Dual-drive configurations with electronic gantry synchronization enable long axes (up to 6-8 m) with maintained accuracy, though they require matched servo drives and cross-coupling control algorithms. **Cost:** \$500-5,000+ per axis depending on diameter, length, and preload class.

Lead Screws (Section 3) sacrifice efficiency ($\eta = 20\text{-}40\%$ typical for ACME threads) in exchange for self-locking capability (lead angle $\lambda < 5^\circ$ with friction angle $\phi \approx 6\text{--}8^\circ$). This inherent safety is critical for vertical axes (Z-axis, gantry lifts) where power loss must not allow gravity-driven motion. PV limits (pressure \times velocity product) for bronze nuts typically fall in the range 0.5-1.5 MPa·m/s; exceeding these limits causes rapid wear and thread galling. Polymer nuts (Delrin, PTFE) extend PV capacity to 2-3 MPa·m/s but introduce compliance ($k \approx 50\text{--}100 \text{ N}/\mu\text{m}$ vs. 150-200 N/ μm for bronze). **Applications:** Manual mills, Z-axis counterbalance systems, low-speed positioning (<0.1 m/s). **Cost:** \$100-800 per axis.

Rack & Pinion (Section 4) enables travel lengths from 3-50 m with maintained accuracy (+/- 0.05-0.15 mm over full length when segment pitch errors held to +/- 0.02 mm). AGMA stress verification is essential: bending stress σ_b must remain below material endurance limit (typically 150-250 MPa for through-hardened steel, 400-600 MPa for case-carburized), and Hertzian contact stress σ_c must not exceed 1,000-1,500 MPa to prevent pitting. Dual-pinion anti-backlash designs (spring-loaded opposing pinions with 50-200 N preload) reduce backlash from 0.10-0.30 mm to <0.05 mm. Long-axis synchronization requires encoder feedback on the machine table (not just motor encoders) to compensate for elastic windup and thermal expansion. **Applications:** Gantry routers, plasma tables, waterjet cutters. **Cost:** \$1,000-8,000+ per axis depending on length and precision class.

Belt Drives (Section 6) achieve the highest speeds (>1 m/s continuous, 2-5 m/s rapids) and longest practical travels (up to 4-6 m single-span, 10+ m with idlers) at lowest cost. Effective axial stiffness $k = EA/L$ depends critically on belt material: steel-reinforced belts deliver $k \approx 200\text{--}300 \text{ N}/\mu\text{m}$ but exhibit positive thermal expansion ($\alpha \approx +11.5 \times 10^{-6} \text{ K}^{-1}$); aramid (Kevlar) belts offer $k \approx 150\text{--}250 \text{ N}/\mu\text{m}$ with negative CTE ($\alpha \approx -2.0 \times 10^{-6} \text{ K}^{-1}$) enabling passive thermal compensation when paired with aluminum extrusion frames. Resonance management is crucial: fundamental frequency $f_n = \frac{1}{2L}\sqrt{T/\mu}$ typically falls in 10-30 Hz range for 1-3 m spans, necessitating notch filters or idler-based segmentation (shortening effective L to raise f_n). Backlash (0.3-1.0 mm from tooth clearance, belt hysteresis, and pulley runout) limits accuracy to +/- 0.05-0.15 mm unless dual-belt anti-backlash is implemented. **Applications:** Laser cutters, large-format 3D printers, pick-and-place systems. **Cost:** \$200-1,500 per axis.

Linear Guides (Section 5) provide the stiffness backbone (typically 50-80% of total axis stiffness) regardless of drive type. ISO 14728 life ratings predict carriage life under combined loads:

$$L_{10} = \left(\frac{C}{P}\right)^{3.33} \times 10^6 \text{ mm}$$

for ball guides, where dynamic load rating C ranges from 5-50 kN and equivalent load P includes radial, moment, and preload components with hardness, temperature, contamination, and lubrication correction factors. Preload classes (Z0 = 1%, ZA = 2%, ZB = 5%, ZC = 8% of C_0) trade increased stiffness (Hertzian contact stiffness $k \propto F^{1/3}$, so doubling preload yields ~26% stiffness gain) against reduced life (~50% life reduction for ZC vs. Z0). Installation tolerances are demanding: rail straightness $\leq 0.015 \text{ mm}/\text{m}$, parallelism between rails $\leq 0.020 \text{ mm}/\text{m}$, and flatness of mounting surface $\leq 0.010 \text{ mm}/\text{m}$; violations cause uneven loading and premature failure. **Cost:** \$300-3,000+ per axis depending on size, preload class, and

number of carriages.

9.2 Universal Requirements and Their Implications

Section 7 established four universal requirements transcending specific drive technologies:

Backlash specifications range from $<=0.005$ mm for high-precision mills to $<=0.100$ mm for plasma tables (Table 7-1). Meeting these targets demands technology-appropriate solutions: preloaded ball nuts for ball screws, dual-pinion spring preload (50-200 N) for racks, tensioned dual-belt configurations for belt drives. Measurement per ISO 230-2 bidirectional positioning test provides quantitative verification; laser interferometry confirms both systematic error (encoder miscalibration) and random error (backlash, mechanical compliance).

Stiffness requirements span 10 N/ μm (plasma/waterjet with $+/-0.15$ mm tolerance) to 200 N/ μm (precision mills with $+/-0.005$ mm tolerance) (Table 7-2). Since axis stiffness combines in series ($1/k_{\text{total}} = 1/k_{\text{drive}} + 1/k_{\text{guide}} + 1/k_{\text{coupling}} + 1/k_{\text{frame}}$), every component matters. ASME B5.54 static load testing quantifies actual stiffness; dynamic stiffness $k_{\text{dyn}} = k_{\text{static}} / \sqrt{(1 - r^2)^2 + (2\zeta r)^2}$ drops near structural resonances (frequency ratio $r \approx 1$), driving machine design away from typical servo bandwidths (10-50 Hz).

Thermal behavior dominates error budgets in long-axis machines. Steel components expand $11.5 \mu\text{m}$ per meter per $^{\circ}\text{C}$; aluminum $23.6 \mu\text{m}/\text{m} \cdot ^{\circ}\text{C}$ (Table 7-3). Passive compensation (CTE matching between drive and frame, symmetric heating) can halve thermal error. Active compensation ($x_{\text{corrected}} = x_{\text{cmd}} \times [1 + \alpha_{\text{eff}}(T - T_{\text{ref}})]$) with RTD sensors ($+/-0.5^{\circ}\text{C}$ accuracy) further reduces error to $<10 \mu\text{m}$ over $+/-10^{\circ}\text{C}$ ambient variation, essential for sheet metal work and precision machining. Environmental control ($+/-0.2-3^{\circ}\text{C}$ depending on facility class, Table 7-4) represents a facility-level investment but enables consistent sub- 0.010 mm accuracy.

Safety systems (Table 7-5) include dual-channel E-stops (ISO 13849 Category 3, SIL 2), interlocked guards (Type 4 light curtains with safety distance $S = K(T_s + T_r) + C$ typically yielding 800-1,200 mm standoff for 1,600 mm/s approach speed), and Z-axis gravity brakes ($>=120\%$ of suspended mass). Lockout/tagout per OSHA 1910.147 (6-step procedure) prevents energization during maintenance. Axis-specific hazards include Z-axis drop (requires fail-safe brake or self-locking lead screw), belt stored energy ($U = \frac{1}{2}k\Delta x^2$ can reach 50-200 J in high-tension systems), rack pinch points (require tunnel guards), and rotating coupling entanglement (requires shrouding).

9.3 Cross-Module Integration

Linear motion system performance is intrinsically coupled to upstream (Module 1: Mechanical Frame) and downstream (Module 2: Vertical Axis) design decisions:

Module 1 Integration (Mechanical Frame):

Frame stiffness k_{frame} appears in series with drive stiffness. A gantry beam with insufficient bending stiffness (EI_y inadequate for span L_{beam}) can halve total axis stiffness regardless of ball screw quality. Module 1's structural resonance analysis (modal frequencies, damping ratios) must account for moving mass of linear axes; a 50 kg gantry accelerating at 1 g injects 500 N force at each reversal, potentially exciting frame modes. Surface preparation (grinding/scraping to $<=0.010$ mm/m flatness) enables linear guide installation within tolerance. Thermal design (material selection for CTE matching, convective/radiative heat paths) directly affects compensation

feasibility. **Design implication:** Linear axis procurement must parallel frame design, not follow it sequentially.

Module 2 Integration (Vertical Z-Axis):

Gravity preload ($F_{\text{gravity}} = m_z \times g$) must be included in ball screw L_{10} life calculation; a 200 kg Z-axis applies 2,000 N continuous preload, often dominating over cutting forces. Brake sizing ($\geq 120\%$ mass including tooling/workpiece) prevents drop on power loss. Counterbalance (gas springs, pneumatic cylinders targeting 80-100% weight offset) reduces motor torque and heat generation, indirectly aiding thermal stability. Thermal compensation priority: Z-axis errors project normal to workpiece surface (directly affecting part thickness/depth), whereas X/Y errors often lie in-plane (affecting feature position but not always critical). **Design implication:** Z-axis drive technology often differs from X/Y (lead screw for Z, ball screw for X/Y) to prioritize safety over speed.

9.4 Forward-Looking: Module 4 (Control Electronics) Requirements

Mechanical motion system specifications directly dictate control system requirements, which Module 4 will address in detail:

Servo Drive Torque and Current:

Peak torque $T_{\text{peak}} = \frac{F_{\text{max}} \times \text{lead}}{2\pi\eta} \times \text{safety factor}$ (typically 1.5-2.0) sizes motor and drive. For a 5,000 N cutting force on a 10 mm lead ball screw ($\eta = 0.90$), $T_{\text{peak}} = \frac{5000 \times 0.010}{2\pi \times 0.90} \times 2.0 \approx 17.7$ Nm, requiring a servo drive rated ≥ 20 Nm continuous (25-30 Nm peak). Current loop bandwidth ≥ 2 kHz ensures torque response <0.5 ms, critical for chatter suppression and following error minimization.

Encoder Resolution and Feedback:

Positioning accuracy target dictates encoder resolution. For ± 0.005 mm repeatability on a 5 mm lead screw, encoder must resolve <0.001 mm per count (safety factor 5-10x); this requires 5,000 counts/rev minimum, typically met by 2,500 line/rev encoders (10,000 counts/rev with 4x quadrature). Long axes (racks, belts) benefit from linear scales (glass or magnetic tape encoders) directly measuring table position, bypassing transmission errors.

Backlash Compensation and Feedforward:

Software backlash tables $B(x)$ at 10-20 points along axis compensate wear-induced backlash variation. Feedforward terms ($T_{\text{ff}} = J\alpha + b\omega + F_{\text{friction}}$) inject calculated torque before position error develops, critical for constant-velocity contouring (reduces following error by 50-80%).

Thermal Compensation Algorithms:

Real-time thermal correction $x_{\text{corrected}} = x_{\text{cmd}} \times [1 + \alpha_{\text{eff}}(T - T_{\text{ref}})]$ requires RTD sensors ($\pm 0.5^\circ\text{C}$ accuracy, 1 Hz update rate) at screw bearings, frame reference points, and ambient. Coefficient α_{eff} combines material CTEs weighted by structural geometry; empirical characterization (Section 7.3 procedure) yields ± 0.002 mm accuracy over $\pm 10^\circ\text{C}$ range.

Vibration Rejection and Notch Filters:

Belt resonances (10-30 Hz) and structural modes (50-200 Hz) excite following error oscillations. Notch filters ($H(s) = \frac{s^2 + 2\zeta_n \omega_n s + \omega_n^2}{s^2 + 2\zeta_d \omega_d s + \omega_d^2}$ with $\zeta_d > \zeta_n$) at resonant frequencies attenuate servo response by 20-40 dB, stabilizing motion. Adaptive notch filters (auto-tuning via FFT of following error) maintain performance as belt tension drifts or structural modes shift with thermal expansion.

Gantry Synchronization (Dual-Drive Systems):

Electronic gearing couples dual Y-axis motors with cross-coupling controller: master axis command feeds both drives, while differential error $\Delta x = x_{\text{left}} - x_{\text{right}}$ generates corrective torque proportional to misalignment. Gains $K_p = 50\text{-}200 \text{ N/mm}$ and $K_d = 5\text{-}20 \text{ Ns/mm}$ maintain $<0.02 \text{ mm}$ racking under asymmetric cutting loads (e.g., milling near one side of table). Linear scales on both ends of gantry beam close the feedback loop, immune to ball screw pitch variations.

9.5 Technology Selection Decision Framework

A prioritized decision tree guides technology selection:

Step 1: Travel Length

- $<1 \text{ m}$: Ball screws preferred (highest stiffness/accuracy, cost-effective at short lengths) - $1\text{-}3 \text{ m}$: Ball screws or belt drives (screws if accuracy $<=0.020 \text{ mm}$; belts if speed $>0.5 \text{ m/s}$) - $3\text{-}8 \text{ m}$: Rack & pinion or belt drives (racks if load $>5 \text{ kN}$; belts if speed $>1 \text{ m/s}$) - $>8 \text{ m}$: Rack & pinion only (belt sag and resonance become unmanageable)

Step 2: Accuracy and Backlash

- $<=0.010 \text{ mm}$: Ball screws with preload, ground rails (ZB/ZC class) - $<=0.050 \text{ mm}$: Ball screws, racks with dual-pinion preload, belts with dual-belt preload - $<=0.100 \text{ mm}$: Any drive with proper tensioning/preload (even single-belt acceptable) - $>0.100 \text{ mm}$: Drive backlash non-critical; focus on structural stiffness

Step 3: Speed and Acceleration

- $>1 \text{ m/s}$ rapids: Belt drives (CoreXY, H-bot for XY decoupling) - $0.2\text{-}1 \text{ m/s}$: Ball screws (below critical speed) or belt drives - $<0.2 \text{ m/s}$: Any drive (speed non-limiting); choose based on other factors

Step 4: Load Capacity

- $>10 \text{ kN}$ continuous: Racks (module 3-5 teeth) or large ball screws ($>=40 \text{ mm}$ diameter) - $1\text{-}10 \text{ kN}$: Ball screws (25-40 mm diameter) or racks (module 2-3) - $<1 \text{ kN}$: Ball screws, lead screws, or belts (choose for accuracy/speed needs)

Step 5: Vertical Axis Safety

- Fail-safe required (power loss must not allow drop): Lead screws (self-locking) or ball screws with electromagnetic brake ($>=120\%$ mass) - Counterbalance available: Ball screws with counterbalance (80-100% weight offset) + brake backup - Horizontal only: Safety not applicable; proceed to cost analysis

Step 6: Cost Constraints

- $<\$200/\text{axis}$: Belt drives (GT2, fiberglass reinforcement, aluminum pulleys) - $\$200\text{-}1,000/\text{axis}$: Ball screws (16-25 mm rolled) or lead screws (ACME 1"-2") - $>\$1,000/\text{axis}$: Ball screws (25-40 mm ground/preloaded), racks (ground tooth profile), or belt drives with steel cable and aramid backing

9.6 Closing Remarks and Path Forward

The linear motion system is a **mechanical-control co-design challenge**: mechanical selection dictates control requirements (torque, encoder resolution, bandwidth), while control capabilities enable mechanical designs previously impractical (long belts with resonance compensation, dual-drive racks with electronic synchronization). Disciplined application of the universal requirements

(Section 7) and maintenance protocols (Section 8) ensures that initial performance persists over machine operational life.

Module progression: With mechanical frame (Module 1), vertical axis specialization (Module 2), and linear motion systems (Module 3) complete, the course transitions to **Module 4 (Control Electronics and Servo Systems)**, covering servo drive selection, PID/feedforward tuning, encoder integration, safety circuits, and HMI design. Specialized process modules follow: Module 5 (Plasma Cutting), Module 6 (Spindle Systems), Module 7 (Fiber Laser), and Module 8 (Waterjet), each building on this foundational motion control knowledge.

Design philosophy: Maintain margins in both mechanical and control domains. A 10% stiffness margin and 20% torque margin compound to robust performance even when secondary effects (thermal expansion, wear, supply voltage sag) degrade nominal values. The most successful CNC designs emerge from parallel development of mechanics and controls, not sequential handoffs.

Module 3 concludes here. The subsequent modules await your continued study.

References

Comprehensive Module 3 Standards (All Drive Technologies)

1. **ISO 3408 Series (2006)** - Ball screws - Parts 1-5: Complete specification covering vocabulary, nominal dimensions, acceptance tests, load ratings, and rigidities
2. **ISO 14728 Series (2017)** - Rolling bearings - Linear motion rolling bearings - Parts 1-3: Dynamic/static load ratings and lubrication
3. **ISO 230 Series (2012-2014)** - Test code for machine tools - Parts 1-3: Geometric accuracy, positioning accuracy, thermal effects
4. **ASME B5.54-2005 (R2019)** - Methods for Performance Evaluation of Computer Numerically Controlled Machining Centers
5. **AGMA 2001-D04** - Fundamental Rating Factors for Gear Teeth (rack and pinion systems)
6. **ISO 5296 Series (2012)** - Synchronous belt drives specifications

Academic References (Primary Textbooks)

7. **Slocum, A.H. (1992).** *Precision Machine Design*. Englewood Cliffs, NJ: Prentice Hall. ISBN: 978-0-13-690918-7
 - Definitive reference on precision mechanical systems design, thermal management, bearing systems, alignment
8. **Budynas, R.G. & Nisbett, J.K. (2020).** *Shigley's Mechanical Engineering Design* (11th ed.). New York: McGraw-Hill Education. ISBN: 978-0-07-339820-4
 - Comprehensive mechanical design covering screws, gears, bearings, belts with worked examples
9. **Norton, R.L. (2020).** *Machine Design: An Integrated Approach* (6th ed.). Hoboken, NJ: Pearson. ISBN: 978-0-13-481834-4
 - Integrated approach to machine component design with extensive case studies

Cross-Module Integration (Course Modules)

10. **Module 1: Mechanical Frame Design** - Mounting surface flatness requirements (+/-0.010 mm/m), frame stiffness contributions to total system compliance
11. **Module 2: Vertical Axis & Gravity Compensation** - Z-axis brake sizing (>=120% mass), counterbalance systems, lead screw self-locking applications
12. **Module 4: Motion Control Systems** - Servo motor sizing based on linear motion inertia/force requirements, encoder resolution selection, thermal compensation algorithms
13. **Modules 5-8: Process Modules** - Cutting force magnitudes and directions: Module 5 (Milling 1-20 kN), Module 6 (Turning 2-15 kN), Module 7 (Fiber Laser <0.5 kN), Module 8 (Waterjet 0.5-3 kN)
14. **Module 11: Large-Format FDM 3D Printers** - Case study integrating belt drives (XY CoreXY kinematics), linear guides (MGN rails), lead/ball screws (Z-axis), thermal management

Forward-Looking Technologies

15. **Linear Motors** - Direct drive systems eliminating mechanical transmission, achieving >5 m/s speeds, +/-0.001 mm accuracy, but higher cost (\$5,000-20,000/axis)
 16. **Active Vibration Control** - Piezoelectric actuators, magnetostrictive dampers for chatter suppression in precision machining
 17. **Smart Bearings** - Embedded sensors (temperature, vibration, load) enabling real-time condition monitoring and predictive maintenance
-